NOTE TO USERS

RNA Sequences And Structures Cleaved By A Novel Mammalian Endoribonuclease *In Vitro*

Alaeddin Walid Tafech

B.Sc., University of British Columbia, 2003

Thesis Submitted In Partial Fulfillment Of

The Requirements For The Degree Of

Master Of Science

in

Mathematical, Computer, and Physical Sciences

(Chemistry)

The University Of Northern British Columbia

December 2005

Your file Votre référence
ISBN: 978-0-494-28395-0
Our file Notre référence
ISBN: 978-0-494-28395-0

Abstract

Endoribonucleases have been implicated in post-transcriptional regulation in virtually all organisms. In vertebrates, the regulation of gene expression by mRNA turn-over is not well-understood as only few endoribonucleases have been purified and eventually cloned. Our lab has purified a novel endoribonuclease from rat livers that cleaves within the Coding Region Determinant (CRD) of the c-*myc* mRNA. c-Myc is a transcription factor belonging to the Myc family and it is over-expressed in many human cancers. mRNA stability involves an enhanced half-life of the mRNA in the cytoplasm and is one method leading to mRNA over-expression. This type of over-expression has been observed in liver cancers, where the c-*myc* mRNA is stable compared to mRNA in the normal liver. The aim of this thesis was to determine the sequence and structure cleavage specificity of the endoribonuclease to nts 1705-1792 of the c-*myc* CRD region. To further confirm the cleavage specificity of the endoribonuclease, nts 3018-3159 of the human β-globin mRNA was used as a substrate in addition to a series of mutants encompassing the 1705-1792 c-*myc* CRD region. Prior to determination of preferential cleavage sites generated by the endonuclease, the *in vitro* secondary structures of the 1705-1792 c-*myc* CRD and the 3018-3159 β-globin RNAs were determined using enzyme probes. The RNase probing data were then used as a constraint with the structure generated by the Mfold software program to obtain the experimental structure. The RNA substrates were then incubated with the endoribonuclease and the cleavage sites were identified. Results revealed that this endonuclease preferentially cleaves UA, CA and UG dinucleotides, regardless of strandedness and single-stranded CU dinucleotides. This study has the potential to enhance our knowledge on how the mammalian endoribonuclease may function in cells.

Table of Contents

List of Tables

Table Page

List of Figures

Acknowledgements

First of all, I would like to thank my supervisor, Dr. Chow H. Lee, for his guidance, supervision, and patience during the two years of my Masters studies. I also would like to thank my colleagues Joel C. Urquhart and Kirk Bergstrom for their advice and their technical support. My thanks also extends to my committee members, Dr. Stephen Rader and Dr. Brent Murray and also to Dr. Andrea Gorrell, for their constant support and advice. Finally, I would like to thank Ric Bennett and Fergil Mills for assisting me in generating the CRD mutants.

Candidate's Publications Relevant to this Thesis

Articles:

1. Bergstrom K, Urquhart JC, **Tafech A**, Doyle E, Lee CH. (2005) Purification and characterization of a novel mammalian endoribonuclease. *J Cell Biochem*, in press. (Epub: 10.1002/jcb.20726).

2. **Tafech A,** Bassett T, Sparanese D, Lee CH. Destroying RNA as a Therapeutic Approach. *Curr Med Chem*, (accepted).

3. **Tafech A**, Bennett WR, Lee CH. Identification of RNA sequences and structures involved in site-specific cleavage by a novel mammalian endoribonuclease. Manuscript in preparation.

Abstracts:

1. Bergstrom K, Urquhart JC, **Tafech A,** Lee CH. (2004) Biochemical properties of an endoribonuclease that is capable of cleaving coding region determinant of c-*myc* mRNA *in vitro*. *9th Annual Meeting of the RNA Society.*

2. **Tafech A,** Lee CH. (2005) *In vitro* secondary structure of the c-*myc* coding region determinant (CRD) RNA and the structure/sequence cleaved by a polysome-associated CRD c-*myc* endonuclease-2 (PAC-2). *10th Annual Meeting of the RNA Society.*

3. **Tafech A,** Lee CH. (2005) *In vitro* secondary structure of the c-*myc* coding region determinant (CRD) RNA and the structure/sequence cleaved by a polysome-associated CRD c-*myc* endonuclease-2 (PAC-2). *RiboWest Conference.*

Chapter 1

Introduction

1.0 Overview of messenger RNA turn-over

In the last two decades, mRNA decay has emerged as a major control point in gene expression in virtually all organisms (Brewer, 2002; Decker and Parker, 1994; Dodson and Shapiro, 2002; Ross, 1995). The amount of protein that can be translated from mRNA is dependent upon the amount of time the mRNA persists in the cytoplasm (Coburn and Mackie, 1999; Dodson and Shapiro, 2002).

Degradation by mRNA turn-over is thought to play a critical role in four essential cellular processes: (i) the setting of the basal level of gene expression, (ii) elimination of aberrant mRNAs containing Premature Termination Codons (PTCs) or lacking codons, (iii) processing of pre-mRNAs, and (iv) defense against infectious double-stranded viral RNAs (Baker and Condon, 2004; Parker and Song, 2004).

The deadenylation-dependent and deadenylation-independent pathways are two models that have been suggested to regulate mRNA decay (Bremer et al., 2003; Guhaniyogi and Brewer, 2001). The deadenylation-dependent pathway involves the shortening/removal of the poly(A) tail, followed by the removal of the 5' cap, and lastly the exonucleolytic degradation by the 5' to 3' and/or the 3' to 5' exonucleases (Brewer, 1999; Brewer, 2002; Chernokalskaya et al., 1997; Dodson and Shapiro, 2002; Guhaniyogi and Brewer, 2001; Tourriere et al., 2001; Wennborg et al., 1995) . In contrast, the deadenylation-independent pathway involves the cleavage of the mRNA without prior deadenylation (Baker and Condon, 2004; Brewer, 2002; Coller and Parker, 2004; Decker and Parker, 1994; Dodson and Shapiro, 2002; Schoenberg and Cunningham, 1999). It involves the rate-limiting step of

endonucleolytic cleavage within the body of the mRNA followed by exonucleolytic decay of the remaining message (Chernokalskaya et al., 1997; Dodson and Shapiro, 2002). The importance of this pathway stems from the fact that it is responsible for the fluctuations in the half-lives of many unstable mRNAs (Caruccio and Ross, 1994; Dodson and Shapiro, 2002; Ross, 1995).

The intrinsic half-lives of many mRNAs are dictated by both the *cis* determinants within the mRNA and the trans-acting factors that bind to them (Dodson and Shapiro, 2002; Guhaniyogi and Brewer, 2001; Wang and Kiledjian, 2000). *Cis* determinants can be located at any region within the mRNA, including the 3'UTR and Coding Region Determinants (CRD). The most common *cis* determinant, the AU-Rich Element (ARE), is found within the 3' UTR of mRNAs (Chen and Shyu, 1995; Ross, 1995) and has been implicated in mRNA instability, although there are few exceptions (Dodson and Shapiro, 2002). Examples of mRNAs containing destabilizing AREs in their 3'UTR are c-*myc* (Chen and Shyu, 1995), c-*fos* (Chen and Shyu, 1995), VEGF (Levy et al., 1998), and apolipoprotein II (Binder et al., 1989). The coding regions of mRNAs have also been implicated in the control of mRNA stability. Examples include: c-*myc* (Yeilding et al., 1998), c-*fos* (Schiavi et al., 1992), and β-tubulin (Bachurski et al., 1994) mRNAs. Secondary structural features are also thought to play a role in mRNA stability by inhibiting mRNA cleavage mediated by exoribonucleases and single-strand RNA-specific endoribonucleases (Coburn and Mackie, 1999).

1.0.1 Messenger RNA turn-over in prokaryotes

A model organism for studying mRNA decay is *Escherichia coli*, which has a typical mRNA half-life of 60-120 seconds (Coburn and Mackie, 1999). The poly(A) tail in bacteria functions to promote mRNA degradation (Coburn and Mackie, 1999; Steege, 2000) by

allowing exoribonucleases to access the 3' stem-loops, which normally act to stabilize the mRNA (Coburn and Mackie, 1999; Steege, 2000). It is believed that with the presence of the single-stranded poly(A) tail docking site, exoribonucleases such as polynucleotide phosphorylase (PNPase) and RNase II can cleave the mRNA in a 3' to 5' direction (Callaghan et al., 2003; Grunberg-Manago, 1999).

The short mRNA half-life observed in *E.coli* is mainly a consequence of the deadenylation-independent pathway, which recently has emerged as a major pathway for degradation of many bacterial mRNAs (Chernokalskaya et al., 1997; Coburn and Mackie, 1999). Six major endoribonucleases that have been implicated in bacterial mRNA decay are RNase E, RNase G, RNase III, RNase P, MazF, and PemK (Kushner, 2002; Li and Altman, 2003; Nicholson, 1999; Steege, 2000; Zhang et al., 2004) (Table 1.1). RNase II, polynucleotide phosphorylase (PNPase), and oligoribonuclease have been specifically implicated in 3' to 5' exonucleolytic cleavage of bacterial mRNAs (Cheng and Deutscher, 2005).

mRNA degradation in bacteria is thought to involve the initial rate-limiting step of endonucleolytic attack by RNase E (Coburn and Mackie, 1999). This is followed by 3' to 5' exonucleolytic attack by PNPase and RNase II (Baker and Mackie, 2003; Condon and Putzer, 2002; Grunberg-Manago, 1999; Kushner, 2002; Mishra, 2002; Nicholson, 1999; Rauhut and Klug, 1999; Steege, 2000). The mRNA decay process in bacteria has been further elucidated by the discovery of a multi-protein complex termed the degradosome. This complex is thought to be composed of RNase E (Coburn and Mackie, 1999), PNPase, RNA helicase, and several other ATP-dependent enzymes (Grunberg-Manago, 1999; Kushner, 2002; Redko et al., 2003).

Endoribonucleases that degrade mRNAs in *E.coli*

RNase E

In the last 10 years, RNase E has emerged as the primary endonuclease responsible for the rate limiting step of bacterial mRNA degradation (Callaghan et al., 2003; Coburn and Mackie, 1999; Kushner, 2002; Redko et al., 2003; Wennborg et al., 1995). It regulates the degradation, and thus the half-life, of many bacterial mRNAs, in addition to its role in processing ribosomal RNAs (Coburn and Mackie, 1999; Wennborg et al., 1995). Targets of RNase E include 9S RNA, the 5'UTR of *ompA* RNA, and the 5' UTR of phage T4 gene 32 mRNA (Ghora and Apirion, 1978; Lundberg et al., 1995; Lundberg et al., 1990; Mudd et al., 1988). RNase E was found to cleave single-stranded RNA regions near the 5'-terminus region, in close proximity to the translation initiation site (Nicholson, 1999). It is also believed that RNase E cleaves upstream of the stabilizing 5' secondary structural features, thereby generating fragments that are then susceptible for degradation by 3' to 5' exonucleases (Baker and Mackie, 2003; Grunberg-Manago, 1999). Furthermore, it has recently been shown that RNase E preferentially cleaves 5' to AU dinucleotides in A/U rich regions (Coburn and Mackie, 1999). An experiment was performed to investigate the structural requirement of RNase E, *in vitro*, to its 9S and 20S RNA targets by generating several structural mutants (Cormack and Mackie, 1992; Mackie and Genereaux, 1993). The conclusion was that RNase E cleaves its target sequences only when present in single-stranded domains.

RNase G

RNase G has been implicated in the maturation of the 5'end of 16S RNA, rRNA processing and M1 RNA processing (Jiang and Belasco, 2004; Wachi et al., 1999). This

endonuclease comprises 489 amino acid residues and shares extensive homology to the endonucleolytic domain (amino half) of RNase E (Jiang and Belasco, 2004). Therefore, it is not too surprising that both RNase E and RNase G have similar cleavage specificity as they both prefer to cleave 5' to AU dinucleotides (in AU-rich regions) only when present in single-stranded conformations (Hua et al., 1993; Jiang and Belasco, 2004; Tock et al., 2000).

RNase III

RNase III has also been implicated in the rate-limiting step of endonucleolytic degradation of many bacterial mRNAs, although not to the same degree as RNase E (Condon and Putzer, 2002). It has little RNA sequence specificity (Condon and Putzer, 2002; Lamontagne et al., 2004) and it has an absolute requirement for double-stranded regions, as it was found to be incapable of cleaving single-stranded regions *in vitro* (Robertson et al., 1968). RNase III was also found to be capable of autoregulating itself by cleaving its own stem-loop structure (Condon and Putzer, 2002).

RNase P

RNase P is a ribonucleoprotein that is responsible for the cleavage of precursor tRNA molecules to generate mature tRNA 5' ends (Altman et al., 1993; Mishra, 2002; Nicholson, 1999). It consists of a 377 nt RNA subunit encoded by *rnpB* gene and ~ 130 kDa protein subunit encoded by the *rnpA* gene (Altman et al., 1993; Nicholson, 1999). In addition to its role in tRNA maturation, it is also likely to play a role in bacterial mRNA turn-over as it was found to cleave polycistronic mRNAs *in vitro* such as tryptophanase (*tnaA*). RNase P was able to cleave between the single-stranded U47 and G48 within the *tnaA* operon RNA (Li and Altman, 2003). It has been hypothesized that the products generated by RNase P are

subsequently degraded by RNase E, followed by 3' to 5' degradation by PNPase (Li and Altman, 2003).

MazF

MazF is a dimeric endoribonuclease that preferentially cleaves RNA 3' to the first adenosine residue in ACA sequences only in single-stranded conformations (Zhang et al., 2005; Zhang et al., 2003). However in another study, this endoribonuclease showed different sequence specificity and it was found to cleave 3' to N residues within NAC sequences (where N = an A or U) in single-stranded conformations (Munoz-Gomez et al., 2004).

PemK

Another endonuclease implicated in *E.coli* mRNA decay is PemK, which functions to block protein synthesis (Zhang et al., 2004). It preferentially cleaves its target mRNA 5'or 3' to the adenosine residue of the UAH sequence, only when present in single-stranded regions (Zhang et al., 2004).

Table 1.1. Bacterial endonucleases and their cleavage sites.

Name of endonuclease	Cleavage site	RNA Structure specificity of the endonuclease	References
RNase E	5' to AU dinucleotides in AU rich regions (upstream of stem-loops)	Single-stranded	(Coburn and Mackie, 1999)
RNase G	Similar to RNase E	Single-stranded	(Wachi et al., 1999)
RNase III	Little sequence specificity	Double-stranded	(Lamontagne and Elela, 2004)
RNase P	Between U47 and G48 in the *tna* operon	Single-stranded	(Li and Altman, 2003)
MazF	3' to the first adenosine residue in ACA sequences or 3' to N residues in NAC sequences (N = A or U).	Single-stranded	(Munoz-Gomez et al., 2004)
PemK	5' or 3' to the adenosine residue in UAH sequences (H= C, A, or U)	Single-stranded	(Zhang et al., 2004)

1.0.2 Messenger RNA turn-over in lower eukaryotes (yeast)

The deadenylation-dependent pathway is best defined in yeast and it appears to be the major mechanism for the regulating of mRNA decay in yeast (Brewer, 1999; Chernokalskaya et al., 1997; Coller and Parker, 2004; Decker and Parker, 1994; Decker and Parker, 2002; Guhaniyogi and Brewer, 2001; Wang and Kiledjian, 2000). This pathway begins with deadenylation of the mRNA by poly(A) nuclease (PAN), followed by decapping of the mRNA by DCP1 (Bremer et al., 2003; Decker and Parker, 2002; Dodson and Shapiro, 2002; Liu et al., 2002; Rodgers et al., 2002; Uchida et al., 2004). The deadenylated and decapped mRNA is then degraded rapidly by the 5' to 3' exonuclease XRN1 (Beelman and Parker, 1995; Bremer et al., 2003; Brewer, 2002; Cunningham et al., 2001; Decker and Parker, 2002; Dodson and Shapiro, 2002; Rodgers et al., 2002; Wilusz et al., 2001). A 3' to 5' exonucleolytic pathway is also observed in yeast. This pathway also depends on the deadenylation and decapping of the mRNA and involves a heteropentameric protein complex (namely, the exosome) consisting of several exonucleases (Brewer, 1999; Brewer, 2002; Decker and Parker, 1994). Although less prominent, the deadenylation-independent mRNA decay pathway is also likely to occur in yeast (Bremer et al., 2003). Endonucleases that have been identified to degrade mRNA in yeast are Rnt1p (Elela et al., 1996) and RNase MRP (Cai et al., 2002) (Table 1.2).

Rnt1p

Rnt1p has been implicated in yeast pre-mRNA processing by cleaving double-stranded regions found within unspliced pre-mRNAs and lariat introns (Danin-Kreiselman et al., 2003). This creates entry sites for the XRN1 or exosomes, which degrade the mRNA body (Danin-Kreiselman et al., 2003). Unlike the sequence non-specific bacterial RNase III, Rnt1p

was found to be sequence-specific as it cleaves double-stranded regions only near 5' NGNN 3' tetra-loops (Lamontagne and Elela, 2004).

RNase MRP

RNase MRP (Mitochondrial RNA Processing) is a ribonucleoprotein that is thought to possess one catalytic RNA subunit and ten protein subunits (Schmitt and Clayton, 1992). This endonuclease has been implicated in mitochondrial rRNA processing and CLB2 (cyclin B gene) mRNA decay (Gill et al., 2004). RNase MRP was found to cleave CLB2 mRNA in the 5' UTR at several yet undefined sites *in vitro*, followed by a rapid XRN1-dependent 5' to 3' exonucleolytic degradation (Gill et al., 2004).

A summary of the cleavage sites and structure specificity of the two yeast endonucleases is shown in Table 1.2. With the purification of these two novel endonucleases, it is becoming clear that endonucleases play an important role in yeast mRNA decay.

Table 1.2. Yeast endonucleases and their cleavage sites.

Name of endonuclease	Cleavage site	RNA Structure specificity of the endonuclease	References
Rnt1p	In proximity to 5' NGNN 3' tetra-loops (N= any nucleotide)	Double-stranded	(Lamontagne and Elela, 2004)
RNase MRP	5' UTR of CLB2 mRNA	Not known	(Gill et al., 2004)

Other means of post-transcriptional regulation of mRNA in yeast includes RNA-interference (RNAi) (Lingel and Izaurralde, 2004; Vermeulen et al., 2005), Non-sense Mediated Decay (NMD) and Non-Stop mediated Decay (NSD) (Baker and Condon, 2004). RNA interference involves the reliance on two main endoribonucleases, which include the Dicer and Argonaute2 proteins. The structure and sequence specificity of these proteins to RNAs will be discussed in section 1.2.1.

Non-sense mediated decay involves the removal of mRNAs containing a premature termination codon (PTC) (Culbertson and Neeno-Eckwall, 2005; Huang et al., 2004). This pathway involves deadenylation-independent decapping, followed by 5' to 3' degradation of the mRNA, which occurs due to the recognition of PTCs (Cougot et al., 2004; Gatfield and Izaurralde, 2004; Stevens et al., 2002). Although a minor pathway, a 3' to 5' exonucleolytic degradation of mRNAs containing PTCs is also thought to occur by exosome degradation (Butler, 2002; Cougot et al., 2004; Gatfield and Izaurralde, 2004; Mitchell and Tollervey, 2000). Exosomes have also been implicated in NSD, which involves the recognition and removal of mRNAs lacking a proper stop codon (Cougot et al., 2004).

1.1 The cellular-*myc* (c-*myc*) gene

c-*myc* is a member of the *myc* gene family, which includes N-*myc,* L-*myc,* B-*myc,* and R-*myc* (Hodgson SV, 1993). All of these members are characterized by their function as transcription factors (Facchini and Penn, 1998; Gardner L, 2002; Hodgson SV, 1993; McAllister RM, 1993; Supino et al., 2001). c-*myc,* however, was found to be the only transcription factor involved in the normal cell growth. It is overexpressed in 80% of breast cancers, 70% of colon cancers, 90% of gynecological cancers, and 50% of hepatocellular carcinomas and many hematological tumors (Gardner L, 2002). Based on these findings, it is estimated that c-*myc* overexpression contributes to the death of approximately 100,000 U.S cancer patients per year which represents 14.3% of all cancer deaths (Gardner L, 2002). These findings underscore the importance of studying this proto-oncogene.

1.1.1 The c-Myc protein and its role in the normal cell and in cancer

c-*myc* structure and function

The c-Myc protein consists of an N-terminal transactivating domain, a nuclear localization signal in the middle domain, and a C-terminal DNA-binding domain (Facchini and Penn, 1998; Gardner L, 2002). The C-terminal domain contains the dimerization motif, which is required for the formation of a heterodimer with a protein called Myc-associated factor X or Max (Facchini and Penn, 1998; Gardner L, 2002). Such dimerization has been shown to be a prerequisite for the function of c-Myc as a transcription factor (Sommer et al., 1998). In addition to Max, c-Myc can be regulated by other proteins which can either induce or inhibit its activity (Facchini and Penn, 1998; Gardner L, 2002). As a transcription factor, it can act as an activator or repressor to regulate a variety of genes such as those involved in gene expression and cell-cycle control (Facchini and Penn, 1998; Gardner L, 2002).

Over the last decade, great progress has been made in understanding the role of c-Myc in both normal and cancer cells (Gardner L, 2002). This intense effort has revealed that c-Myc is implicated in such cellular processes as the cell-cycle, apoptosis, and differentiation (Facchini et al., 1997; Facchini and Penn, 1998; Gardner L, 2002; Henriksson and Luscher, 1996; Levens, 2003; McEwan et al., 1996). In the normal cell, c-*myc* is tightly regulated. This regulation is dependent on external signals such as growth factors and extracellular matrix contacts, as well as internal signals stemming from the cell-cycle (Gardner L, 2002). Normally, the resting cell has little c-*myc* expression, however, upon stimulation by growth factors, c-*myc* expression is induced and a burst of c-*myc* mRNA and protein can be observed (Campisi et al., 1984; Kelly et al., 1983; Moore et al., 1987). This expression declines, but

remains constant throughout the cell-cycle until the generation of the resultant resting daughter cells (Campisi et al., 1984; Kelly et al., 1983; Moore et al., 1987).

Regulation of c-*myc* gene expression

In order for c-*myc* to appropriately respond to internal and external signals (hence promoting normal cellular growth), its activity must be regulated rapidly and efficiently. This regulation is achieved by a wide variety of intricate mechanisms. These mechanisms include regulation at the transcriptional, post-transcriptional, and post-translational levels (Facchini and Penn, 1998). Transcriptional level regulation is thought to be mediated by environmental signals activating the signal transduction pathway, which then exert their effects on the several regulatory elements of the c-*myc* gene (Facchini and Penn, 1998). Transcription of c-*myc* can also be regulated by negative feedback autoregulation as demonstrated in *in vivo* studies (Grignani et al., 1990; Penn et al., 1990). This type of regulation involves the binding of the Myc-Max heterodimer to the regulatory elements leading to the suppression of c-*myc* gene transcription (Facchini et al., 1997; Facchini and Penn, 1998). Regulation at the post-transcriptional level has been intensely studied recently and may involve the activity of exonucleases and/or endonucleases (Brewer, 2002; Guhaniyogi and Brewer, 2001). This type of regulation will be discussed in section 1.1.2. Finally, post-translational regulation involves protein phosphorylation and the protein-protein interactions (Facchini and Penn, 1998).

In contrast to the tight regulation observed in normal cells, c-Myc-induced cancers exhibit abnormal or, more specifically, constitutive expression of c-*myc* (Facchini et al., 1997; Facchini and Penn, 1998). This results from the breakdown of one or more of the regulatory mechanisms described earlier (Facchini et al., 1994). As a consequence, the function of c-Myc is exaggerated, leading to a constant progression through the cell-cycle

and therefore contributing to the conversion of normal cells into cancer cells (Facchini et al., 1997; Facchini and Penn, 1998). Although the oncogenic activity of c-Myc, alone, is a strong promoter of cellular proliferation, additional cooperating oncogenic mutations are required for the transformation to a malignant phenotype, hence, supporting the characteristic multi-step process of carcinogenesis (Facchini and Penn, 1998; Tannock IF, 1998).

The activation of c-*myc*, or its conversion from a proto-oncogene to an oncogene, occurs via several gross genetic aberrations including chromosomal translocation/rearrangement, gene amplification, proviral insertion, and mRNA stabilization (Marcu et al., 1992; Spencer and Groudine, 1991). The best known example to illustrate the chromosomal translocation aberration involves Burkitt's lymphoma. This type of cancer involves the juxtapositioning of the c-*myc* locus near the regulatory region of the IgG heavy chain in B-cells (Spencer and Groudine, 1991). The IgG regulatory region is highly active in lymphocytes as it is constantly responding to antigens and consequently producing antibodies (Facchini et al., 1997; Gardner L, 2002). The result is a 10-20 fold overexpression of the c-*myc* gene (Facchini and Penn, 1998).

Gene amplification involves an increase in the copy number of c-*myc*, resulting in an exaggeration of c-Myc's activity (Gardner L, 2002). The first proto-oncogene observed to be amplified was in fact the c-*myc* amplification in patients with myelocytic leukemia. These cancer cells contained 8-30 copies of the c-*myc* gene (Facchini and Penn, 1998). Another example of gene amplification includes SCLC (small cell lung cancer) cell lines, which contain 50 copies of the c-*myc* gene per cell (Catapano et al., 2000; Gardner L, 2002).

c-*myc* induced cancers due to retroviral insertion involves the insertion of regulatory regions near c-*myc*, leading to its activation (Tannock IF, 1998). It may also involve the

insertion of retroviral sequences in the c-*myc* coding region, leading to the formation of an abnormal and constitutive c-*myc* protein (Tannock IF, 1998). The role of mRNA stabilization in the overexpression of c-*myc* mRNA in human cancers is currently under investigation. It is thought to involve protein shielding of destabilizing regions from endonucleases that infer mRNA instability. An example includes the stability of c-*myc* mRNA in liver cancer (Lee et al., 1998a).

1.1.2 Pathways of c-*myc* mRNA degradation and *in vivo* evidence for post-transcriptional regulation of c-*myc* mRNA

One pathway in which the short half-life of c-*myc* mRNA is regulated includes the deadenylation-dependent pathway (Brewer, 1998; Brewer, 1999). This pathway has been shown to occur *in vivo*, where a sequential decay pathway involving deadenylation, followed by 3' to 5' degradation of the mRNA was observed (Brewer, 1998; Brewer, 1999) in the AU-rich element within the 3' UTR (Bremer et al., 2003; Brewer, 1999; Doyle et al., 2000). A 3' to 5' exonuclease that cleaves c-*myc* mRNA, *in vitro*, within an AU-rich region of the 3'UTR has been purified (Brewer and Ross, 1988). However, it is still not known if this exonuclease is the one observed *in vivo* (Brewer, 1999).

In addition to the 3' to 5' exonucleolytic cleavage, c-*myc* mRNA can be degraded endonucleolytically by the RasGAP-associated G3BP (Tourriere et al., 2001) , an RNase E-like endonuclease (Wennborg et al., 1995), and ~39 kDa endonuclease (Lee et al., 1998b) (see section 1.2.1). Both the RasGap-associated G3BP and the RNase E-like endonucleases are associated with ribosomes and cleave AU-rich elements within the 3'-UTR of c-*myc* mRNA *in vitro* (Tourriere et al., 2001; Wennborg et al., 1995).

In addition to the 3'-UTR, c-*myc* mRNA can be cleaved endonucleolytically within its coding region (Doyle et al., 2000; Guhaniyogi and Brewer, 2001; Hanson and

Schoenberg, 2001; Pistoi et al., 1996). The implicated endonuclease is a ~39 kDa protein which requires magnesium for activity (Lee et al., 1998b). Studies done *in vitro* revealed that this endonuclease cleaves within the coding region determinant (CRD), which encompasses the last 182 nucleotides of the protein coding sequence (Figure 1.1). Although *in vivo* cleavage of the CRD by this endonuclease is not yet known, there is evidence implicating the CRD in c-*myc* mRNA stability. Upon insertion of the c-*myc* CRD into the coding region of the stable globin mRNA, the globin mRNA was rendered unstable in cells (Herrick and Ross, 1994). Furthermore, deletion of both the 5' and 3' UTRs of c-*myc* mRNA did not alter the half-life of the mRNA in cells, supporting the involvement of the coding region in c-*myc* mRNA instability (Bonnieu et al., 1990; Lachman et al., 1986). Finally, post-transcriptional down-regulation of c-*myc* mRNA, upon the conversion of myoblasts to myotubes, required the CRD (Kren et al., 1996; Lee et al., 1998b; Wisdom and Lee, 1990; Wisdom and Lee, 1991; Yeilding et al., 1998). Down-regulation of the mRNA does not occur upon deletion of the CRD (Wisdom and Lee, 1990; Yeilding et al., 1998). This evidence, along with the finding that c-*myc* mRNA can be degraded endonucleolytically in cells, as evidenced by the presence of CRD decay products, (Hanson and Schoenberg, 2001; Pistoi et al., 1996) highlights the importance of finding the endonuclease that can cleave within the CRD of the c-*myc* mRNA.

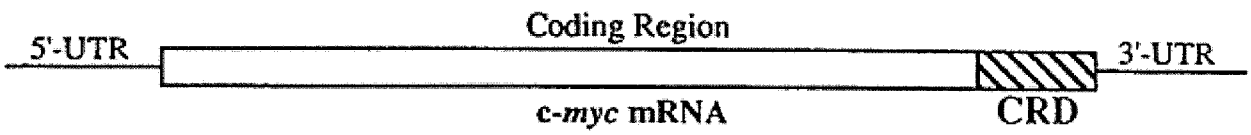

Figure 1.1 A schematic representation of the *c-myc* mRNA. The coding region determinant (CRD) is implicated in the regulation of c-*myc* mRNA turnover by the 39 kDa endonuclease.

The CRD is also the binding site for an RNA-binding protein. Based on *in vitro* experiments, a protein that binds with considerable specificity to sequences located in the CRD RNA has been identified and is termed the CRD-binding protein or CRD-BP (Bernstein et al., 1992; Lee et al., 1998b; Prokipcak et al., 1994). The binding of CRD-BP to the CRD region indicates a potential role for this protein in regulating c-*myc* mRNA decay. CRD-BP is thought to protect the CRD of c-*myc* mRNA from endonucleolytic attack (Bernstein et al., 1992; Doyle et al., 2000; Lee et al., 1998b; Prokipcak et al., 1994). However, this hypothesis is yet to be tested either *in vitro* or *in vivo*. An antisense oligonucleotide targeting the 1763-1777 CRD region (5' AGCCACAGCAUACAU 3') was found to be the most effective in inhibiting c-*myc* expression, suggesting that this region is an important binding site for CRD-BP (Coulis et al., 2000).

1.2 Overview of messenger RNA turn-over in higher eukaryotes

The deadenylation-dependent and deadenylation-independent pathways have been demonstrated in mammals. However, the details by which most mammalian mRNAs are degraded are not well-understood (Brewer, 1999; Brewer, 2002; Ross, 1995). It has been hypothesized that many mammalian mRNAs are degraded by a deadenylation-dependent mechanism *in vivo* (Dodson and Shapiro, 2002; Ross, 1995; Wilusz et al., 2001). This involves the initial rate-limiting step of a 3' to 5' exonucleolytic removal of the poly(A) tail by poly(A) ribonucleases. (Cunningham et al., 2001; Decker and Parker, 2002; Dodson and Shapiro, 2002; Uchida et al., 2004). Recently, a human cytoplasmic poly(A) ribonuclease deadenylase was identified and it was termed human PABP-dependent poly(A) nuclease (hPAN) (Uchida et al., 2004). It is a magnesium-dependent 3' to 5' exonuclease, that is stimulated to degrade the mRNA by binding to the Poly(A) binding protein (PABP) *in vivo*

(Uchida et al., 2004). Another deadenlyase was found in vertebrates and it was termed PARN (polyA ribonuclease) (Korner and Wahle, 1997). Unlike hPAN, PARN is stimulated to cleave the mRNA by binding to the 5' cap structure (Decker and Parker, 2002; Korner and Wahle, 1997). After deadenylation, subsequent decay steps, which involve the mRNA body, generally occur so quickly that decay intermediates are not detected, hence, hampering further analysis of the decay pathways (Brewer, 1999). Nonetheless, recent evidence implicates mammalian mRNA involvement in the 5' to 3' and 3' to 5' exonucleolytic decay pathways.

Evidence for 5' to 3' exonucleolytic degradation

The implication that mammalian mRNAs can be degraded in a 5' to 3' deadenylation-dependent pathway similar to the one in yeast, is based on three main findings. The first finding includes the identification of the poly(A) ribonucleases mentioned previously. The other two findings involve the discovery of XRN1 and DCP1 mammalian homologues (Bashkirov et al., 1997; Cunningham et al., 2001; Dodson and Shapiro, 2002; Ross, 1995). The human decapping enzyme, DCP1, and the 5' to 3' exonuclease, XRN1, were found to co-localize in cytoplasmic foci termed, GW (because they contain a protein that is highly abundant with glycine and tryptophan amino acids) bodies, which represent sites of active mRNA degradation (Cougot et al., 2004).

Evidence for 3' to 5' exonucleolytic degradation

In addition to the 5' to 3' deadenylation-dependent pathway, a 3' to 5' deadenylation-dependent pathway is also thought to regulate mammalian mRNA decay (Coburn and Mackie, 1999; Cunningham et al., 2001; Hanson and Schoenberg, 2001; Liu et al., 2002). This is evident from two observations, which include the discovery of an exosome

homologue in *HeLa* cell lines (Mitchell et al., 1997) and the 3' to 5' exonucleolytic decay of the H4 human histone mRNA (Ross et al., 1986). The mammalian exosome has been purified and its composition appears to be similar to its yeast counterpart (Chen et al., 2001).

Evidence for endonucleolytic degradation

The deadenylation-independent pathway is also thought to regulate mammalian mRNA turn-over (Cunningham et al., 2001; Grunberg-Manago, 1999; Hanson and Schoenberg, 2001). This is determined mainly through the identification of endonucleolytic cleavage sites in many mammalian mRNAs (Caruccio and Ross, 1994; Dodson and Shapiro, 2002). The identity and properties of mammalian endonucleases that target specific mRNAs for decay under normal physiological condition remain elusive, as only few mammalian mRNA endonucleases have been purified and subsequently characterized (Table 1.3) (Caruccio and Ross, 1994; Claverie-Martin et al., 1997; Dodson and Shapiro, 2002). The search for mammalian endonucleases is essential for understanding the post-transcriptional control of mammalian gene expression (Brewer and Ross, 1988; Wennborg et al., 1995). Endoribonucleolytic digestion is responsible for the decay of several vertebrate mRNAs including those for albumin (Cunningham et al., 2001), human transferrin receptor (Binder et al., 1994), insulin-like growth factor II (Meinsma et al., 1992), chicken apolipoprotein II (Binder et al., 1989), human α–globin (Wang and Kiledjian, 2000), human β-globin (Stevens et al., 2002), human c-*myc* (Lee et al., 1998b), *Xenopus* vitellogenin (Cunningham et al., 2000), $p27^{KIP1}$ (Zhao et al., 2000) and interleukin II (Hua et al., 1993). The cleavage specificity of the endonucleases for these mRNAs is discussed in section 1.2.1.

Stress-regulated pathways for mRNA degradation

Post-transcriptional regulation also plays a role in mammalian cellular processes such as RNAi, NMD, and NSD. Similar to yeast, RNAi in mammals relies on the Dicer and Argonaute2 proteins (Liu et al., 2004; Vermeulen et al., 2005) (see section 1.2.1). The NMD pathway in mammals is also thought to be similar to the one in yeast and is believed to occur via the 5' to 3' (involving decapping and 5' to 3' exonucleolytic digestion) or the 3' to 5' (deadenylation followed by 3' to 5' degradation) degradation pathways (Chen and Shyu, 2003; Lejeune et al., 2003). The exonucleolytic enzymes involved in the NMD pathway are thought to be the same enzymes responsible for the degradation of normal mRNAs (XRN1 and the exosome) (Lejeune et al., 2003). In contrast, the NMD pathway in *Drosophila* was found to rely on endonucleolytic cleavage near the premature termination codon of the aberrant mRNA rather than the deadenylation-dependant pathway (Gatfield and Izaurralde, 2004). This pathway is thought to involve the rate-limiting step of endonucleolytic cleavage, followed by 5' to 3' degradation of the 3' fragment by XRN1 and 3' to 5' degradation of the 5' fragment by the exosome (Gatfield and Izaurralde, 2004). The endonuclease responsible for mediating the NMD pathway in *Drosophila* has yet to be identified.

Mammalian mRNAs containing non-stop codons are degraded by the NSD pathway (Frischmeyer et al., 2002; van Hoof et al., 2002). This pathway is thought to be mediated by deadenylation, followed by 3' to 5' degradation of the mRNA body by the exosome (Frischmeyer et al., 2002; van Hoof et al., 2002).

mRNA-binding proteins

mRNA-binding proteins are also thought to be implicated in mammalian post-transcriptional mRNA decay by binding to *cis*-elements within the mRNA. Proteins, such as

tristetraprolin (Lai et al., 2002), KSRP (Chen et al., 2001), TIA –1 (Piecyk et al., 2000) and TIAR (Piecyk et al., 2000; Wilusz et al., 2001), have been implicated in mRNA destabilization. The destabilizing function is thought to mediated through the recruitment of an exosome that degrades the mRNA in a 3' to 5' direction (Brewer, 2002). In contrast, mRNA-binding proteins such as HuC (Ma et al., 1997), HuD (Manohar et al., 2002), HuR (Ma et al., 1996), CRD-BP (Bernstein et al., 1992), α-CP (Ji et al., 2003; Kong et al., 2003), vigilin (Cunningham et al., 2000), and La antigen (Heise et al., 2001) are thought to mediate mRNA stabilization by shielding the mRNA from endonucleolytic attack (Brewer, 2002). The AUF1 mRNA-binding protein is thought to mediate both mRNA stabilization and destabilization, depending on cell-types (Loflin et al., 1999; Xu et al., 2001).

1.2.1 Endoribonucleases that degrade mRNAs in vertebrates

Although less well-studied, endonuclease-mediated mRNA decay appears to be more common than previously expected. A summary of the characterized endonucleases and their cleavage sites is shown in Table 1.3. The following is a more detailed insight into the vertebrate endonucleases that have been characterized.

PMR-1

Polysomal Ribonuclease 1 (PMR-1) is a member of the peroxidase gene family and is the most extensively studied mRNA endoribonuclease in vertebrates (Cunningham et al., 2001; Stevens et al., 2002; Yang and Schoenberg, 2004). It is a 62 kDa liver polysomal endoribonuclease that is activated by estrogen to degrade polysomal-associated serum protein mRNAs such albumin mRNA (Yang and Schoenberg, 2004). Degradation occurs in the 3'UTR of albumin mRNA upon estrogen induction of *Xenopus* hepatocytes *in vivo* (Cunningham et al., 2001; Stevens et al., 2002; Yang and Schoenberg, 2004). PMR-1 is also

thought to degrade vitellogenin mRNA in the 3' UTR *in vitro* and *in vivo* (Cunningham et al., 2000). Upon estrogen stimulation, however, the 3'UTR of vitellogenin mRNA is thought to be shielded from PMR-1-induced degradation by the RNA-binding protein, vigilin (Cunningham et al., 2000; Stevens et al., 2002). PMR-1 preferentially cleaves UG dinucleotides (3' to the uridine residue) present in ApyrUGA elements both *in vitro* and *in vivo* (where pyr can be either a C or U residue) (Bremer et al., 2003; Hanson and Schoenberg, 2001) in single-stranded regions only (Hanson and Schoenberg, 2001). PMR-1, however, is not thought of as a restriction endonuclease in that non-consensus sequences can also be cleaved (Hanson and Schoenberg, 2001). The N-terminal domain of PMR-1 is thought to be important for endonucleolytic degradation of substrates (Yang and Schoenberg, 2004). In particular, it is believed that one or more tyrosines in the N-terminal domain play a role in the endonucleolytic degradation of albumin mRNA (Yang and Schoenberg, 2004).

A ~26 kDa endonuclease that cleaves Hepatitis B viral RNA

This endonuclease is a 26 kDa cytokine-activated endoribonuclease that was purified from liver nuclear extracts (Heise et al., 2001). Upon HBV infection, cytokines such as IFN-γ and TNF-α become up-regulated and an enhanced activity of the endoribonuclease is observed (Heise et al., 2001). Such activation may be due to translational modification, or the inactivation of an inhibitor (Heise et al., 2001). Up-regulation of the cytokines also leads to the decrease of the RNA binding protein, La antigen, which may act to sterically hinder the endonuclease from accessing the cleavage site (Heise et al., 2001). Upon incubation of the endonuclease with a viral RNA transcript encompassing nucleotides 1243-1333, it preferentially cleaved 3' to the two adenosine residues in the 5'-CCAUACU-3' motif located 5' to a stem-loop structure, which is also binding site for the La antigen (Heise et al.,

2001). Despite this knowledge, it is currently not known whether surrounding sequences or structural features play a role in the recognition of the site cleaved by the endoribonuclease, whose identity remains unknown (Heise et al., 2001).

RNase L

RNase L is an endonuclease that also relies on hormonal activation. It is 740 kDa endoribonuclease that targets viral RNAs for degradation (Silverman, 2003) and is believed to play a role in defense against viral RNA upon interferon activation (Li et al., 2000). RNase L preferentially cleaves at single-stranded UA and UU dinucleotides (Han et al., 2004; Mishra, 2002), causing the mammalian infected cells to undergo apoptosis (Pandey and Rath, 2004). The endonucleolytic domain of RNase L is found in the C-terminal region (Silverman, 2003). This region is also thought to be a kinase-like domain, based on sequence homology studies (Mishra, 2002; Silverman, 2003).

RasGap-associated G3BP

RasGAP-associated G3BP is a 52 kDa endonuclease that was found to cleave within the 3'UTR of c-*myc* mRNA *in vitro* (Barnes et al., 2002; Guitard et al., 2001; Tourriere et al., 2001). This endonuclease is unique in that it requires phosphorylation (Tourriere et al., 2001) and phosphorylation-dependent protein-protein interaction to regulate its activity in c-*myc* mRNA degradation (Irvine et al., 2004). G3BP prefers to cleave 3' to cytidine residues in CA dinucleotides only when present in single-stranded regions (Tourriere et al., 2001). Recent evidence indicate the importance of G3BP *in vivo,* as inactivation of the G3BP-encoding gene in animal models led to embryonic lethality and growth retardation (Zekri et al., 2005). The endonucleolytic domain of G3BP has yet to be identified as it has no sequence homology with any other known proteins.

A ~65 kDa RNase E-like endonuclease that cleaves c-*myc* mRNA

Another enzyme implicated in c-*myc* mRNA cleavage includes the RNase E-like endonuclease. This enzyme is 65 kDa in size and was purified from different human cell-lines (Wennborg et al., 1995). Similar to bacterial RNase E, it cleaves *E.coli* 9S RNA and outer membrane protein RNA (*omp*A). It preferentially cleaves 3' to the 2nd U residue in the 5'AUUUA 3' destabilizing motif present in the 3' UTR (Wennborg et al., 1995). This enzyme was also found to cleave c-*myc* mRNA within the 5' AUUUA 3' motif that is present in the 3' UTR (Wennborg et al., 1995). This endonuclease, whose identity is yet unknown, was found to cross-react with antibodies against bacterial RNase E (Wennborg et al., 1995).

A ~39 kDa endonuclease that cleaves c-*myc* mRNA

A ~39 kDa liver polysomal endonuclease that was purified from rat livers, has been found to cleave within the CRD of c-*myc* mRNA *in vitro* (Lee et al., 1998b). This enzyme is magnesium-dependent and is not inhibited by RNase A class inhibitors such as RNasin (Lee et al., 1998b). Major cleavage occurs at two sites in the first 88 nucleotides of the A-rich region, 5'-CAAUGAAAAG-3', which corresponds to nucleotides 1727 to 1736 (Lee et al., 1998b). The identity of this endonuclease remains unknown.

Dicer

Dicer is a 218 kDa RNase III orthologue (Parker et al., 2004; Provost et al., 2002) implicated in RNAi and miRNA function, and is thought to be activated upon infection with viruses containing double-stranded RNAs (Rand et al., 2004; Zhang et al., 2004). In an *in vitro* setting, Dicer attacks the ends of double-stranded RNA with no sequence specificity into small interfering RNAs of ~21 nucleotides and excises miRNAs that act to promote

RNA interference (Doi et al., 2003; Fortin et al., 2002; Nicholson and Nicholson, 2002; Provost et al., 2002; Rand et al., 2004; Zhang et al., 2004).

Argonaute2

Argonaute2 is a component of RISC that recognizes and cleaves mRNAs that are complementary to the siRNAs (Hutvagner and Zamore, 2002; Schwarz et al., 2002). This protein is thought to be ~40 kDa in size due to the presence of the ~20 kDa PAZ domain and ~20 kDa PIWI domain (Liu et al., 2004; Parker et al., 2004). The PIWI domain, which is located in the C-terminal is thought to contain the endonucleolytic domain, based solely on structural similarity of this region with RNase H (Parker et al., 2004).

An endonuclease that cleaves β-globin mRNA

A polysomal endoribonuclease has been purified from mouse erythroleukemia cells and is thought to cleave normal β-globin (Stevens et al., 2002). In addition, the polysomal endonuclease is also believed to be activated by the presence of a premature termination codon to cleave aberrant mRNAs (Stevens et al., 2002). It preferentially cleaves single-stranded UG (3' to uridines) dinucleotides and to some extent UC (3' to uridines) sites (Stevens et al., 2002). These sites were also found to be cleaved *in vivo* using S1 nuclease mapping and primer extension (Stevens et al., 2002). The size and identity of this endonuclease are not known.

ErEN

ErEN is a ~ 40 kDa endonuclease that is part of a multiprotein complex (~ 160 kDa) and functions to cleave within the 3' UTR region of α-globin mRNA (Rodgers et al., 2002; Wang and Kiledjian, 2000). It preferentially cleaves at nucleotide 63 (3' to the cytidine residue in the CU dinucleotide) in the CU-rich element (Rodgers et al., 2002). It is not known, however,

whether the cleaved dinucleotide is present in a single-stranded or a double-stranded region. The cleavage products were detected both *in vitro* and *in vivo* (Wang and Kiledjian, 2000).

It has been shown, *in vitro*, that α-globin mRNA becomes shielded from endonucleolytic degradation upon the binding of a protein complex, termed the alpha complex (α-CP), to the 3'UTR (Rodgers et al., 2002; Wang and Kiledjian, 2000). It is also thought that the binding of the poly(A) binding protein to the poly(A) tail inhibits cleavage by ErEN (Rodgers et al., 2002; Wang and Kiledjian, 2000). The precise identity of this endonuclease remains unknown.

An endonuclease that cleaves Tfr mRNA

A single-strand RNA specific endoribonuclease is thought to cleave within the 3' UTR of the human transferrin receptor (Tfr) mRNA, more specifically, 3' to the first guanosine residue within the 5' GAACAAG 3' motif (Binder et al., 1994). This enzyme is thought to be regulated by iron levels in the cytoplasm (Posch et al., 1999). When iron is scarce, a binding protein termed the Iron-Responsive Element Binding Protein (IREBP) binds to the iron-responsive element (IRE) in the 3' UTR (Binder et al., 1994). However, when iron is abundant, the IREBP is displaced and the Tfr mRNA is cleaved within the 3' UTR of the IRE (Binder et al., 1994; Rodgers et al., 2002). The size and identity of this endonuclease are not known.

An endonuclease that cleaves IGFII mRNA

Another single-strand RNA-specific endonuclease includes the enzyme that was found to cleave within the 3' UTR of the Insulin Growth Factor II (IGFII) mRNA (Meinsma et al., 1992; van Dijk et al., 1998; van Dijk et al., 2001). This endonuclease cleaves within purine-rich regions located between a putative hairpin structure and a guanosine-rich sequence

(Nielsen and Christiansen, 1992). It is also thought that an RNA binding protein termed the IGFII Cleavage Unit Binding Protein (ICU-BP) interacts with the stem structure to shield IGFII mRNA from endonucleolytic cleavage (Scheper et al., 1996). The size and identity of this endonuclease remain unknown.

A ~ 120 kDa endonuclease that cleaves Xlhbox2B mRNA

A ~ 120 kDa endonuclease purified from *Xenopus* oocytes was found to cleave the *Xenopus* homeobox mRNA, Xlhbox2B, with the same specificity both *in vitro* and *in vivo* (Brown and Harland, 1990). The site of this cleavage is between the coding region and a 600 nt region in the 3' UTR (Brown and Harland, 1990), and is also the site of RNA binding proteins that act to shield the mRNA from endonucleolytic attack (Rodgers et al., 2002). The identity of this endonuclease remains unknown.

An endonuclease that cleaves $p27^{KIP1}$ mRNA

The mRNA of the cell-cycle regulator, $p27^{KIP1}$, is thought to be cleaved endonucleolytically 3' to the uridine residue (in bold) within the U-rich element, 5'-GUUUUGUUUUUUUU-3' present in the 3'UTR (structure specificity of the enzyme is not yet unknown) (Zhao et al., 2000). This U-rich element is also the binding site of HuR, which is an mRNA-binding protein implicated in the stability of many mRNAs (Brennan and Steitz, 2001; Zhao et al., 2000). The size and identity of this endonuclease remain unknown.

ARD-1

The activator of RNA decay, ARD-1 is a cDNA encoded by human cells whose endoribonucleolytic activity was found to be similar to *E.coli* RNase E (similar cleavage sites) (Claverie-Martin et al., 1997). It was found to be 13.3 kDa in size and cleaves single-

stranded regions only within AU rich elements (Claverie-Martin et al., 1997). This endonuclease has sequence homology to RNase E (Claverie-Martin et al., 1997).

An endonuclease that cleaves apolipoprotein II mRNA

An endonuclease has been purified from chicken liver and is thought to cleave within the 3' UTR of the apolipoprotein II mRNA (Binder et al., 1989; Hua et al., 1993). More specifically, it preferentially cleaves 3' to any adenosine or uridine within single-stranded 5'-AAU-3' and 5'-UAA-3' elements present in the 3' UTR (Binder et al., 1989; Hua et al., 1993). The size and identity of this endonuclease are not known.

A 60-70 kDa endonuclease that cleaves interleukin II mRNA

An RNasin-resistant 60-70 kDa endonuclease purified from the cytoplasm of T lymphocytes was found to cleave interleukin II mRNA (Hua et al., 1993). This cleavage occurred within the 5'UUAUUUAU 3' motif present in the coding region (structure specificity and exact sequence cleaved is not known) (Hua et al., 1993). The identity of this endonuclease remains unknown

Table 1.3. Vertebrate mRNA-endonucleases and their cleavage sites.

mRNA	Cleavage site	Name of endonuclease	Putative binding protein	mRNA-specificity of binding-proteins
Albumin	Single-stranded 5' ApyrUGA-3' (3' to uridine residue in bold) ; 3'-UTR	PMR-1	-	-
Vitellogenin	Single-stranded ApyrUGA (3' to uridine residue in bold); 3'-UTR	PMR-1	Vigilin	3'UTR containing the 2 cleaved ApyrUGA sequences (Cunningham et al., 2000)
c-*myc*	Single-stranded , 5'CA 3' dinucleotides	RasGAP-associated G3BP	-	-
c-*myc*	5' CAAUGAAA 3'; coding region (A-rich-region)	_	CRD-BP	CRD region (nucleotides 1705-1786) (Prokipcak et al., 1994)
c-*myc*	Single-stranded 5'-AUUUA-3' in 3'UTR	RNase E-like endonuclease	-	-
Complementary mRNA to siRNA	-	Argonaute2	-	-
β-globin mRNA	Single-stranded 5' UG 3' and 5' UC 3'; 3'UTR	-	-	-
α-Globin	5' CC**C**UCCUUCCACC 3' (cleaves 3' to the C residue in bold)'; 3'-UTR	ErEN	αCP	5'CCGAUGGGCCUCCCAACGGGCCCUCCUCCC **C**UCCUUGCACC3'; 3'UTR (Wang and Kiledjian, 2000).
Tfr	Single-stranded , 5' **G**AACAAG 3' (cleaves 3' to the guanosine residue in bold); 3'-UTR	-	IREBP	Stem-loops B and E (near cleavage site); 3' UTR (Koeller et al., 1989)
IGF II	Single-stranded; Adjacent to G-rich sequence and duplex structure ; 3' UTR	-	ICU-BP	Elements I and II; 3'UTR (element II contains cleavage site) (Scheper et al., 1996).
Xlbbox2R	5' CACCCUACCUACCCAACUA 3'	-	Endonuclease inhibitor	Not identified
HBV RNA	Single-stranded 5' CC**A**U**A**CU 3' (3' to adenosines in bold)	-	La antigen	Stem-loop 2 (nts 1272-1295) containing the last 3 nucleotides of the consensus cleavage site (5'ACU 3') (Heise et al., 1999a; Heise et al., 1999b)
$P27^{kip1}$	5'GUU**U**UGUUUUUUU 3' (3' to the uridine residue in bold); 3'UTR	-	HuR	U-rich element in 3' UTR containing cleavage sites (Zhao et al., 2000)
Viral RNA	Single-stranded 5' UA 3' and 5'UU 3'	RNase L	-	-
Viral RNA	Double-strand RNA	Dicer	-	-
-	Single-stranded AU rich regions	ARD-1	-	-
Apolipoprotein II	Single-stranded 5'-UAA-3' and 5'AUU-3' trinucleotides; 3'-UTR	-	-	-
Il-2	5' UUAUUUAU 3', coding region	-	-	-

1.3 A novel mammalian endoribonuclease that was identified based on its ability to cleave a specific coding region of c-*myc* RNA *in vitro*

1.3.1 Significance of this endoribonuclease

During the development of an improved purification strategy to purify the ~39 kDa endonuclease that cleaves the c-*myc* CRD RNA (Lee et al., 1998b), another novel endoribonuclease comprising of five polypeptides was accidentally discovered (Bergstrom et al., in press). The purpose of this project is to characterize the sequence/structure cleavage specificity of this mammalian endoribonuclease to the 1705-1792 c-*myc* CRD region.

In rodent livers, c-*myc* mRNA levels increase transiently following partial hepatoectomy and then decrease as liver regeneration is completed (Kren et al., 1996). These fluctuations in mRNA levels were determined to be independent of the c-*myc* gene promoter, but rather relied heavily on a c-*myc* mRNA *cis*-element, namely the coding region encompassing the CRD (Morello et al., 1990). The implication of c-*myc* mRNA decay in controlling gene expression in the liver is further supported by the observations that c-*myc* mRNA is cleaved endonucleolytically in cells (Hanson and Schoenberg, 2004; Pistoi et al., 1996), and that it was found to be relatively stable in liver cancer (Lee et al., 1998a). Therefore, the study of an enzyme that has the capability of degrading c-*myc* mRNA has the potential to enhance our knowledge of mammalian mRNA stability and provide insight into how c-*myc* mRNA is post-transcriptionally regulated.

In addition, the significance of understanding and identifying this endonuclease stems from the fact that little, in general, is known about mammalian endonucleases. Knock-out experiments such as the one performed against the RasGap-G3BP and RNase L genes have highlighted the significance and role of endoribonucleases *in vivo*. Vigorous investigations into the role of the endonuclease under study are required. For instance, it is not known if this

endonuclease is stress-regulated, similar to endonucleases such as RNase L, Dicer, PMR-1, and the endonucleases capable of cleaving the Tfr and HBV RNAs. It is also not known if the endonuclease under study is part of a larger protein complex that regulates c-*myc* gene expression. Lastly, further studies on this endonuclease will confirm whether it is distinct from the other endonucleases capable of cleaving c-*myc* mRNA such as RasGAP-associated G3BP, the ~65 kDa RNase-E like enzyme, and the ~39 kDa endonuclease.

1.3.2 The significance of determining RNA secondary structure

There are two essential properties of RNA molecules: first, that they intrinsically form stable secondary structures both *in vivo* and *in vitro*, and second, that secondary structural features play a critical role in regulating several cellular process (Buratti and Baralle, 2004; Klaff et al., 1996). As indicated previously, endonucleases may cleave their target sequences in single-stranded regions only, double-stranded regions only, or in both. Therefore, in order to characterize the sequence and structural specificity of the mammalian endonuclease to the CRD region of c-*myc* mRNA, the secondary structure of the CRD RNA corresponding to nts 1705-1792 of c-*myc* must first be determined.

In addition to mRNA turn-over, RNA secondary structures are thought to be involved in cellular process such as splicing (Buratti and Baralle, 2004), protein-binding (Buratti and Baralle, 2004), translation (Doktycz et al., 1998), and pathogenesis (Buratti and Baralle, 2004). Most chloroplast mRNAs, for example, contain a stem-loop structure in the 3'UTR which renders the mRNA stable by impeding 3' to 5' exonucleases from attacking them (Yang and Stern, 1997). Removal of this stem-loop thus renders the mRNA unstable and decreases its half-life (Yang and Stern, 1997). Secondary structural features are also thought to play a role in the processing of yeast precursor mRNAs (Buratti and Baralle, 2004). In

Saccharomyces cerevisiae, it is thought that secondary structures between the 5' splice site and the branch point are capable of promoting U1snRNP assembly in the early splicing stages (Buratti and Baralle, 2004; Charpentier and Rosbash, 1996). Stem-loops have also been implicated in putative protein-binding. The HuR protein, for example, is involved in mRNA turn-over by binding to specific mRNA subsets and this relies heavily on secondary structural features (Buratti and Baralle, 2004).

mRNA translation is another cellular process which is thought to involve secondary structural features (Doktycz et al., 1998). It is thought that RNA secondary structures 3' to the initiation codon can enhance the efficiency of translation by slowing the initiation-codon scanning mechanism, and that structural features in the 5' UTR strongly inhibit translation (Doktycz et al., 1998). In addition to splicing, secondary structural features have also been implicated in pathogenesis. Mutations in the *tau* gene have been implicated in diseases such as frontotemporal dementia and Parkinson's disease (Buratti and Baralle, 2004). NMR studies have shown that mutations in the intronic region near the 5' splice site of exon 10 of the *tau* gene strongly correlates with an alternate secondary structure (Buratti and Baralle, 2004).

1.4 Objectives

The novel rat liver endonuclease, which consists of five polypeptides, has been purified based on its ability to cleave within the CRD of c-*myc* mRNA *in vitro* (Bergstrom et al., in press). The full-length CRD region corresponds to nts 1705-1886 of the c-*myc* mRNA, whereas the region used to purify the novel endonuclease corresponds to nucleotides 1705-1792 (Figure 1.2). The 1705-1792 CRD RNA was used for the characterization of the novel endonuclease.

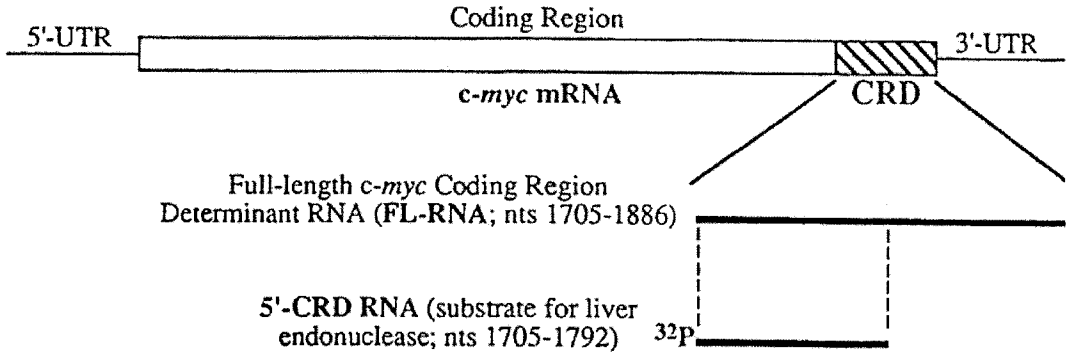

Figure 1.2. A Schematic representation illustrating the full CRD region (1705-1886) and the 1705-1792 CRD region. The 1705-1792 CRD region was used for the study of the sequence and structure cleavage specificity of the novel mammalian endonuclease.

The first aim of this project was to determine the *in vitro* secondary structure of the CRD region spanning nts 1705-1792. Secondary structure determination of the CRD region will allow: (i) determination of whether the enzyme preferentially cleaves its target sequences in single-stranded or double-stranded regions or both, (ii) an understanding of the potential secondary structure of the 1705-1792 CRD region *in vivo*, (iii) an understanding of the potential cleavage specificity of the endonuclease *in vivo*. The second aim of this project was to characterize the sequence/structure cleavage specificity of the novel mammalian endonuclease by generating a series of mutants encompassing nts 1705-1792 of the CRD region. To confirm the sequence and structure specificity of the mammalian endonuclease, β-globin RNA (3018-3159) was randomly chosen as a substrate for this study. Determination of the sequence and structural specificity of the endonuclease to the CRD mutants will: (i) confirm whether the endonuclease is a single-stranded or a double-stranded RNA-cleaving enzyme, (ii) confirm the sequence specificity of the endonuclease to the RNA, (iii) constitute the first step toward understanding the sequence and structural specificity of the endonuclease *in vivo*, (iv) confirm whether the endonuclease is indeed a novel mammalian endonuclease, distinct from other currently known vertebrate endoribonucleases.

Chapter 2

In Vitro Secondary Structure Determination of the 1705-1792 Coding Region Determinant (CRD) Region of the c-*myc* mRNA and the β-globin mRNA Corresponding to Nucleotides 3018-3159.

This chapter aims at determining the secondary structure of the *in vitro*-transcribed 1705-1792 CRD RNA and the RNA corresponding to nts 3018-3159 of β-globin. This is accomplished by using the Mfold software program, in conjunction with RNase probing experiments. Determination of the secondary structure of the 1705-1792 CRD RNA will provide insight into the structure specificity requirement for cleavage by the novel mammalian endonuclease under study. In addition, secondary structure determination of the 3018-3159 β-globin RNA will further confirm the sequence and structure specificity requirement for RNA cleavage by the novel enzyme.

2.0 Methods

2.0.1 Linearization and *in vitro* transcription of the pUC19 and the SPκβc plasmids containing the 1705-1792 CRD DNA insert and nucleotides 3018-3159 of the β–globin DNA, respectively.

The pUC19 plasmid (5 ug) containing the 1705-1792 c-*myc* cDNA (5'-ACCAGATCC CGGAGTTGGAAAACAATGAAAAGGCCCCCAAGGTAGTTATCCTTAAAAAAGCCA CAGCATACATCCTGTCCGTCCAAGC-3') and an SP6 promoter site (5' to the cDNA) was linearized with the restriction enzyme *Eco*R1 (Invitrogen Life Technologies, Carlsbad, CA) in a 20 uL final volume consisting of the following final concentrations: 1 U/uL of *Eco*R1, 1X Reaction Buffer, and made up to volume with sterile water. The digestion was performed at 37^0C for 3 hours. After linearization, 1 uL of the linearized plasmid and 1 uL of the uncut plasmid were run on a 1% agarose gel to check for digestion. The gel was run for about 1.5 hours at 46 mA and was visualized using the ChemiImager^{TM} System (Alpha

Innotech Corporation, San Leandro, CA). The reaction mixture was then made up to 200 uL with sterile water in preparation for the standard phenol/chloroform extraction. This involves adding ½ volume of phenol (100 uL) and ½ volume of chloroform:isoamylalcohol ($CHCl_3$: IAA) (49:1). The solution was mixed thoroughly by repeated inverting and then was centrifuged at 12,000 rpm for 5 minutes. The aqueous layer (top layer) containing the linearized plasmid was carefully extracted and one volume of $CHCl_3$: IAA was subsequently added. The solution was then mixed again by inverting and then centrifuged at 12,000 rpm for five minutes. The top layer was then extracted again and standard ethanol precipitation was performed. Standard ethanol precipitation involves the addition of $1/10^{th}$ volume of 3M sodium acetate (NaAc) pH 5.2, followed by two volumes of 100% ethanol, mixing thoroughly by inverting, and DNA precipitation at -20^0C for at least 15 minutes. The solution was then centrifuged at 12,000 rpm for 10 minutes and the supernatant was then gently poured off. Seventy percent ethanol was then added (200 uL) to the DNA pellet and it was again centrifuged for 5 minutes at 12,000 rpm. The supernatant was then carefully removed and the pellet was allowed to dry at room temperature for 15 minutes. The dried pellet was resuspended in sterile water to a final concentration of 0.2-0.3 ug/uL.

The linearized plasmid (1 ug) was then used as a template for *in vitro* transcription using the MEGAscript SP6 Kit (Ambion, Inc., Austin, Texas). The transcription reaction was performed in a 20 uL final volume containing the following reagents: 1X reaction buffer, 5 mM rNTPs, 8 mM DTT (Invitrogen Life Technologies, Carlsbad, CA), 3 units/µl of RNasin (Promega, Madison, WI), and 2 uL of the SP6 enzyme mix. The *in vitro* transcription reaction was performed at 37^0C for 1.5 hours, followed by the addition of 1 uL DNase I (Ambion, Inc., Austin, Texas) and incubation at 37^0C for 15 minutes. The reaction mixture

was then made up to 200 uL with diethylpyrocarbonate (DEPC) H_20, followed by standard phenol/chloroform extraction and standard ethanol precipitation. The RNA pellet was then resuspended in 50 uL DEPC-H_20 and the unincorporated rNTPs were removed using the ProbeQuant™ G-50 Micro Column (Amersham Biosciences UK Limited, Little Chalfont, Buckinghamshire, England) according to the manufacturer's protocol. To check the quality of the RNA, 1 uL of the RNA sample was added to 5 uL cocktail mix [10 X MOPS (N-morpholino propanesulfonic acid, EDTA, sodium acetate, sterile water, DEPC-H_2O), formaldehyde, formamide, ethidium bromide, and DEPC-H_2O) and 2 uL loading dye, and run on a 1.3% agarose gel (containing formaldehyde) at 50 mA for 1 hour. The RNA was visualized using the ChemiImager™ System.

The SPκβc plasmid (5 μg) containing nucleotides 3018-3159 of the human β-globin DNA (5'ACATTTGCTTCTGACACAACTGTGTTCACTAGCAACCTCAAACAG ACACCATGGTGCACCTGACTCCTGAGGAGAAGTCTGCCGTTACTGCCCTGTGGGC AAGGTGAACGTGGATGAAGTTGGTGGTGAGGCCCTGGGCAG-3') was linearized with the restriction enzyme *Fok*I (New England Biolabs, Beverly, MA) in a 20 uL final volume consisting of the following final concentrations: 1 U/uL of *Fok*I, 1X React 2, and made up to volume with sterile water. The digestion was performed at 37^0C for 3 hours. Subsequent steps were identical to the ones described for the pUC19 plasmid. The *in vitro* transcription reaction was performed using the MEGAscript SP6 Kit (Ambion, Inc., Austin, Texas), identical to the procedure described for the 1705-1792 CRD RNA.

2.0.2 Dephosphorylation, 5'-end labeling, and gel-purification of the 1705-1792 CRD and the 3018-3159 β–globin transcripts.

In order to 5' end-label the transcript with γ^{32}P-ATP, it was necessary to dephosphorylate the 1705-1792 CRD transcript. Dephosphorylation was performed in a 100 uL final volume consisting of the *in vitro* transcribed 1705-1792 CRD RNA (9 ug) and the following reagents, having the final concentrations of: 0.1 U/uL Calf Alkaline Phosphatase (CIAP) (Roche Diagnostic Inc, Mannheim, Germany), 1X dephosphorylation buffer, 0.4 units/µl of RNasin, 5 mM DTT, and made up to 100 uL with DEPC-H_20. The reaction mixture was then incubated for 30 minutes at 37^0C. After making up the volume to 200 uL with DEPC-H_20, the following reagents were added to ensure the dissociation of protein-RNA complexes and the denaturing of ribonucleases (Boyer, 1992): 1 uL of 0.5M EDTA pH 8, 4 uL of 5 M NaCl, and 10 uL of 20% SDS. The standard chloroform/phenol extraction was then performed, followed by ethanol precipitation, and resuspension of the pellet using DEPC-H_20 to give a final concentration of 0.25-0.5 µg/µL. The dephosphorylated RNA was checked on a 1.3% agarose gel to ensure the presence of RNA before proceeding with 5'-end labeling.

The 5'-end labeling of the dephosphorylated transcript was performed in a 25 µL final volume consisting of 5 µg of the dephosphorylated transcript and 30 µCi of γ^{32}P-ATP (Amersham GE Healthcare, Montreal, Quebec). End-labeling of the RNA was done using the following reagents with final concentrations of: 12 mM DTT, 2.5 U/µL of RNasin, 1.6 U/µL of T4 Polynucleotide Kinase (PNK) (New England Biolabs, Beverly, MA), 1X PNK buffer, and made up to 25 µL with DEPC-H_20, followed by incubation for 1 hour at 37^0C. After making up the reaction mixture to 50 µL with DEPC-H_20, the excess γ^{32}P-ATP was removed using a G-50 spin column and the solution was then made up to 200 µL with DEPC-H_20,

followed by phenol/chloroform extraction and ethanol precipitation. The pellet was resuspended in 20 μL 9M urea/phenol loading dye (0.02% w/v bromophenol blue, 0.02% w/v xylene cyanol, and 10% v/v saturated phenol) and loaded onto a 6% polyacrylamide/7M urea gel, which was run at 25 mA with 0.5X TBE buffer (tris base, boric acid, EDTA) until the bromophenol dye was near the bottom of the gel. The gel was then exposed for 10 seconds, scanned using the Cyclone PhosphoImager and visualized using the OptiQuant software (Hewlett Packard, Palo Alto, CA). The portion of the polyacrylamide gel containing the 1705-1792 radioactively-labeled RNA transcript was excised and the ^{32}P-labeled RNA was eluted with 400 μL of Probe Elution Buffer [PEB(NH_4OAC, EDTA pH 8, SDS, and DEPC-H_20)]: Phenol (1:1) solution for 6 hours at 37^{0}C, followed by standard phenol/chloroform extraction and ethanol precipitation. The radioactive pellet was then resuspended in approximately 100 μl DEPC-H_20 to give a final count of approximately 30,000 cpm/μL.

Dephosphorylation, 5'-end labeling, and gel-purification of the 3018-3159 β–globin transcript was identical to the procedure described for the 1705-1792 CRD RNA.

2.0.3 Utilization of enzyme probes for secondary structure determination

The 5'-end labeled 1705-1792 RNA transcript (30,000 cpm) was partially digested with RNase T1 (cleaves 3' to single-stranded guanosines) (Roche Diagnostic Inc, Mannheim, Germany), RNase T2 (preferentially cleaves 3' to single-stranded adenosines, but also 3' to the other 3 nucleotides) (Invitrogen Life Technologies, Carlsbad, CA), RNase A (cleaves 3' to single-stranded uridines and cytidines) (Ambion, Inc., Austin, Texas), and RNase V1 (cleaves 3' to double-stranded nucleotides or stacked bases) (Ambion, Inc., Austin, Texas) (Ehresmann et al., 1987) (see Table 2.1 for a summary of the RNase probes and their

cleavage sites). Digestion by RNase T1 was done under both RNA native and denaturing conditions in order to confirm the strandedness of the guanosine residues. Digestion of the 5' end-labeled transcript under RNA denaturing conditions was done in 1X sequencing buffer containing 20 mM sodium citrate pH 5, 7M urea, and 1 mM EDTA (Ambion, Inc., Austin, Texas), which according to Ehresmann et al. (1978), RNase T1 remains active under these conditions. Digestion of the transcript under native conditions was done in a buffer containing 100 mM Tris-HCl pH 7.5, 1M NH_4Cl, and 100 mM $MgCl_2$ (10X PA buffer). Digestion of the 5' end-labeled transcript with RNase T2, RNase A, and RNase V1 was done in a buffer consisting of 100 mM Tris pH 7, 1M KCl, and 100 mM $MgCl_2$ (10X Structure Buffer) (Ambion, Inc., Austin, Texas). In order to identify the cleavage sites that were generated, a partial alkaline digestion of the end-labeled transcript was done (Ehresmann et al., 1987). This involved incubation with 10X alkaline buffer containing 50 mM sodium carbonate ($NaHCO_3/Na_2CO_3$) pH 9.2, and 1 mM EDTA. The alkaline ladder and enzyme digestions were all performed in a 20 µl final volume containing 2 µl of the respective reaction buffer, the 5' end labeled transcript (30,000 cpm), and made up to 20 µl with sterile water. Partial alkaline digestion was done at 95^0C for 3 minutes, followed by ethanol precipitation and resuspension in 9M urea/phenol loading dye to give final counts of 25,000 cpm/µl and then loading 2 µl. Prior to enzymatic digestion, the RNA transcript was heated for 5 minutes at 50-55^0C and then allowed to refold for 10 minutes at room temperature. Partial digestion of the RNA transcript with RNase T1 under RNA denaturing conditions involved the addition of 1 unit of RNase T1 and then incubation at room temperature for 5 minutes, whereas for partial digestion under RNA native conditions, 0.05 units of RNase T1 was added and incubation was done for 30 seconds on ice. Partial digestion with RNase T2

(0.02 units) and RNase A (2 x 10^{-4} mg) was performed for 15 minutes at room temperature, whereas for RNase V1 (1 x 10^{-4} units), the mixture was incubated for 5 minutes at room temperature. The reactions were terminated by the addition of 1 µl saturated phenol and 1 µl yeast tRNA (10 mg/ml), followed by standard ethanol precipitation and resuspension in 9M urea/phenol loading dye to give final counts of 15,000 cpm/µl. Two microlitres of samples were typically loaded onto the gel for visualization. To check for RNA integrity, undigested 1705-1792 CRD RNA was also ran (input RNA).

After pre-running the 12% polyacrylamide/7M urea gel with 0.5X TBE buffer for 45 minutes, the samples were loaded and the gel was run for 2.5 hours at 30 mA until the bromophenol dye was near the bottom of the gel. The gel was then fixed in 10% methanol/10% acetic acid solution for 10 minutes, exposed for 16 hours, scanned using the Cyclone PhosphoImager and visualized using the OptiQuant software.

Structure probing of the 3018-3159 β-globin RNA was identical to the procedure described for the 1705-1792 CRD RNA, except for the following modifications. The 3018-3159 β-globin RNA was incubated with 1 unit of RNase T1 for 15 minutes at room temperature under both RNA denaturing and RNA native conditions. In addition, the 3018-3159 β-globin RNA was incubated with 1 µl of $1X10^{-3}$ U/µl RNase V1 for 15 minutes at room temperature. After loading the samples onto the gel, the samples were run for two hours and four hours under the same electrophoresis conditions described for the 1705-1792 CRD RNA.

Table 2.1. The enzymes probes and their cleavage specificity.

Enzyme Probe	Cleavage specificity
RNase T1	3' to unpaired guanosines
RNase T2	3' to unpaired adenosines > guanosines, cytidines, uridines
RNase A	3' to unpaired cytidines and uridines
RNase V1	3' to paired or stacked nucleotides

2.1 Results

2.1.1 Digestion of the pUC19-myc 1705-1792 and SPκβc-globin 3018-3159 plasmids and the generation of *in vitro* transcribed RNA

pUC19-myc 1705-1792 plasmid

Upon agarose gel electrophoresis, the undigested pUC19 plasmid containing the 1705-1792 CRD insert showed two bands (Figure 2.1). The intense, low molecular band at approximately 2,500 bp represented the supercoiled conformation of the plasmid, whereas the faint high-molecular weight band corresponded to the relaxed form of the recombinant pUC19 plasmid (nicked plasmid). Upon digestion of recombinant pUC19 with *Eco*RI, one band that ran between the nicked and the supercoiled plasmids was observed, indicating that most, if not all, of the recombinant pUC19 plasmids were linearized.

The linearized plasmid was then used as a template for *in vitro* transcription using SP-6 RNA polymerase. Upon agarose gel electrophoresis, a single band was observed at approximately 90 nucleotides (Figure 2.2). This band represented the 88 nucleotide 1705-1792 RNA, in addition to the *Bam*HI and *Eco*RI restriction sites.

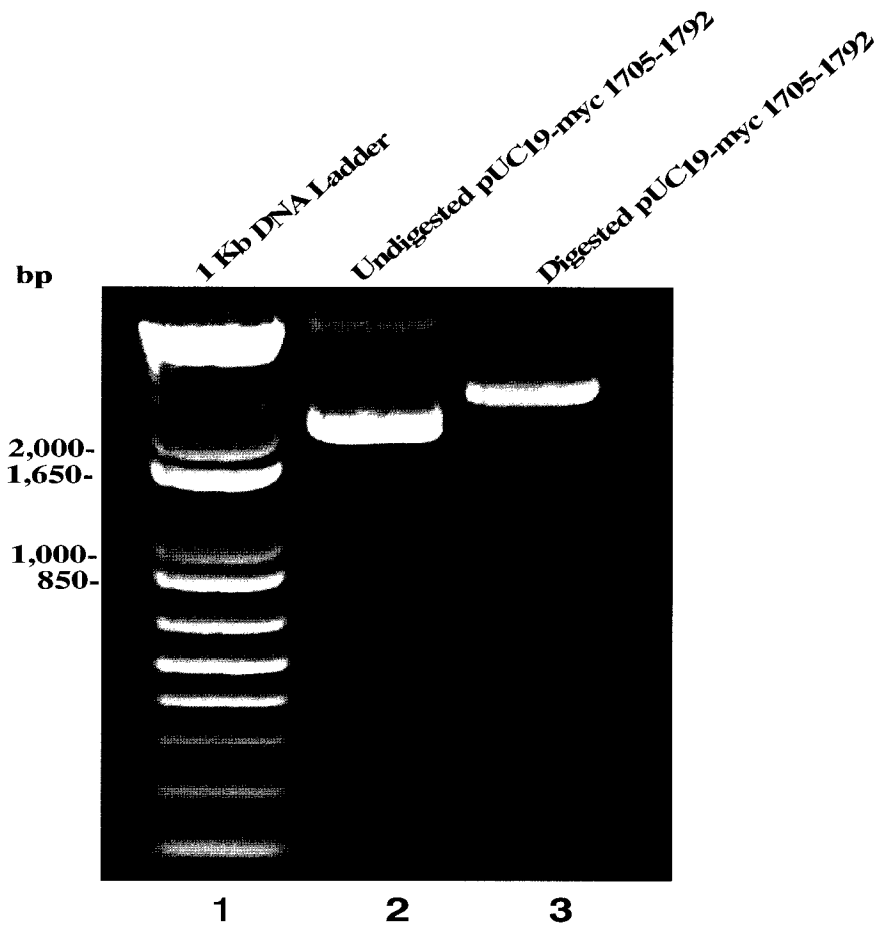

Figure 2.1. Linearization of 1705-1792 pUC19 plasmid with *Eco*R1 in preparation for *in vitro* transcription. The undigested pUC19 plasmid (lane 2) was compared to an *Eco*R1 digested plasmid (lane 3) parallel to a 1 Kb DNA ladder (lane 1). The samples were run on a 1% agarose gel containing ethidium bromide and visualized using ChemiImager™ System (Alpha Innotech Corporation, San Leandro, CA).

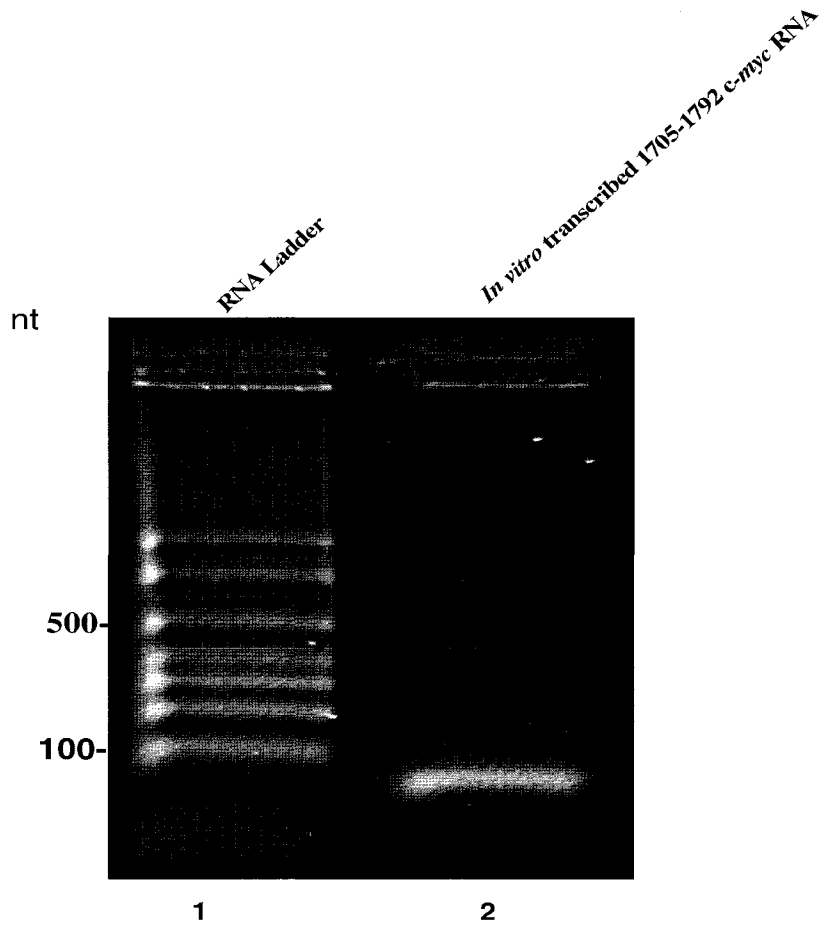

Figure 2.2. *In vitro* transcription using the 1705-1792 pUC19 plasmid as a template. The linearized 8257 pUC19 plasmid was *in vitro* transcribed using the MEGAscript SP6 Kit (Ambion, Inc., Austin, Texas) and ran on a 1.3% agarose gel. Lane 1 represents the RNA ladder and lane 2 corresponds to the *in vitro* transcribed 1705-1792 CRD RNA.

SPκβc-globin 3018-3159 plasmid

Upon agarose gel electrophoresis, the undigested SPκβc-globin plasmid was represented by four bands at approximately 2,500 bp, 3,000 bp, 5,000 bp, and 12,000 bp (Figure 2.3). The band at 5,000 bp may represent the relaxed form of the recombinant plasmid, while the band at 2,500 bp may represent the supercoiled form of the plasmid. The 3,000 bp band may represent the linearized form of the plasmid, which might have been present due to contamination with restriction endonucleases that were left behind from the bacterial crude extract or it might have been due to mechanical shearing of the plasmid. The band at 12,000

bp may represent multimerization of the SPκβc-globin plasmid, to generate this slow-running complex. Upon cleavage of the SPκβc-globin plasmid with *Fok*I, three bands were generated at approximately: 650 bp, 700 bp, and 1,000 bp (Figure 2.3). These bands were most likely due to the digestion of the plasmid at the multiple *Fok*I restriction sites.

The linearized plasmid was then used as a template for *in vitro* transcription using the SP-6 RNA polymerase. In a 1% formaldehyde agarose gel, one major band was observed between the 100 and 200 nucleotide markers (Figure 2.4). This is in good agreement with the expected size of the 142 nt β-globin RNA (3018-3159).

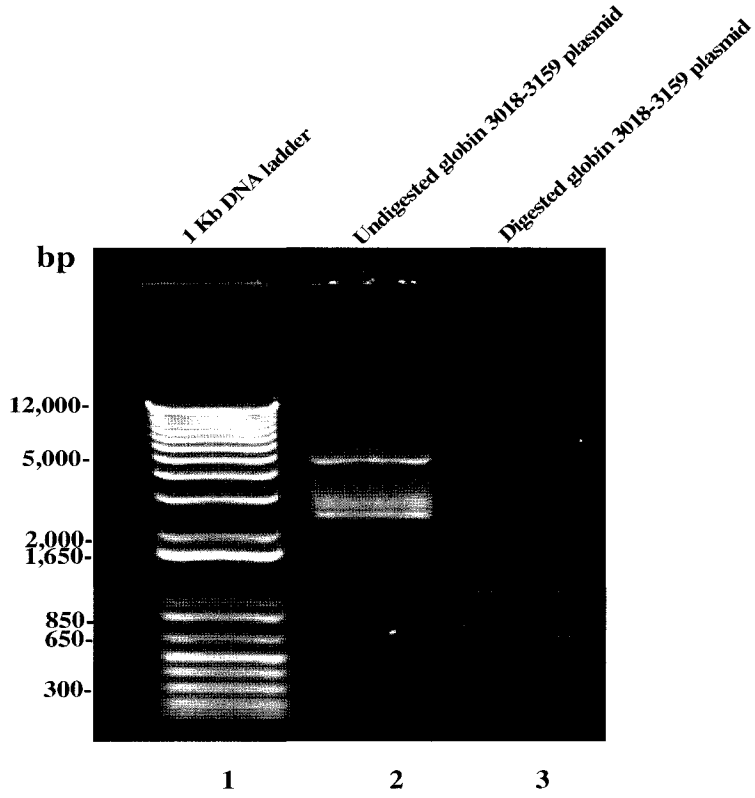

Figure 2.3. Linearization of the SPκβc-globin 3018-3159 plasmid with *Fok*I in preparation for *in vitro* transcription. The undigested SPκβc-globin 3018-3159 plasmid (lane 2) was compared to an *FokI* digested plasmid (lane 3) parallel to a 1 Kb DNA ladder (lane 1). The samples were run on a 1% agarose gel containing ethidium bromide and visualized using ChemiImager™ System (Alpha Innotech Corporation, San Leandro, CA) (Courtesy of Dan Sparanese).

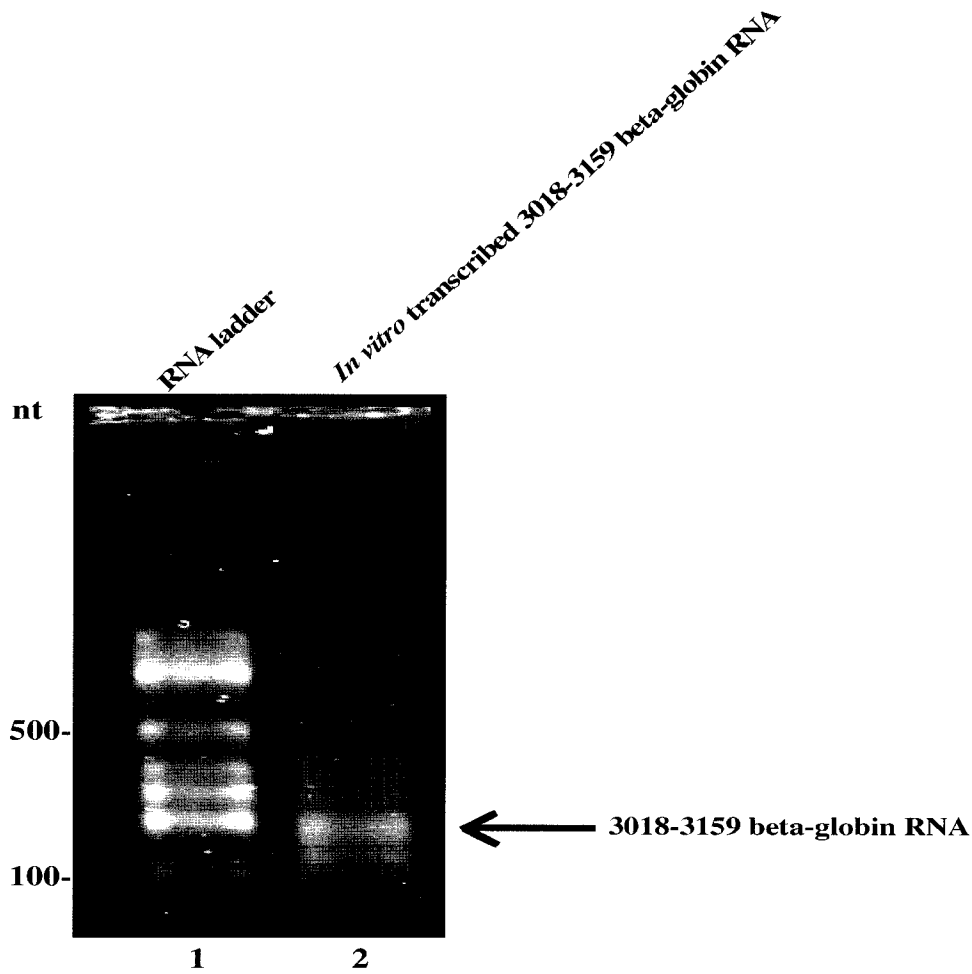

Figure 2.4. *In vitro* transcription using the 3018-3159 β-globin plasmid as a template. The linearized 3018-3159 β-globin plasmid was *in vitro* transcribed using the MEGAscript SP6 Kit (Ambion, Inc., Austin, Texas) and ran on a 1.3% agarose gel. Lane 1 represents the RNA ladder and lane 2 corresponds to the *in vitro* transcribed 3018-3159 β-globin RNA (Courtesy of Dan Sparanese).

2.1.2 Visualization of the gel-purified 5'-end labeled RNA on a 6% polyacrylamide/ 7M urea gel

c-*myc* nts 1705-1792

In order to obtain an uncontaminated RNA substrate for secondary structure determination and cleavage specificity analysis, the 5' end-labeled transcript was gel-purified on a 6% polyacrylamide/7M urea gel. On a 6% denaturing polyacrylamide gel, the xylene cyanol

(XYC) dye has a size of 106 nt, while the bromophenol blue (BPB) dye has a size of 26 nt. Therefore, the 1705-1792 CRD RNA (~88 nucleotides) is expected to migrate slightly faster than xylene cyanol dye. Upon running the labeled transcript on the polyacrylamide gel, an intense band slightly below the xylene cyanol marker was observed (see arrow; Figure 2.5a). This band corresponded to the 1705-1792 CRD RNA, which has an approximate size of 88 nucleotides. In addition to this intense band, multiple faint degradation products were also observed (Figure 2.5a). Upon gel-purification, the 1705-1792 CRD bands were successfully excised, leaving behind most of the unwanted degradation products (Figure 2.5b).

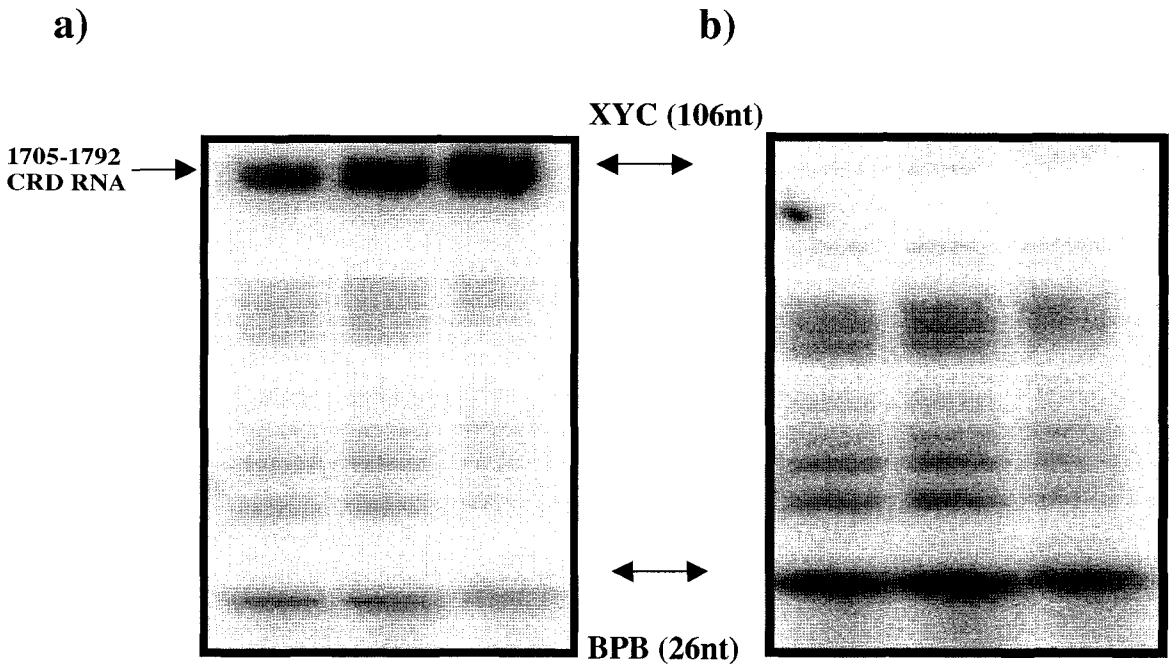

Figure 2.5. Gel-purification of the 5' end-labeled 1705-1792 CRD transcript. The 5' end labeled transcript was run on a 6% polyacrylamide/7M urea gel and the samples were divided into 3 wells (a). After gel-purification, the gel was re-exposed for 10 seconds and visualized to ensure the excision of the 1705-1792 CRD RNA (b). XYC and BPB indicate the approximate locations of the xylene cyanol and the bromophenol dyes, respectively.

β-globin nts 3018-3159

Upon running the ^{32}P-labeled β-globin RNA on a 6% polyacrylamide/7M urea gel, an intense band corresponding to the ~ 142 nt 3018-3159 β-globin RNA was observed, in addition to multiple degradation products (Figure 2.6a). The 3018-3159 β-globin RNA migrated slightly slower than the xylene cyanol band (106 nt) (Figure 2.6a). The 3018-3159 β-globin RNA was successfully excised from the gel, leaving behind most of the unwanted degradation products (Figure 2.6b).

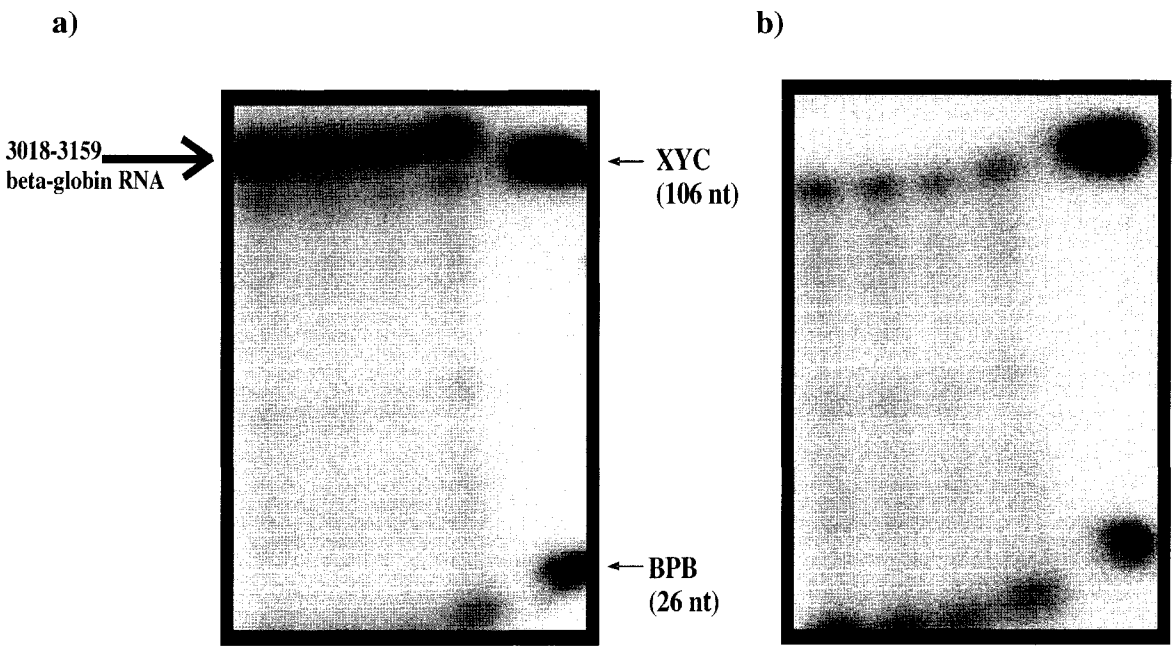

Figure 2.6. Gel-purification of the 5' end-labeled 3018-3159 β-globin transcript. The 5' end labeled transcript was run on a 6% polyacrylamide/7M urea gel and the samples were divided into 4 wells (a). After gel-purification, the gel was re-exposed for 10 seconds and visualized to ensure the excision of the 3018-3159 β-globin RNA (b). XYC and BPB indicate the approximate locations of the xylene cyanol and bromophenol dyes, respectively (Courtesy of Dan Sparanese).

2.1.3 The secondary structures of the 1705-1792 c-*myc* CRD and 3018-3159 β–globin RNAs *in vitro*

c-*myc* nts 1705-1792

The 5' end-labeled 1705-1792 CRD transcript digested with the different RNases was run on a 12% polyacrylamide/7M urea gel for 2 hours (Figure 2.7a) and 3 hours (Figure 2.7b), respectively, in order to obtain a better resolution of cleavage sites near the top and bottom of the gel. However, only the cleavage sites between nucleotides 1719 and 1780 of the CRD region were easily identifiable upon running the gel for the indicated time periods.

Upon digestion of the labeled transcript with RNase T1 under RNA-denaturing conditions, it appeared that the 1705-1792 RNA substrate has been completely digested (Lane 3). This was not the case, however, as will be explained in the discussion section. Six cleavage fragments were generated by RNase T1 under RNA-denaturing conditions: G1731, G1745, G1746, G1749, G1764, and G1770 (Lane 3, Figure 2.7a). However, upon digestion of the 5' end-labeled transcript with RNase T1 under RNA-native conditions, only fragments corresponding to G1731, G1749, and G1770 were observed (Lane 4, Figure 2.7a). It is important to point out that cleavage at G1749 appeared more intense under native conditions than denaturing conditions (Lane 4, Figure 2.7a). Upon cleavage with RNase T2 under RNA native condition, a laddering pattern was observed and was mostly prominent between nucleotides 1719-1734, 1739-1744, 1747-1752, and 1768-1775 (Lane 5, Figure 2.7a). In addition, there was RNase T2 cleavage at positions U1757 and A1758. Digestion with RNase A generated several fragments including intense cleavage at C1727, U1751, C1768, C1771, U1773, and C1775 (lane 6, Figures 2.7 a and b). Weak cleavage sites generated by RNase A include C1741, C1742, U1747, and U1750. It is also important to note that all of the cleavage sites generated by RNase A were also cleaved by RNase T2 (Lanes 5 and 6,

Figures 2.7 a and b). Cleavage with RNase V1 generated two intense bands at positions A1743 and C1768, in addition to the weak bands observed at positions C1771 and U1773 (Lane 7). Furthermore, laddering patterns were observed between nucleotides 1721-1724, 1727-1734, 1743-1745 and 1754-1757 (see Brackets 1-4, respectively; Figures 2.7a and 2.7b).

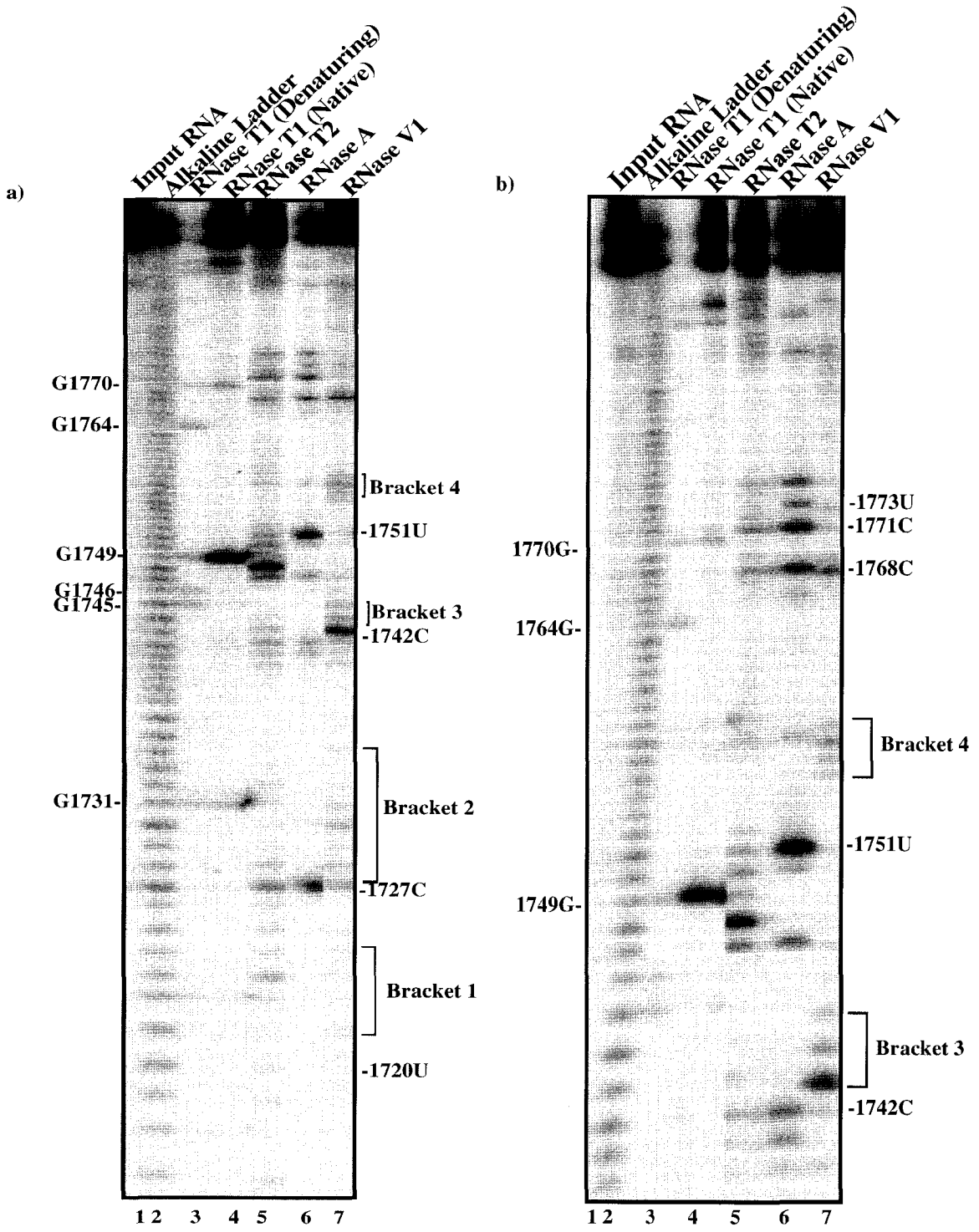

Figure 2.7. Structure probing of the 5' end-labeled *in vitro* transcribed 1705-1792 CRD RNA on a 12% polyacrylamide/7M urea gel that was run for 2 hours (a) and 3 hours (b), For band identification purposes, guanosine residues on the left of the diagram indicate several sites cleaved by RNase T1 under RNA denaturing conditions, whereas numbering on the right indicates some of the sites cleaved by RNase A. Brackets 1-4 indicate the four laddering regions generated by RNase V1.

Upon folding the 1705-1792 CRD region using the Mfold software program (Zuker, 2003), the secondary structure shown in Figure 2.8 was obtained. The RNase probing data was then used as a constraint with the structure generated by Mfold to obtain a structure that best fit the probing data (Figure 2.9). The experimental data is in agreement with the structure determined by Mfold, although the experimentally determined structure appeared to be very dynamic in solution. The experimental structure shown in Figure 2.9 consists of a summary of the cleavage sites and cleavage intensities generated at each position cleaved by the various RNases. Cleavage intensity was determined by judging the strength of each cleavage site relative to the overall cleavage within each lane. The secondary structure has five stems, two containing four base pairs (stems I and V) and the remaining three consisting of three base-pairs (stems II, III, and IV). In addition, there is one hairpin loop (nts 1747-1753) and four internal bulges consisting of an average of eight nucleotides (Figure 2.9).

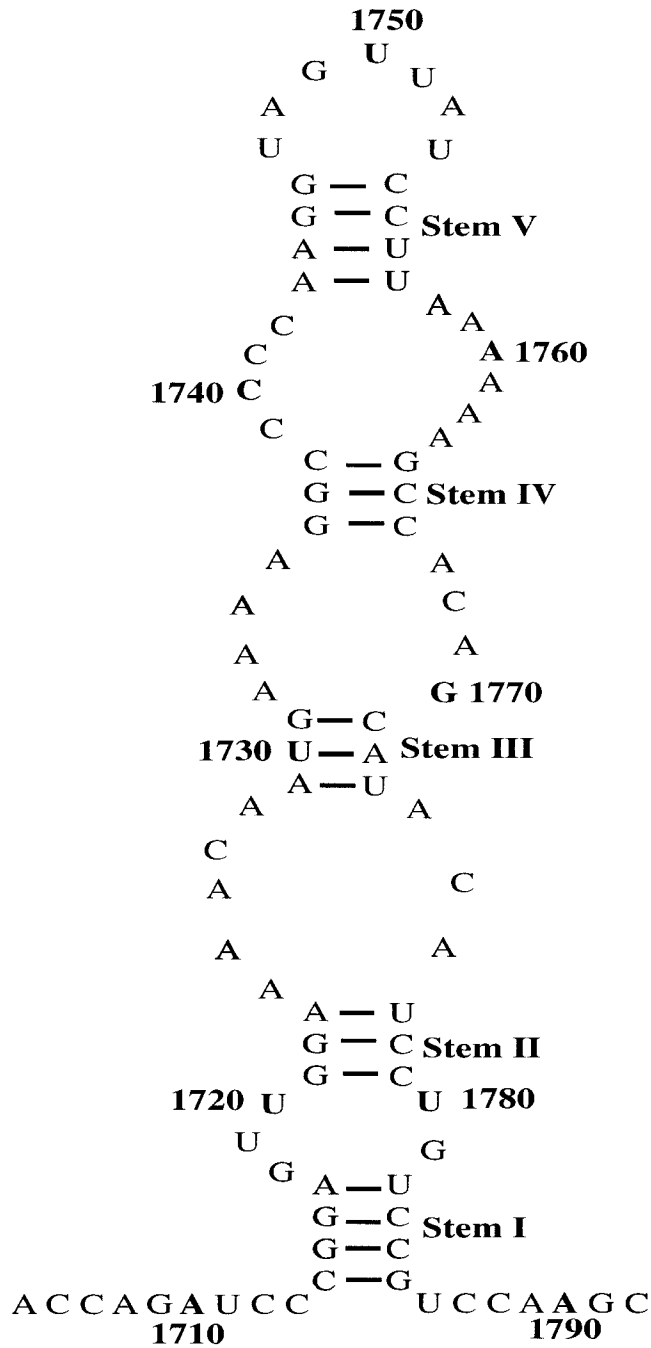

Figure 2.8. The 1705-1792 CRD secondary structure determined by the Mfold software program. This structure was generated by entering the primary sequence into the Mfold program (Zuker, 2003) to obtain a structure with the lowest free-energy.

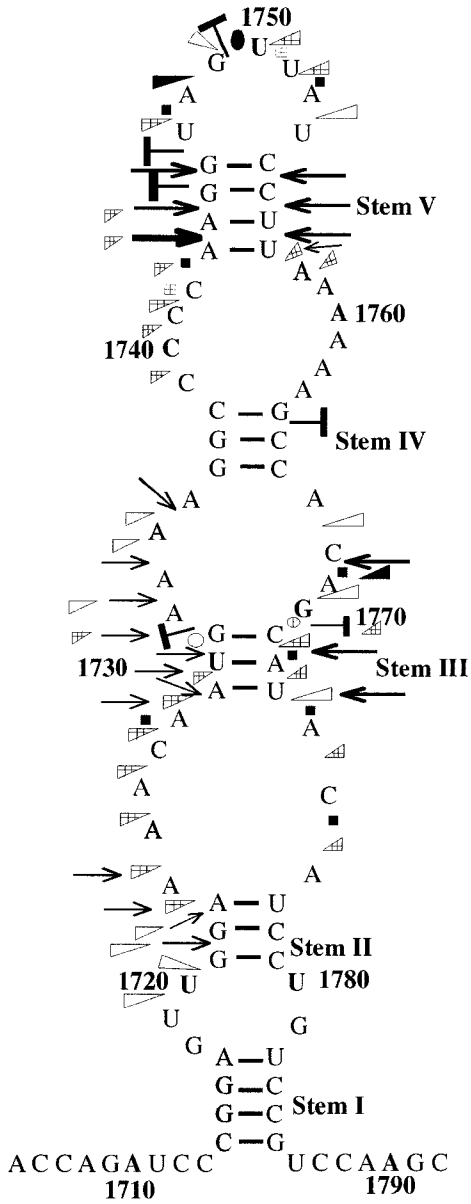

	T1 (D)	T1 (N)	T2	A	V1
Strong					
Moderate					
Weak					

Figure 2.9. Secondary structure model for the 1705-1792 CRD RNA showing locations of bases accessible for enzyme probes. This secondary structure was obtained by using the probing data as constraint with the Mfold program (Zuker, 2003). Hatched and open symbols represent moderate and weak cleavage, respectively, while filled symbols represent strong modification. RNase V1 cleavage sites are indicated by arrow intensity. D and N indicate cleavage with RNase T1 under RNA denaturing or native conditions, respectively.

β-globin nts 3018-3159

The 5'end-labeled 3018-3159 β-globin RNA transcripts digested with the different RNase probes were run on a 12% polyacrylamide/7M urea gel for 2 hours (Figure 2.10a) and 4 hours (Figure 2.10b), respectively. This was done in order to obtain a better resolution of cleavage sites near the top and bottom of the gel. However, only cleavage sites between nucleotide 1 and 84 (numbering starts from the 5' end) were easily identifiable upon running the gel for the indicated time periods.

Upon digestion of the 5' end-labeled 3018-3159 β-globin RNA with RNase T1 under RNA denaturing conditions, sixteen cleavage sites were easily identifiable: G7, G13, G22, G24, G32, G45, G53, G54, G62, G69, G71, G72, G74, G77, G81, and G84 (lane 3, Figures 2.10 a and b). Upon cleavage of the labeled transcript with RNase T1 under RNA-native conditions, the same cleavage sites generated by RNase T1 under RNA denaturing conditions were also cleaved, except for G53 and G54 (lane 4, Figures 2.10 a and b). It is also important to point out that upon cleavage 3' to G81 by RNase T1 under RNA-native conditions, an intense cleavage fragment is obtained in comparison with the cleavage fragment generated by RNase T1 under RNA denaturing conditions (lanes 3 and 4, Figure 2.10b). Cleavage of the 5' end-labeled transcript with RNase T2 generated three laddering regions, in addition to cleavage 3' to U80 and G81 (lane 5, Figure 2.10 a and b). The laddering regions were observed between nucleotides 1-12, 18-20, and 39-44 and include intense cleavage 3' to A18 and A19 (lane 4, Figure 2.10a). Upon partial digestion with RNase A, nineteen cleavage sites were generated including an intense cleavage 3' to C2 (lane 6, Figure 2.10a). The remaining eighteen sites cleaved by RNase A include: U4, U6, C8, U10, C11, U12, C15, C17, C20, U21, C27, U30, C33, C39, C43, C47, C50, and U80. The following sites cleaved by RNase

A were also cleaved by RNase T2: C2, U4, U6, C8, U10, U11, U12, C20, C39, and C43. Upon cleavage of the 5' end-labeled transcript with RNase V1, the following nucleotides were cleaved: C17, C27, C29, U30, A35, A39, and C50 (lane 7, Figure 2.10a and b). In addition, laddering regions were observed between nucleotides 1-6 and 10-15 (see Brackets 1 and 2, respectively, Figure 2.10a). The following sites cleaved by RNase V1 were also cleaved by RNase T2: 1-6, 10-12, and A39. Furthermore, RNase V1 sites that were also cleaved by RNase A include: C2, U4-U6, U10, C11, U12, C15, C17, C27, U30, A35, A39, and C50.

Upon folding the 3018-3159 β-globin RNA using the Mfold program (Zuker, 2003), only one structure was in close agreement with the experimental data (Figure 2.11a). The experimental data were then used a constraint in conjunction with the structure generated by Mfold to obtain the experimental structure shown in Figure 2.11b. The determined structure consists of 7 stems, 6 internal bulges, 2 hairpin loops, and 1 multibranched loop. Stems II, III, and VI consist of two base pairs, while stems I, IV, V, VII consist of three, six, five, and three base-pairs, respectively. Four of the stems in the determined structure were also present in the structure generated by Mfold and include: stems I, II, III, V, and VI. In addition, stems IV and VII were also present in the structure generated by Mfold, except that that some base-pairs were eliminated or added. There is also a large internal loop located between stems VI and VII and the large multi-branched loop surrounding stems IV, V, and VI. The experimental structure shown in Figure 2.12 consists of a summary of the cleavage sites generated at each position cleaved by the particular RNase probe.

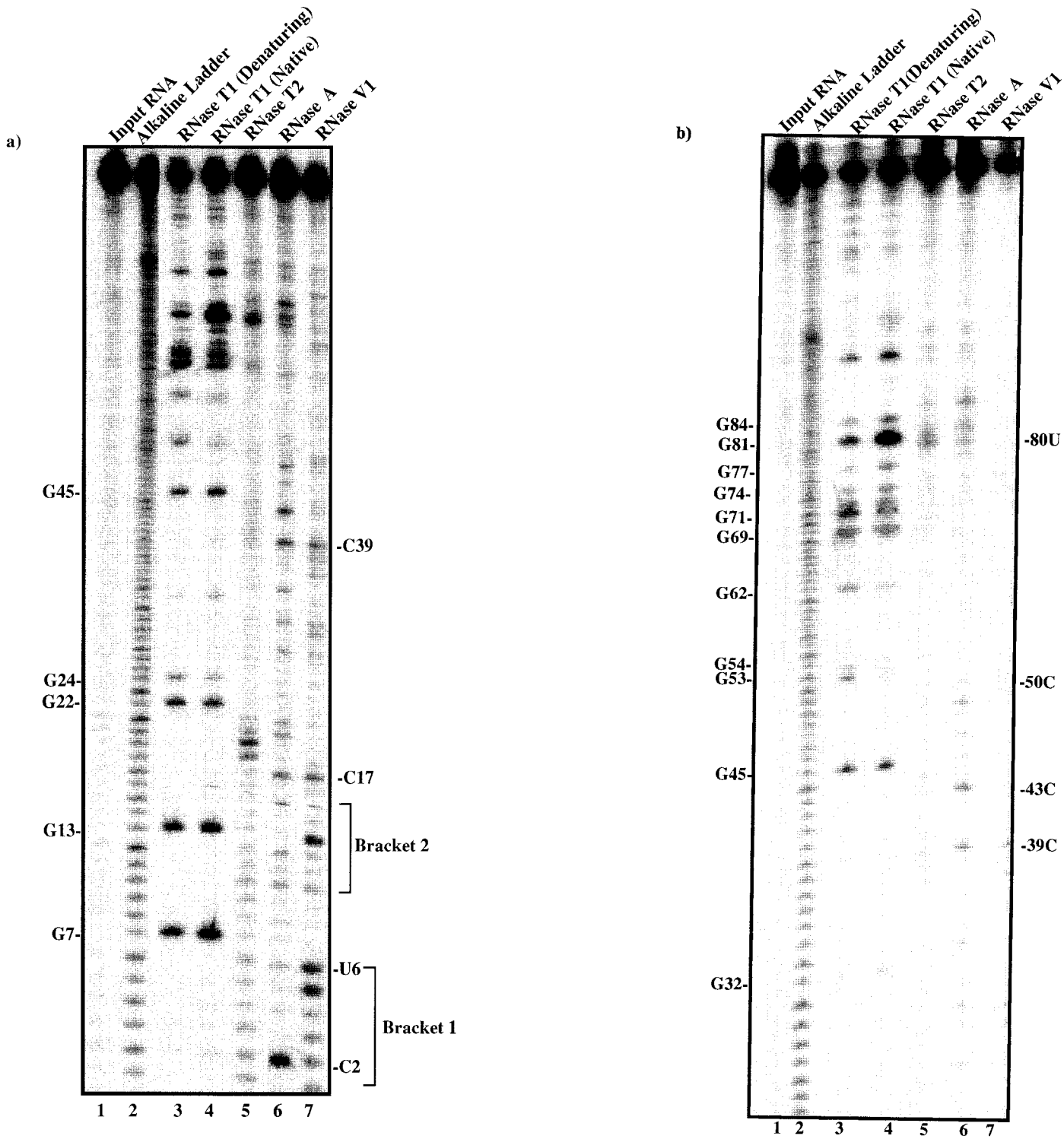

Figure 2.10. Structure probing of the 5' end-labeled β-globin RNA corresponding to nucleotides 3018-3159 on a 12% polyacrylamide/7M urea gel. The samples were run for 2 hours (a) and 4 hours (b), fixed, scanned, and then visualized. Several guanosine residues are indicated on the left of the diagram, whereas some of the sites cleaved by RNase A are indicated on the right of the diagram. Brackets 1 and 2 indicate the two laddering regions generated by RNase V1.

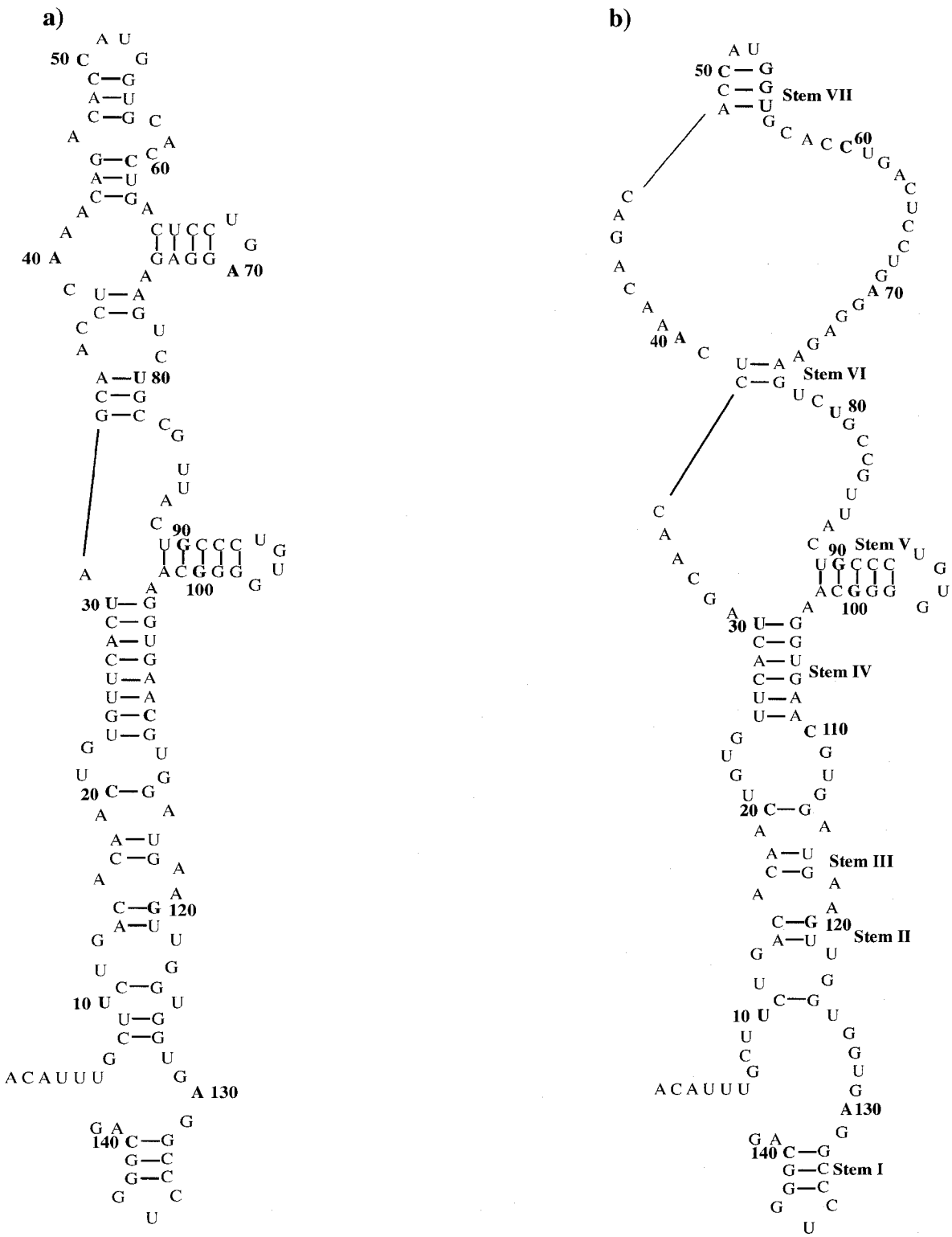

Figure 2.11. The secondary structure of the β-globin RNA corresponding to nucleotides 3018-3159. The structure determined by Mfold (a) was used in conjunction with the probing data to obtain a consensus structure (b).

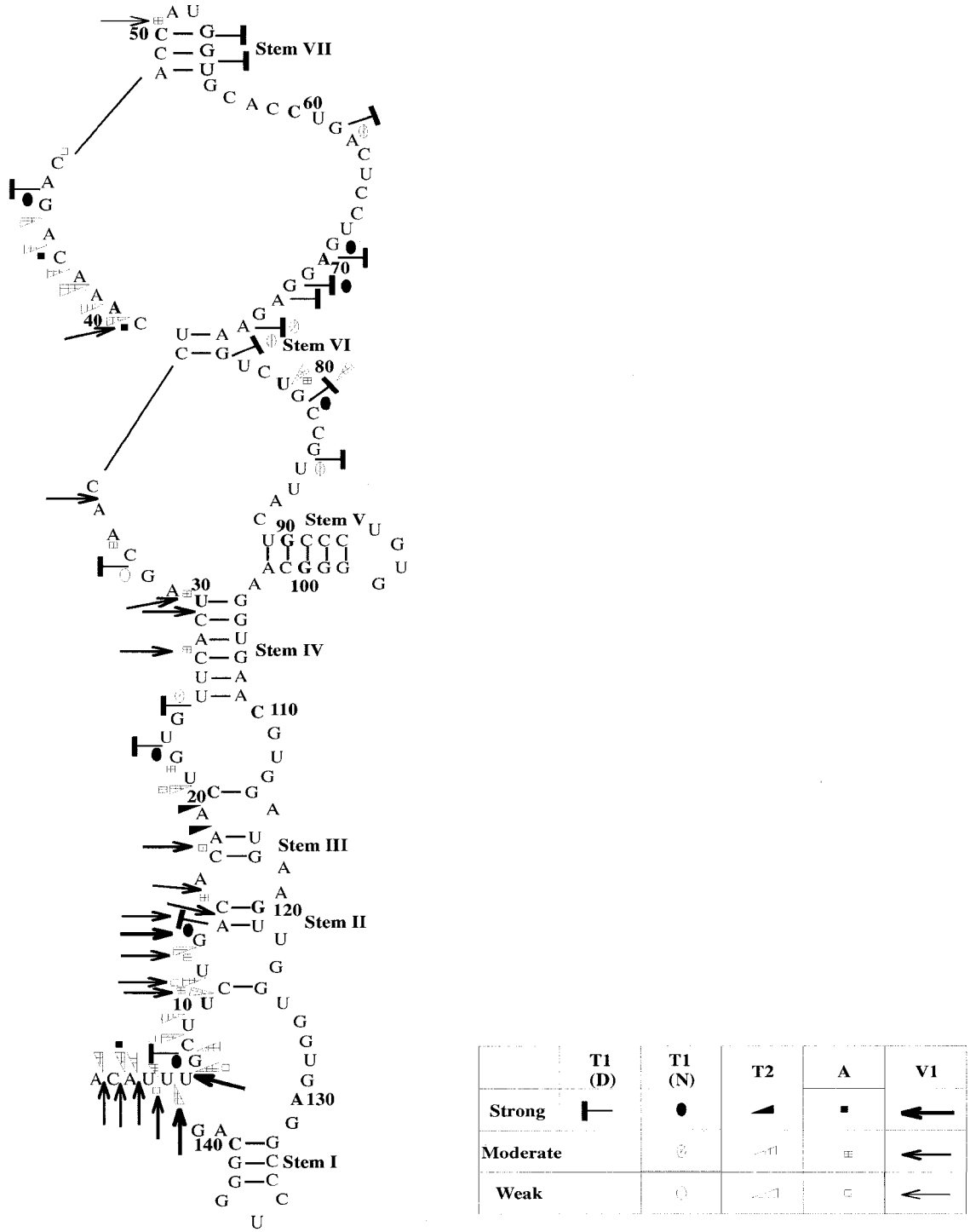

Figure 2.12. Secondary structure model for the 3018-3159 β-globin RNA showing locations of bases accessible for enzyme probes. This secondary structure was obtained by using the probing data as constraint with the Mfold program (Zuker, 2003). Hatched and open symbols represent moderate and weak cleavage, respectively, while filled symbols represent strong modification. RNase V1 cleavage sites are indicated by arrow intensity. D and N indicate cleavage with RNase T1 under RNA denaturing or native conditions, respectively.

2.2 Discussion

c-*myc* CRD nts 1705-1792

Cleavage of the 1705-1792 end-labeled CRD transcript with RNase T1 under RNA denaturing condition generated several bands corresponding to guanosine residues. The lack of a 1705-1792 intact CRD RNA (lane 3, Figure 2.7) might be due to the partial loss of the RNA during ethanol precipitation or due to the higher RNase T1 activity on the denatured RNA. These partial digestion conditions were used in subsequent experiments, where it was clearly shown that the cleavage sites generated were the result of partial digestion, rather than complete digestion.

Digestion of the 5' end-labeled transcript with RNase T1 under both denaturing and native conditions is essential in order to gain insights into the nature of the strandedness of the guanosine residues (Ehresmann et al., 1987). The presence of a guanosine cleavage site upon RNase T1 digestion under both RNA denaturing and native conditions would indicate that the guanosine residue remains single-stranded upon refolding (Ehresmann et al., 1987). The cleavage of guanosine residues: 1731, 1749, and 1770 by RNase T1 under both RNA denaturing and native conditions indicates their localization in a single-stranded domain. The presence of a guanosine cleavage site generated by RNase T1 under denaturing conditions and its disappearance under native conditions, indicates that the guanosine residue is present in a double-stranded region. This is observed with G1745, G1746, and G1764, indicating that these guanosine residues are present in a stem region. The presence of a more intense cleavage site upon RNase T1 cleavage under RNA native conditions compared to denaturing conditions, indicates the localization of the guanosine residue in a single-stranded region that is relatively highly accessible by RNase T1. This finding was observed with G1749 and

G1770, however, due to the difference in input RNA loaded between the native and denaturing conditions, such correlation cannot be made in this case.

RNase T2 prefers to cleave 3' to single-stranded adenosine residues (Ehresmann et al., 1987). However, it is also capable of cleaving 3' to U, G, and C residues present in single-stranded domains (Ehresmann et al., 1987; Walker and Avis, 2005). The cleavage of the two RNase T1-cleaved residues, G1749 and G1770, by RNase T2 and the lack of cleavage of these sites by the double-strand specific enzyme, RNase V1, confirms the single-strandedness of these guanosine residues. Furthermore, the ability of RNase T2 to cleave 3' to any single-stranded nucleotide explains why residues that were cleaved by RNase A were also cleaved by RNase T2. The intense cleavage generated by RNase T2 3' to nucleotide 1748 and the absence of cleavage at this site by RNase V1 indicates that this adenosine residue is present in a highly accessible single-stranded region. Furthermore, the presence of a cleavage 3' to A1758 by RNase T2 and the absence of cleavage at this site by RNase V1 indicates the single-strandedness of this residue. The nucleotides involved in the two RNase V1 laddering regions, namely the regions consisting of nts 1721-1724 and nts 1727-1734, were also cleaved by RNase T2. Cleavage 3' to nucleotide C1727 was also observed by RNase A. Therefore, the cleavage by both RNase T2 and RNase V1 of nucleotides 1721-1723 and 1729-1731, which comprise stems II and III, respectively, indicate that these two stems are unstable, possibly due to the "breathing" of this dynamic structure that results in the generation of two alternative structures, an entirely open structure and a double-stranded structure. The dynamic nature of stem III is further confirmed by cleavage 3' to nucleotides C1771 and U1773 by both the single-strand specific enzymes, RNase T2 and RNase A and the double-strand specific enzyme, RNase V1. RNase V1 is also known to be capable of

cleaving some stacked unpaired bases (Ehresmann et al., 1987; Lowman and Draper, 1986). Such cleavage by RNase V1 might be the case for nucleotides 1724, 1727, 1728, 1732, 1733, 1734, and 1768, which span single-stranded regions in proximity to stems II, III and IV, therefore allowing the stacking of these bases. The observation that nucleotides 1747-1752 were cleaved by the single-stranded specific enzyme, RNase T2, and not by RNase V1, indicates with high confidence that this laddering region is single-stranded. Stem V was also found to be unstable, based on cleavage by RNase T2 and RNase V1 of similar sites within this stem. Evidence for the existence of this stem is based on the cleavage 3' to nucleotides 1743-1745 and 1754-1757 by RNase V1 and the lack of cleavage 3' to G1745 by RNase T1 under RNA native conditions. The dynamic nature of stem V is deduced based on cleavage within this stem by RNase T2 of the three sites that were cleaved by RNase V1, A1743, A1744, and U1757. The instability of stem V might be due to the "breathing" of the AU base-pairs within this stem, which allows cleavage by RNase T2. The results discussed, therefore, point to an overall unstable and dynamic secondary structure. However *in vivo,* this structure could be stabilized by RNA-binding proteins and/or divalent cations, which may allow such an unstable structure to exist.

Mfold analysis on the full-length c-*myc* CRD RNA (1705-1886) (Figure 2.13) and the full-length c-*myc* mRNA (Figure 2.14) was performed to gain an insight into the folding of the 1705-1792 CRD region within these RNAs. The most energetically-favorable secondary structures of both RNAs were chosen and it was shown that stems IV and V were conserved between these two RNAs. It is likely, therefore, that both stems IV and V are also conserved *in vivo*. In addition, the full-length CRD RNA structure has a Tm value of 63.4^0C, while the full-length c-*myc* mRNA structure has a Tm value of 74^0C. These values are greater than

room temperature, indicating that both of these structures are likely to be stable and non-dynamic at room temperature. This enhances the likeliness that the two conserved stems exist within c-*myc* mRNA *in vitro* and *in vivo*.

It is essential to point out that the *in vitro*-transcribed 1705-1792 CRD RNA contains five nucleotides that belong to the *Eco*RI restriction site (GAATT). These five nucleotides, however, were not included in the determined secondary structure. Upon Mfold analysis of the 1705-1792 c-*myc* CRD RNA with the presence of the five nucleotides, the CRD structure was identical to the determined secondary structure, as the five nucleotides were not involved in any base-pairing interactions (data not shown). Therefore, this validates the cleavage specificity characterization of the novel endonuclease on the presented secondary structure of nts 1705-1792 of the c-*myc* CRD RNA.

In order to investigate whether the determined secondary structure is evolutionarily-conserved, phylogenetic RNA analysis was performed by comparing the human 1705-1792 c-*myc* CRD region with those of the rat (*Rattus norvegicus*), mouse (*Peromyscus leucopus*), cat (*Felis catus)*, and cow (*Bos taurus*) (Figure 2.15). The baboon (*Papio hamadryas*) and chimpanzee (*Pan troglodytes*) CRD sequences are 100% homologous to the human c-*myc* CRD region and, therefore, were not included in this analysis. The alignment of the sequences revealed that most of the nucleotides were conserved between these species, except for the following variable sites: 1730, 1769, 1772, and 1785. None of these variable sites, however, appear to covary with each other, indicating their lack of involvement in an evolutionary conserved secondary structure. A detailed alignment analysis is needed to reveal with high certainty those sites that covary with each other, and therefore play important roles in secondary structure formation.

Upon folding of these homologous RNA sequences using the Mfold software program, variable secondary structures were obtained (Figure 2.16). None of these structures, however, were identical to the human 1705-1792 CRD structure, indicating the lack of an evolutionary conserved secondary structure between these species in the 1705-1792 CRD region. However, six of the residues that are thought to localize within double-stranded domains within the human 1705-1792 CRD region are also localized in double-stranded regions in the four secondary structures. These nucleotides include: G1721, G1722, G1745, G1746, G1764, and C1765 (underlined in Figure 2.16). Therefore, it is likely that these nucleotides are double-stranded in the human CRD region, hence, supporting the experimental probing results.

The existence of an *in vivo* secondary structure that is different from the one obtained *in vitro* cannot be excluded (Thisted et al., 1995), which is mainly due to the presence of RNA-binding proteins and cations. RNA-binding proteins are thought to bind secondary structural features such as the hairpin, bulge, and internal loops (Richardson et al., 1998). CRD-BP is an RNA binding protein implicated in CRD binding (Prokipcak et al., 1994) and may interact with the secondary structural features to promote a conformational change *in vivo*. Such a conformational change may also arise due to the presence of ribosomes and endonucleases that have also been implicated in c-*myc* mRNA metabolism. In addition to RNA-binding proteins, divalent and monovalent cations are also thought to induce RNA structural conformational changes (Batey et al., 1999; Shiman and Draper, 2000). Monovalent and divalent cations (particularly magnesium) interact with the negatively-charged phosphate backbone, thereby inducing a third level of RNA organization termed the tertiary structure (Shiman and Draper, 2000). Now that the *in vitro* secondary structure of the 1705-1792 CRD

region has been determined, one can assess the sequence and structure cleavage specificity of the mammalian endoribonuclease.

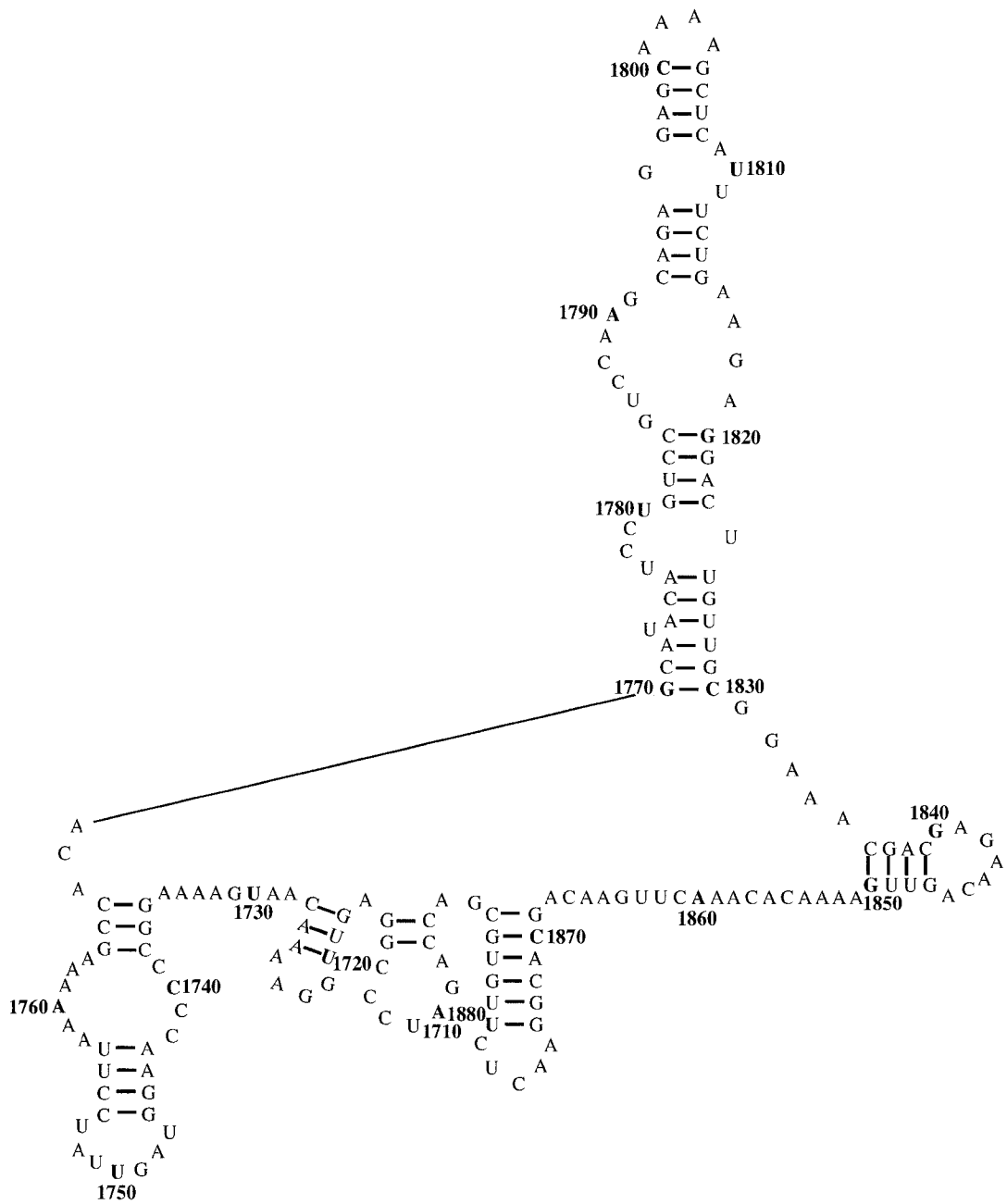

Figure 2.13. The 1705-1886 c-*myc* CRD RNA structure generated by the Mfold software program.

A)

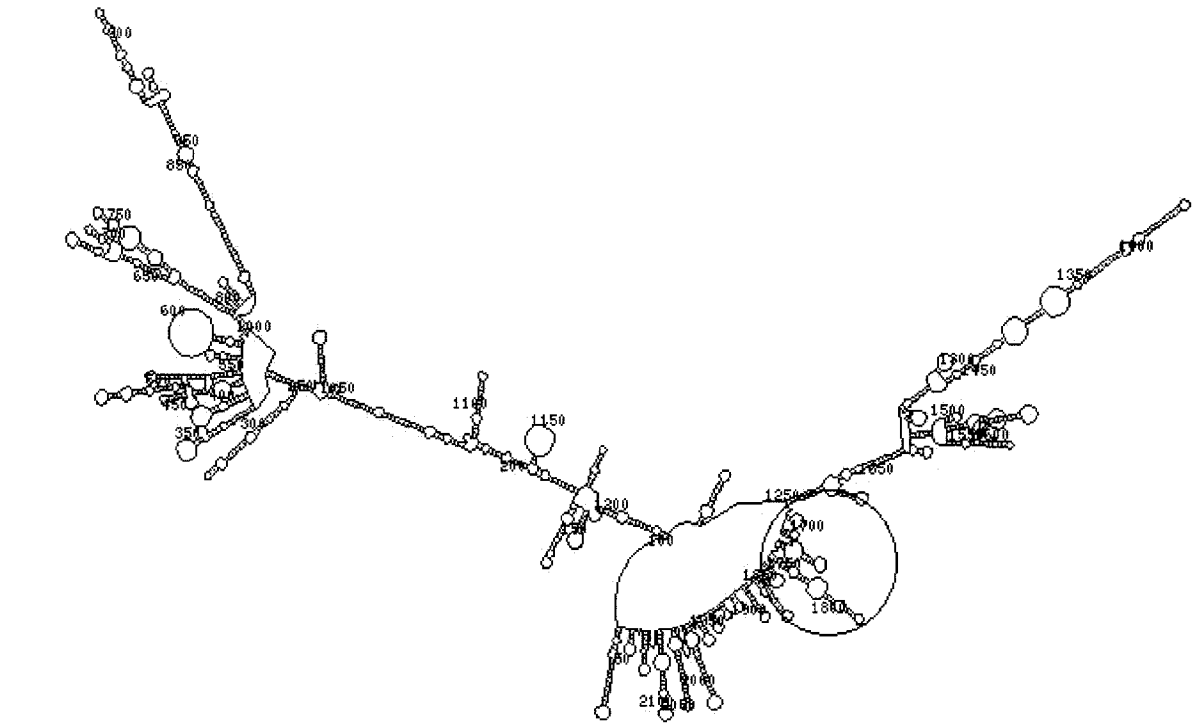

B)

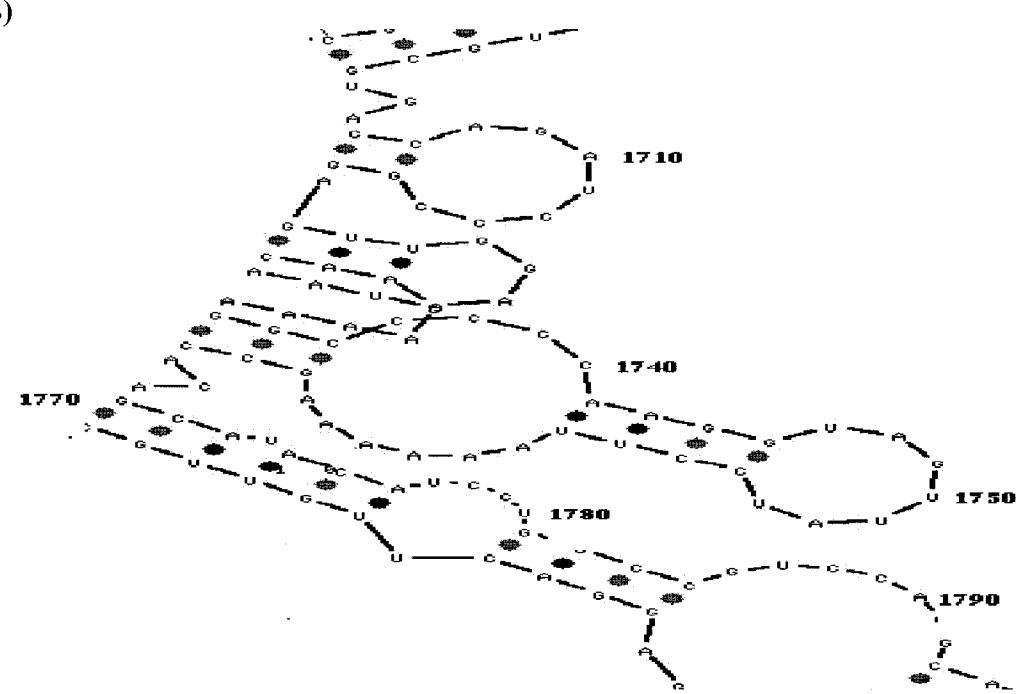

Figure 2.14. The secondary structure of the full-length c-*myc* mRNA generated by the Mfold software program. A, represents the condensed secondary structure of the c-*myc* mRNA. The circled region indicates the 1705-1792 CRD region. B, represents a 10X magnification of the circled region.

	1710	1720	1730	1740
Human	ACCAG**A**TCCCGGAGT	**T**GGAAAACAA**T**GAAA	AGGCC**C**CCAAGGTAG	
Rat	ACCAGATCCCTGAGT	TGGAAAACAACGAAA	AGGCCCCCAAGGTAG	
Mouse	ACCAGATCCCGGAGT	TGGAAAACAATGAAA	AGGCCCCCAAGGTAG	
Cat	ACCAGATCCCAGAGT	TGGAAAACAACGAAA	AGGCCCCCAAGGTGG	
Cow	ACCAGATCCCAGAGT	TGGAGAACAATGAAA	AAGCCCCCAAGGTAG	

	1750	1760	1770	1780	1790
Human	**T**TATCCTTAAA**A**AAG	CCACA**G**CATACATCC	**T**GTCCGTCCA**A**GC		
Rat	TTATCCTCAAAAAAG	CCACCGCCTACATCC	TGTCCGTCCAAGC		
Mouse	TTATCCTCAAAAAAG	CCACCGCCTACATCC	TGTCCATCCAAGC		
Cat	TGATCCTTAAAAAAG	CCACCGCGTACATCC	TGTCCGTCCAAGC		
Cow	TTATCCTTAAAAAAG	CCACAGCGTACATCC	TGTCGGTCCAAGC		

Figure 2.15. Sequence alignment of the human 1705-1792 c-*myc* CRD DNA with the CRD sequences present in rat, mouse, cat, and cow using the BCM Search Launcher (Smith et al., 1996). Bold letters correspond to the numbering above. The accession numbers for the CRD sequences are as follows: human, V00568; rat, Y00396; mouse, AY294987; cat, M15078; cow, AF519455.

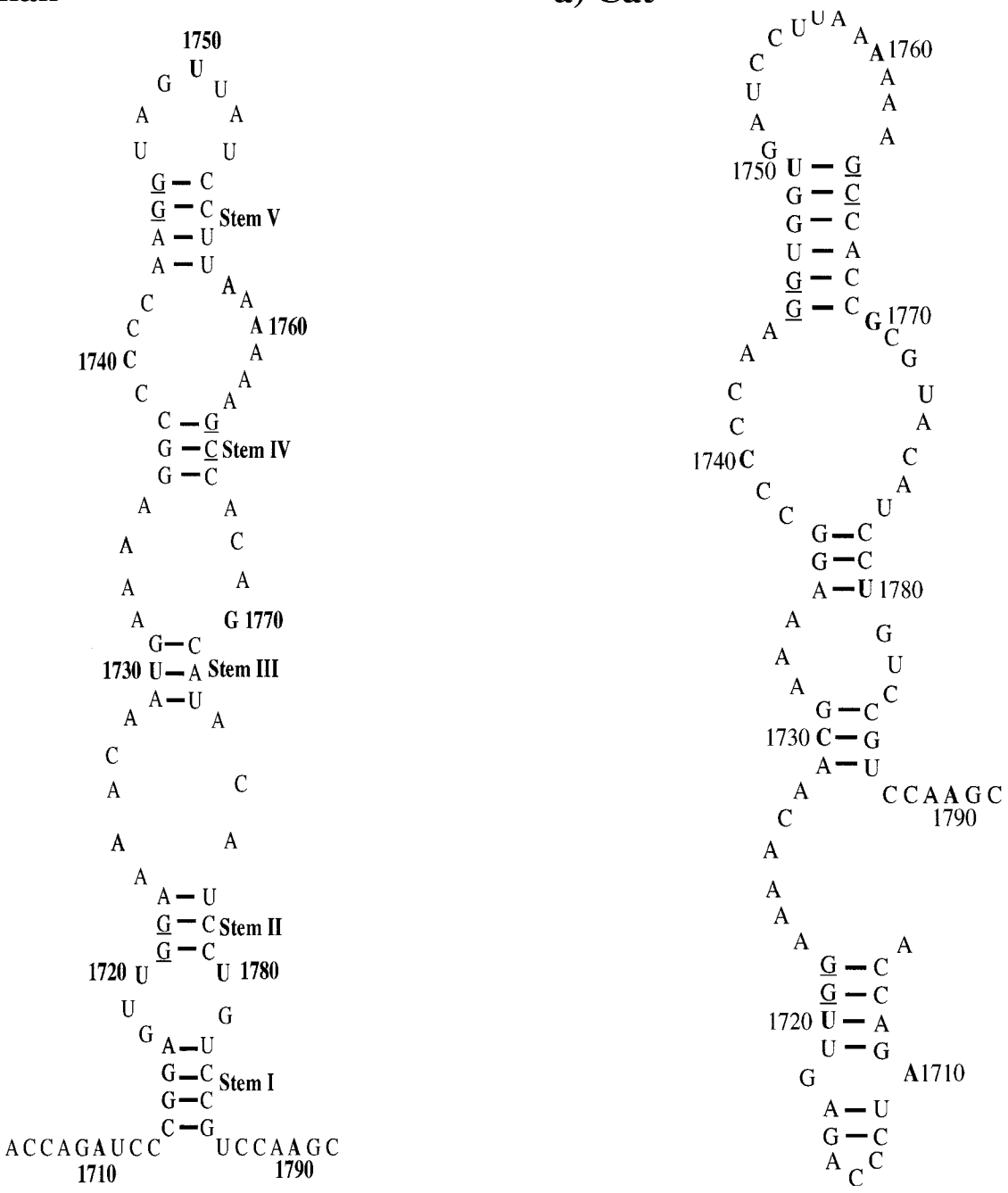

Figure 2.16. Comparison between the human 1705-1792 CRD RNA secondary structure with those structures generated by Mfold (Zuker, 2003) for a) cat, b) mouse, c) rat, and d) cow. Underlined nucleotides indicate residues that were double-stranded in the human CRD and remained double-stranded in the secondary structures of all four species.

b) Mouse

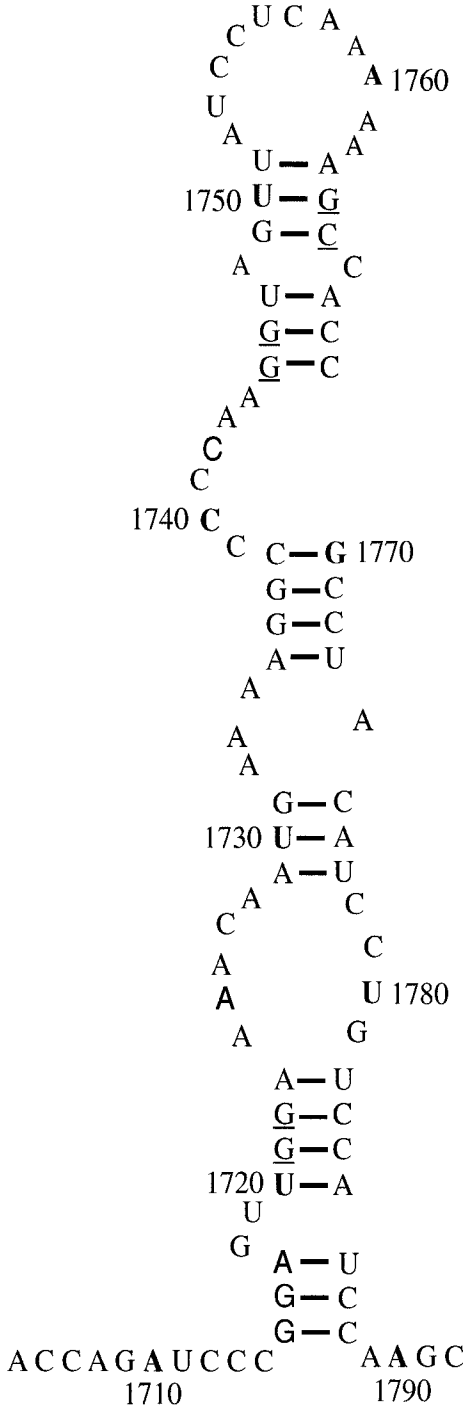
1760
1750
1740
1770
1730
1780
1720
ACCAGAUCCC
1710
AAGC
1790

C) Rat

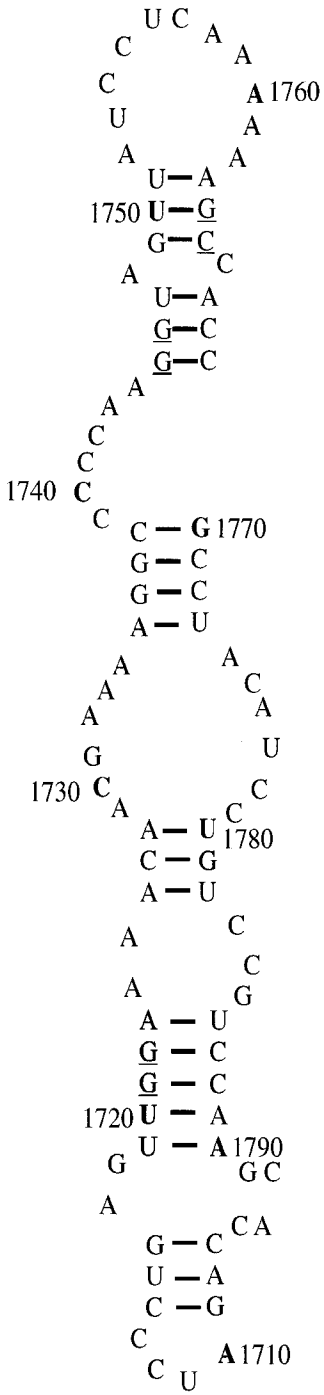
1760
1750
1740
1770
1730
1780
1720
1790
1710

d) Cow

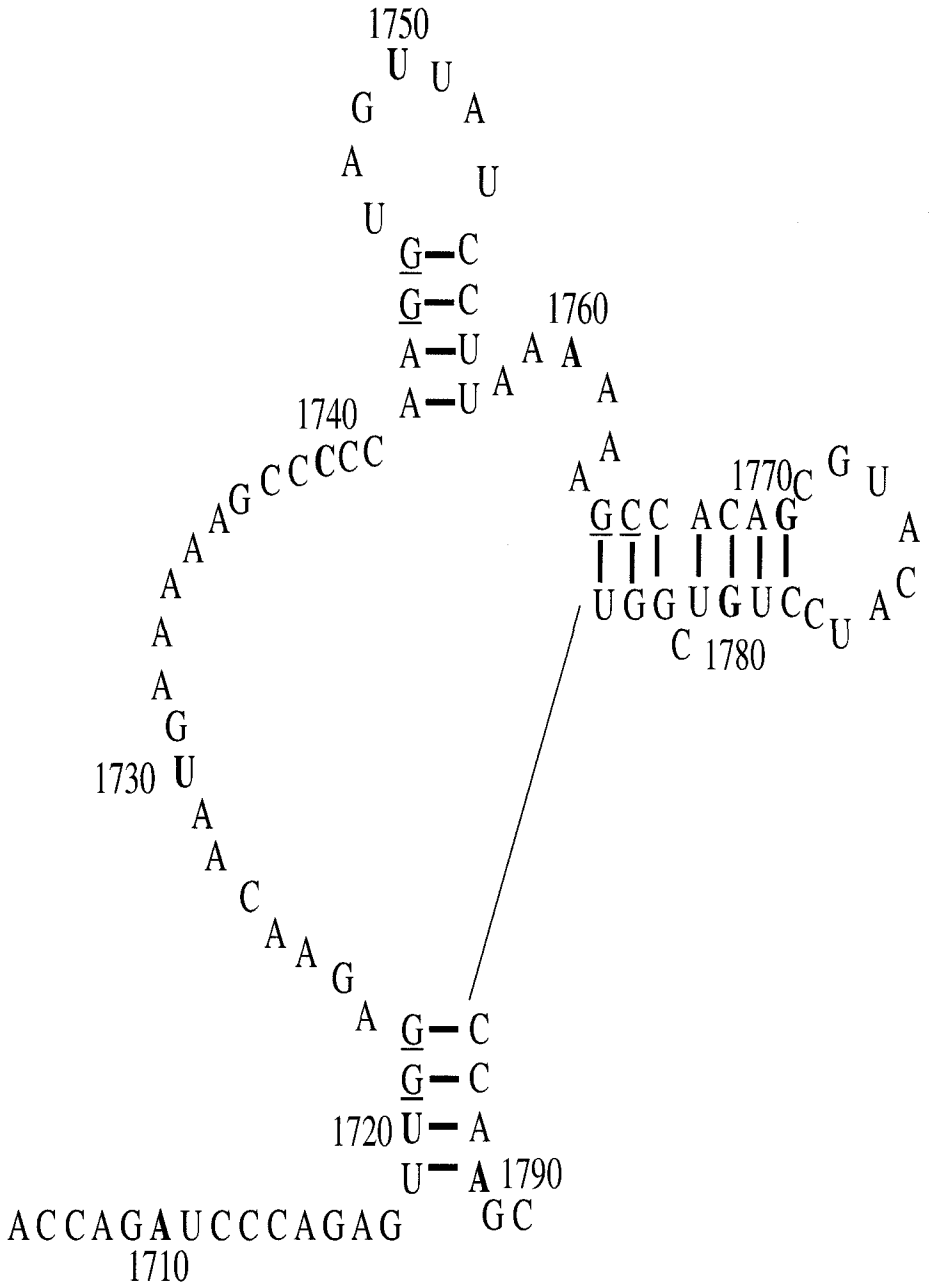

β-globin nts 3018-3159

Upon cleavage of the β-globin nts 3018-3159 RNA with RNase T1 under RNA-denaturing conditions, sixteen cleavage sites were generated. Fourteen of these cleavage sites were also obtained upon cleavage by RNase T1 under RNA native conditions including: G7,

G13, G22, G24, G32, G45, G62, G69, G71, G72, G74, G77, G81, and G84. The cleavage of these sites by RNase T1 under both RNA native and denaturing conditions indicate that these sites are localized within single-stranded domains. The lack of cleavage at G53 and G54 by RNase T1 under RNA native conditions indicates the inaccessibility of these sites for cleavage, and hence their presence in double-stranded domains. The intense cleavage at G81 by RNase T1 under native conditions in comparison with RNA denaturing conditions indicates that this site is present in a highly accessible region in the secondary structure. Upon cleavage with RNase T2, a laddering region is observed between nucleotides 1-12. Some of the nucleotides cleaved within this ladder were also cleaved by RNase V1 including A1, C2, A3, U4, U6, U10, C11, and U12. Cleavage of nucleotides 1-6 by RNase V1 might be due to the proximity of these nucleotides to a stem-rich area, which allows base-stacking to occur. The localization of nucleotides 1-6 in a single-stranded region is further highlighted by the intense cleavage at C2 by RNase A and the cleavage by RNase A of the following sites: U4, U5, and U6. The lack of cleavage by RNase V1 and the presence of cleavage by RNase T2 3' to nucleotides 7-9, indicates the localization of these nucleotides in a single-stranded domain. Cleavage 3' to nucleotides U10, C11, and U12 by RNase V1 and the single-strand specific enzymes RNase T2 and RNase A, indicates their presence in a dynamic structure that can alternate between open and double-stranded conformations. This dynamic structure also includes G13, which is cleaved by RNase T1 under both RNA denaturing and native conditions and by the double-strand specific enzyme, RNase V1. Overall, this indicates that nucleotides 11-13 may be part of stem II and that cleavage of these sites by the RNA single-strand specific enzymes is most likely due to the presence of the unstable G-U base-pairs that may form between U12 and G123, G13 and U122. The presence of the two non Watson-

Crick base-pairings may allow breathing of the stem, and hence accessibility of these sites by the RNA single-strand specific enzymes. Nucleotides A18, A19, and C20 were only cleaved by the single-strand specific enzyme, RNase T2, indicating their single-stranded localization. Furthermore, the third RNase T2 laddering region, encompassing nucleotides 39-44, also lacked RNase V1 cleavage and two nucleotides within this ladder were also cleaved by RNase A, including C39 and C43. Exception to this includes cleavage at C39 by RNase V1, which might be due to the stacking of this base. Cleavage by RNase V1 and RNase A also occurred at several positions including C15, C17, C27, U30, and C50. Cleavage 3' to C17 and C27 by both enzymes is most likely due to the breathing of the unstable AU base-pairs in the respective stems, thereby, allowing access for RNase A to cleave its target sequence. RNase A and RNase V1 cleavage at C15, U30, and C50 occurred at stem-loop junctions. RNase V1 is capable of cleaving at these sites due to their involvement in base-pair formation. However, it is also feasible for single-strand specific enzymes to cleave at such junctions as there is less steric hindrance in this region in comparison with a nucleotide that has a double-stranded 3' neighboring nucleotide.

Overall, the β-globin RNA nts 3018-3159 is an unstable and a dynamic structure. The instability of this structure is mainly the due to the large internal and multi-branch loops, which increase the free-energy of formation of the structure. Furthermore, the dynamic nature of this structure is also a consequence of the breathing of the weak A-U and G-U base pairs, which allows the structure to form alternate secondary structures. This structure is most likely stabilized *in vivo* by the binding of proteins or through electrostatic interactions with the negatively-charged phosphate backbone. Therefore, these two types of interactions may allow for the stabilization of the 3018-3159 β-globin mRNA secondary structure *in vivo*.

Chapter 3

Sequence and Structure Cleavage Specificity of the Novel Mammalian Endoribonuclease

The research described in this chapter was conducted to understand the sequence and structural cleavage specificities of the 1705-1792 c-*myc* CRD region by the novel mammalian endoribonuclease. It was also intended that the research would confirm the sequence and structural specificity of the enzyme using another *in vitro*-transcribed RNA substrate, namely, β-globin RNA corresponding to nts 3018-3159. Further confirmation of the sequence and structural specificity of the enzyme to the 1705-1792 CRD region was obtained by generating a series of mutants encompassing the 1705-1792 CRD region. Understanding the sequence and structural RNA cleavage specificity of the endoribonuclease, *in vitro*, is expected to provide insight into the sequence and structural cleavage specificity of the enzyme in cells.

3.0 Methods

3.0.1 The endoribonuclease assay and the identification of cleavage products

The 5' end-labeled 1705-1792 CRD and the 3018-3159 β-globin RNAs (usually 1-3 μl containing ~30,000 cpm) were incubated with 2 μl (~1-3 units) of the purified endoribonuclease, 18 μl reaction mix and made up to 25 μl with sterile water. Prior to incubation with the endonuclease, the RNA substrate was heated at 50-55^{0}C for 5 minutes and allowed to refold at room temperature for 10 minutes. The reaction mix contained 1M Tris pH 7.4 (2.8 μl), 100 mM DTT (5.6μl), 100 mM MgOAc (5.6 μl), 4M KOAc (3.5 μl), 2.5 mM spermidine (11.2 μl), 40 U/μl RNasin (4 μl), and made up to 252 μl with DEPC-H_2O. However, only 18 μl of reaction mix was required per reaction. Incubation was performed at

37^0C for 5 minutes and was terminated by the addition of 1 µl of phenol. The final volume was then made up to 200 µl with DEPC-H_2O, followed by standard ethanol precipitation and resuspension of the RNA pellet in 9M urea/phenol loading dye to give final counts of 15,000 cpm/µl. Two microlitres were loaded onto the gel for visualization. The negative control (not treated with the endoribonuclease) was done under the same conditions except that 2 µl of sterile water was added instead of the purified endonuclease or nothing was added. The cleavage products were identified by running the samples parallel to an alkaline ladder and a partial RNase T1 digest under the RNA denaturing condition (as described in section 2.0.3). The samples were then loaded and run onto a 12% polyacrylamide/7M urea gel and visualized as described in section 2.0.3.

3.0.2 Site-directed mutagenesis for the generation of the 1705-1792 CRD mutants

In order to determine the sequence and structure cleavage specificity of the mammalian endoribonuclease to the 1705-1792 c-*myc* CRD region, sequence and structural mutations were generated within the 1705-1792 CRD transcript. The mutations that were generated to investigate the sequence specificity of the endonuclease involved generating point mutations within the sites that were cleaved by the endoribonuclease or generating potentially new cleavage sites without altering the structural features of the RNA. Structural mutations were generated by collapsing cleavage sites present in a hairpin-loop into a double-stranded conformation or generating potentially new cleavage sites within a double-stranded region. The 1705-1792 CRD mutants were generated by designed primers (QIAGEN, Mississauga, ON), containing the mutations of interest. The forward primers consisted of (5' to 3'): *Bam*H1 restriction site, SP6 polymerase promoter, and wild-type or mutated CRD sequences. The reverse primers consisted of (5' to 3'): *Eco*R1 restriction site and wild-type or mutated

CRD sequences. Twelve mutants were generated in total, ten of which were designed to test the sequence specificity of the endonuclease. The remaining mutants were designed to examine the structure specificity of the endoribonuclease to the 1705-1792 CRD RNA.

The CRD mutants designed to determine the RNA sequence specificity of the endonuclease include CP-2, CP-3, CP-10C, CP-10G, CP-10U, CP-13, CP-15, CP-19A, CP-19G, and CP-19U. These mutants were generated using the primers shown in Table 3.1. The CP-2 and CP-3 CRD mutants were designed to test the specificity of the endonuclease to UA dinucleotides. The CP-2 CRD mutant involves altering the 1751 uridine residue into an adenosine residue and the 1752 adenosine residue into a uridine residue, thereby, converting the 1751 UA cleavage site into an AU site. The CP-3 CRD mutant focused on another UA site cleaved by the endonuclease (1757 UA), and it involved mutating the uridine at position 1757 into an adenosine residue and the 1758 adenosine into uridine, thereby, generating an AU dinucleotide. The CP-10C, CP-10G, and CP-10U CRD mutants were also designed to test the specificity of the endonuclease to UA dinucleotides. These mutants involved mutating the 1751 UA cleavage site into UC (CP-10C), UG (CP-10G), and UU (CP-10U) dinucleotides.

The CP-13 CRD mutant was designed to examine the specificity of the endoribonuclease to UG dinucleotides. This mutant involved mutating the 1730 uridines residue into a guanosine residue and the 1731 guanosine residue into a uridine residue, thereby, generating a GU dinucleotide.

Four mutants were generated to examine the specificity of the endonuclease to CA dinucleotides. The CP-15 CRD mutant involved mutating the cytidine at position 1727 into an adenosine and the adenosine at position 1728 into a cytidine, thereby, generating a 1727

AC dinucleotide. The CP-19A, CP-19G, and CP-19U CRD mutants involved mutating the cytidine residue at position 1727 into A, G, and U, respectively, thereby generating the following dinucleotides: 1727 AA (CP-19A), 1727 GA (CP-19G), and 1727 UA (CP-19U). In order to confirm the absence of any structural alterations in the ten CRD mutants, the mutants were folded using the Mfold software program (Zuker, 2003).

Two mutants were generated to investigate the structure specificity of the mammalian endonuclease to the 1705-1792 CRD RNA. The two primers used to generate the two structural mutants (CP-22 and CP-24) are shown in Table 3.1. The CP-22 CRD mutant involves altering the adenosine at position 1743 into a uridine residue and the uridine at position 1757 into an adenosine residue. These point mutations generate two additional UA dinucleotides at positions 1743 and 1756 that are localized within a double-stranded domain. The CP-24 CRD mutant involved mutating the adenosine at position 1752 into a uridine and the uridine at position 1753 into an adenosine, thereby allowing for the collapse of the hairpin loop and placing the 1747 UA endonuclease cleavage site into a double-stranded conformation. The presence of the target structural alterations within the two mutants was examined by folding the mutant RNAs using the Mfold program and probing the two structure mutants with RNase A. The RNase A reaction conditions were identical to the conditions described in section 2.0.3.

Table 3.1. The 1705-1792 CRD mutants designed for probing the sequence and structure specificity of the novel mammalian endonuclease.

CRD mutant	**Mutation**	**Sequence of forward primer[1]**	**Sequence of reverse primer[2]**	**RNA sequence[3]**
CP-2	U1751A and A1752U	FUP: 5'- CTC**GGATCC**ATTTAGG TGACACTATAGACCAGATCCCG GAGTTGG-3'	RCP-2: 5'- CTC**GAATTC**GCTTGGAC GGACAGGATGTATGCTGTGGCTTT TTTAAGGAatACT-3'	5'-ACCAGAUCCCGGAGUUGGAAA ACAAUGAAAAGGCCCCCAAGGUA GUAUUCCUUAAAAAAGCCACAGC AUACAUCCUGUCCGUCCAAGC-3'
CP-3	U1757A and A1758U	FUP	RCP-3: 5'-CTC**GAATTC**GCTTGGAC GGACAGGATGTATGCTGTGGCTTT TTTAAGGATAACatCCT-3'	5'-ACCAGAUCCCGGAGUUGGAAA ACAAUGAAAAGGCCCCCAAGGUA GUUAUCCUAUAAAAAGCCACAGC AUACAUCCUGUCCGUCCAAGC-3'
CP-10G	A1752G	FUP	RCP-10G: 5'-CTC**GAATTC**GCTTGG ACGGACAGGATGTATGCTGTGGC TTTTTTAAGGAcAAC-3;	5'-ACCAGAUCCCGGAGUUGGAAA ACAAUGAAAAGGCCCCCAAGGUA GUUGUCCUUAAAAAAGCCACAGC AUACAUCCUGUCCGUCCAAGC-3'
CP-10C	A1752C	FUP	RCP-10C:5'-CTC**GAATTC**GCTTGGA CGGACAGGATGTATGCTGTGGCTT TTTTAAGGAgAAC-3'	5'-ACCAGAUCCCGGAGUUGGAAA ACAAUGAAAAGGCCCCCAAGGUA GUUCUCCUUAAAAAAGCCACAGC AUACAUCCUGUCCGUCCAAGC-3'
CP-10U	A1752U	FUP	RCP-10U:5'-CTC**GAATTC**GCTTGGA CGGACAGGATGTATGCTGTGGCTT TTTTAAGGAaAAC-3'	5'-ACCAGAUCCCGGAGUUGGAAA ACAAUGAAAAGGCCCCCAAGGUA GUUUUCCUUAAAAAAGCCACAGC AUACAUCCUGUCCGUCCAAGC-3'
CP-13	U1730G andG1731U	FCP-13: 5'-CTC**GGATCC**ATTTAG GTGACACTATAGACCAGATCCC GGAGTTGGAAAACAAgtAAA-3'	RUP:5'-CTC**GAATTC**GCTTGGACG GACAGGATGTATGC-3'	5'-ACCAGAUCCCGGAGUUGGAAA ACAAGUAAAAGGCCCCCAAGGUA GUUAUCCUUAAAAAAGCCACAGC AUACAUCCUGUCCGUCCAAGC-3'
CP-15	C1727A and A1728C	FCP-15:5'-CTC**GGATCC**ATTTAG GTGACACTATAGACCAGATCC CGGAGTTGGAAAAacATG-3'	RUP	5'-ACCAGAUCCCGGAGUUGGAAA AACAUGAAAAGGCCCCCAAGGUA GUUAUCCUUAAAAAAGCCACAGC AUACAUCCUGUCCGUCCAAGC-3'
CP-19G	C1727G	FCP-19G:5'-CTC**GGATCC**ATTTA GGTGACACTATAGACCAGATC CCGGAGTTGGAAAAgAAT-3'	RUP	5'-ACCAGAUCCCGGAGUUGGAAA AGAAUGAAAAGGCCCCCAAGGUA GUUAUCCUUAAAAAAGCCACAGC AUACAUCCUGUCCGUCCAAGC-3'

CP-19U	C1727U	FCP-19U:5'-CTC**GGATCC**ATTTA GGTGACACTATAGACCAGATC CCGGAGTTGGAAAAtAAT-3'	RUP	5'-ACCAGAUCCCGGAGUUGGAAA AUAAUGAAAAGGCCCCCAAGGUA GUUAUCCUUAAAAAAGCCACAGC AUACAUCCUGUCCGUCCAAGC-3'
CP-19A	C1727A	FCP-19A:5'-CTC**GGATCC**ATTTA GGTGACACTATAGACCAGATC CCGGAGTTGGAAAAaAAT-3'	RUP	5'-ACCAGAUCCCGGAGUUGGAAA AAAAUGAAAAGGCCCCCAAGGUA GUUAUCCUUAAAAAAGCCACAGC AUACAUCCUGUCCGUCCAAGC-3'
CP-22	A1743U and U1757A	FUP	RCP-22: 5'-CTC**GAATTC**GCTTGGA CGGACAGGATGTATGCTGTGGCTT TTTTtAGGATAACTACCTaGGG-3'	5'-ACCAGAUCCCGGAGUUGGAAA ACAAUGAAAAGGCCCCCUAGGUA GUUAUCCUAAAAAAAGCCACAGC AUACAUCCUGUCCGUCCAAGC-3'
CP-24	A1752U and U1753A	FUP	RCP-24: 5'-CTC**GAATTC**GCTTGGA CGGACAGGATGTATGCTGTGGCTT TTTTAAGGtaAAC- 3'	5'-ACCAGAUCCCGGAGUUGGAAA ACAAUGAAAAGGCCCCCAAGGUA GUUUACCUUAAAAAAGCCACAGC AUACAUCCUGUCCGUCCAAGC-3'

1. Bold letters indicate *Bam*HI restriction site and small letters indicate mutant residues.
2. Bold letters indicate *Eco*RI restriction site and small letters indicate mutant residues.
3. Underlined letters indicate mutation sites.

3.0.3 PCR amplification, digestion, subcloning, and ligation

The plasmid construct containing the wild-type (WT) 1705-1792 cDNA (pUC19-myc 1705-1792) was used as a template for Polymerase Chain Reaction (PCR) to generate products containing the target CRD mutations. The PCR products (5 PCR replicates per mutant) were then cleaved with *Bam*HI and *Eco*RI and subcloned into a pUC19 plasmid cut with *Bam*HI and *Eco*RI. The PCR reaction consisted of the pUC19-myc 1705-1792 template (2 ng), 1 µl of the forward primer (100 ng/µl), 1 µl of the reverse primer (100 ng/µl), 3.5 µl of the 10X PCR buffer (New England Biolabs, Beverly, MA), 3.5 µl of dNTPs (2.5 mM, also containing 50 mM $MgCl_2$), 0.5 µl of *Taq* Polymerase (5 U/ µl) (New England Biolabs, Ontario), and made up to 35 µl with sterile water. The PCR products were then generated using the Minicycler™ Peltier Thermal Cycler (MJ Research, Inc., Reno, NV) using the following steps: step 1, template denaturation at 94^0C for 30 seconds; step 2, primer annealing at 50^0C for 30 seconds; step 3, primer extension at 72^0C for 45 seconds; step 5, repeating the above steps for 29 additional cycles. The five PCR products were then pooled together, ethanol precipitated, resuspended in 10 µl gel-loading dye (0.02% w/v bromophenol blue, 0.02% w/v xylene cyanol), and loaded onto a 2% agarose gel for gel-purification. The gel was run at 35 mA in 0.5X TBE buffer for one hour. The PCR products were then gel-purified using the QIAEX II Gel Extraction Kit (Qiagen, Montreal). Gel-purification involved resuspending the gel containing the PCR products with three volumes (typically ~0.5 ml) of Buffer QX1 (contents not listed in QIAEX protocol), which functions to solubilize the gel, leading to the elution of the PCR products (Qiagen, 1999). This is followed by the addition of 20 µl of the QIAEX II resin (contains a highly electrolytic environment which allows DNA adsorption), and then incubation at 50^0C for 10 minutes

with frequent vortexing to allow for resin suspension. The solution was then centrifuged for 30 seconds at 13,000 rpm to precipitate the resin and the supernatant was removed. The resin pellet was then washed with 500 µl of Buffer QX1 and resuspended by vortexing, followed by centrifugation at 13,000 rpm for 30 seconds and removal of all traces of the supernatant. This washing step functions to remove residual salt contaminants that may later interfere with restriction digestion (according to the manufacturer's instructions). The pellet was then washed twice with 500 µl of Buffer PE (contents not described in protocol), which contains ethanol and efficiently removes salt contaminants (according to the manufacturer's instructions). This involved resuspending the pellet in the washing buffer by vortexing, centrifugation at 13,000 rpm for 30 seconds, and then removing all traces of the buffer. The washed pellet was then air dried until it became white (~30 minutes), resuspended in 20 µl Tris-EDTA buffer, pH 8.0, to allow for DNA elution, followed by incubation for 5 minutes at room temperature. The solution was then centrifuged for 30 seconds at 13,000 rpm and the supernatant containing the PCR product was transferred into another microtube. In order to increase the PCR product recovery, the above steps involving the elution with 20 µl of Tris-EDTA buffer, pH 8.0, were repeated and the supernatant was pooled with the previously eluted DNA solution. The pooled DNA was then ethanol precipitated and resuspended in 10 µl sterile water in preparation for restriction digestion. The PCR product (10 µl) was then digested with 3 µl of *Bam*HI (10 U/µl) (Invitrogen Life Technologies, Ontario), 3 µl of *Eco*RI (10 U/µl) (Invitrogen Life Technologies, Ontario), 2 µl of 10X React 3 Buffer, and made up to 20 µl with sterile water. Digestion of the PCR product was done for 3 hours at 37^0C, followed by standard ethanol precipitation, and resuspension in 21 µl sterile water in preparation for subcloning into the pUC19 plasmid. The pUC19 digestion was performed in a

20 µl final volume containing 3.7 µg of the plasmid, 4 µl of *Bam*HI (10 U/µl), 4 µl of *Eco*RI (10 U/µl), 2 µl of 10X React 3, and made up to 20 µl with sterile water. Incubation was done for three hours at 37^0C, followed by standard chloroform/phenol extraction, standard ethanol precipitation, and resuspension in 70 µl sterile water to obtain a final plasmid concentration of 50 ng/µl.

The digested PCR product was then subcloned into the linearized pUC19 plasmid. The ligation reaction was performed in a 20 µl final volume containing 1 µl of linearized pUC19 (50 ng/µl), 10.5 µl of the digested PCR product, 2 µl of 10X DNA ligase buffer (New England Biolabs, Ontario), and 2 µl (2,000 U/µl) of T4 DNA ligase (New England Biolabs, Ontario), and the solution was then made up to 20 µl with sterile water. The ligation reaction was then incubated for two hours at room temperature.

3.0.4 Preparation of Competent Cells, transformation, and plating

Preparation of competent DH5α cells involved the addition of 10 µl of frozen DH5α stock cells to 3 ml of Luria-Bertani (LB) broth and allowing for overnight agitation at 37^0C. Five hundred microlitres of the overnight grown DH5α cells were then added to 50 ml LB broth and allowed to grow until OD_{600}= 0.6. The 50 ml broth, containing the bacterial cells, was centrifuged at 2,500 rpm for five minutes and the supernatant was removed. The cell pellet was then resuspended in 2.5 ml of cold 50 mM $CaCl_2$, and the volume was made up to 25 ml and stored on ice for 20 minutes. The sample was then centrifuged for five minutes at 2,500 rpm, followed by removal of the supernatant, and resuspension in 3.5 ml of $CaCl_2$. The 3.5 ml solution containing the competent cells was then stored at 4^0C.

Transformation of the ligated plasmid into the competent DH5α cells involved transfecting 200 µl of the competent cells with 7.5 µl of the ligation mix in a pre-chilled

round-bottom flask, followed by thorough mixing and chilling on ice for 30 minutes. The sample was then heat-shocked at 42^{0}C for two minutes, followed by the addition of 1 ml LB broth and agitation at 37^{0}C for 30 minutes. Two microlitres of 1M isopropyl β-D-thiogalactoside (IPTG) and 10 µl (20 mg/ml) of bromo-4-chloro-3-indolyl-beta-D-galactopyranosie (X-GAL) were then added to the 1 ml LB broth solution, and poured into a pre-warmed agar plate containing 0.05 mg/ml ampicillin. The plates containing the cells were incubated in an upright position at 37^{0}C for 30 minutes with the lid partly open, followed by overnight incubation at 37^{0}C in an inverted position.

3.0.5 Colony selection, plasmid extraction, and checking for the presence of insert

Ten white colonies were picked from the agar plate using a pipette tip and added to 3 ml of LB broth (which also had 1.5 µl of 50 mg/ml ampicillin added to it), followed by overnight agitation at 37^{0}C. The plasmid was extracted from the bacterial cells using a mini-prep procedure, which involved transferring 1.5 ml of the overnight grown cells into a microtube, followed by centrifugation at 13,000 rpm for two minutes. The supernatant was then removed and the pellet was resuspended in 500 µl STET buffer (0.1M NaCl, 10 mM Tris-Cl, pH 8.0, 1 mM EDTA, pH 8.0, 5% Triton X-100) and 10 µl of 50 mg/ml lysozyme. The solution was then boiled for one minute and centrifuged for ten minutes at 13,000 rpm to allow for chromosomal DNA precipitation. The chromosomal pellet was removed using a sterile toothpick and 500 µl isopropanol was added to the supernatant containing the recombinant plasmid, followed by incubation at –20^{0}C for 30 minutes. The sample was then centrifuged for ten minutes at 13,000 rpm, followed by the removal of the supernatant, washing the pellet with 200 µl of 70% ethanol, air drying at room temperature for 15 minutes, and then resuspension of the pellet in 25 µl sterile water. A mini-digest was then

performed and was run onto a 2% agarose gel to check for the presence of insert. This involved incubating 2 µl of the mini-prepped plasmid with 1 µl of *Bam*HI (10 U/µl), 1 µl of *Eco*RI (10 U/µl), 2 µl of 10X React 3, and making up the reaction volume to 10 µl with sterile water. The reaction was performed at 37^0C for 30 minutes, followed by the addition of 1 µl of RNase A (10 mg/ml) and 1.5 µl of gel-loading dye and running onto a 2% agarose gel for 1.5 hours at 45 mA. The sample was run parallel to an undigested mini-prepped plasmid. Colonies containing the insert were then stored in 17% glycerol at -80^0C

3.0.6 Plasmid preparation and sequencing of the RNA mutants

In order to obtain a high quantity of recombinant plasmids, the Qiagen Plasmid Midi Kit (Qiagen Inc. Mississauga, ON) was used. One hundred and fifty micrcolitres of the colony (stored in 17% glycerol) containing the mutant insert was added to 150 ml LB broth to which 150 µl of 50 mg/ml ampicillin was added, followed by overnight agitation at 37^0C. The cells were then centrifuged at 6,000 x g for 15 minutes and all traces of the supernatant were removed. Four milliliters of Buffer P1 (50 mM Tris.Cl pH 8, 10 mM EDTA, 100 µg/ml RNase A) were then added to resuspend the cell pellet until no clumps were present. The lysis buffer, P2 [200 mM NaOH, 1% SDS (w/v)] was then added (4 ml) to the cell solution and mixed thoroughly by gently inverting 4-6 times, followed by incubation for five minutes at room temperature. Four milliliters of the pre-chilled P3 Buffer (3.0 M potassium acetate pH 5.5) were immediately added to the solution, followed by gentle inverting 4-6 times and incubation for 15 minutes on ice. The addition of Buffer P3 allows for enhanced precipitation of genomic DNA, proteins, cell debris, and SDS. The sample was then mixed again and immediately centrifuged at 20,000 x g at 4^0C for 30 minutes. The supernatant containing the plasmid was then poured into a new Nalgene tube and centrifuged again at 20,000 x g at 4^0C

for 15 minutes. The supernatant was then poured into the QIAGEN-tip 100 (anion-exchange resin), which was equilibrated with Buffer QBT [750 mM NaCl, 50 mM MOPS pH 7.0, 15% isopropanol (v/v), and 0.15% Triton^R X-100 (v/v)]. The Qiagen-tip was then washed two times with 10 ml of Buffer QC [1.0 M NaCl, 50 mM MOPS pH 7.0, 15% isopropanol (v/v)], which acts to remove all contaminants in plasmid preparations such as carbohydrates (Qiagen, 1999). The plasmid was then eluted with 5 ml Buffer QF [1.25 M NaCl; 50 mM Tris.Cl pH 8.5; 15% isopropanol (v/v)] into a sterilized transparent Nalgene tube. The DNA was then precipitated by the addition of 4 ml isopropanol and immediately centrifuged for 30 minutes at 4^{0}C at 15,000 x g. The supernatant was then carefully removed and the DNA pellet was then washed with 2 ml of 70% ethanol and centrifuged at 5,000 x g for ten minutes. The 70% ethanol was then removed and the pellet was allowed to dry for 30 minutes. The pellet was then resuspended in 100 µl sterile water, quantified at 260 nm, followed by restriction digestion with *Eco*RI and *Bam*HI, and running of samples onto a 2% agarose gel to check for the presence of DNA insert.

3.0.7 *In vitro* transcription, dephosphorylation, 5' end-labeling, and gel-purification

This was identical to the procedures described in sections 2.0.1 and 2.0.2

3.1 Results

3.1.1 Cleavage sites generated by the mammalian endoribonuclease using the 1705-1792 c-*myc* CRD and 3018-3159 β-globin RNAs as substrates.

CRD nts 1705-1792

Upon incubation of the 1705-1792 CRD RNA substrate with the purified mammalian endonuclease for five minutes at 37^{0}C, fourteen cleavage sites were generated (Figure 3.1a and b). These sites included intense cleavage at 1727 CA and 1751 UA, and extremely weak cleavage at 1740 CC, 1741 CC, 1750 UU and 1766 CA. Moderate cleavage was observed at

the following dinucleotides: 1730 UG, 1742 CA, 1747 UA, 1757 UA, 1768 CA, 1771 CA, 1773 UA, and 1775 CA. There are four UA dinucleotides within single-stranded regions in the 1705-1792 CRD RNA and all of which were cleaved by the endoribonuclease (Figure 3.1b). In addition, there are eight CA dinucleotides in the 1705-1792 CRD region, two of which, however, were beyond the detection limit of the polyacrylamide gel (CA dinucleotides at positions 1707 and 1788). The remaining six CA dinucleotides were all cleaved by the endoribonuclease. It is also important to note that five of the CA dinucleotides: 1727, 1742, 1766, 1768, 1775 that were cleaved by the endonuclease are located within single-stranded regions (Figure 3.1b). Three UG dinucleotides are present within the 1705-1792 CRD region. However, two of which were beyond the limits of the gel (UG dinucleotides at positions 1720 and 1780). The identifiable UG dinucleotide at position 1730 (double-stranded) was cleaved by the endoribonuclease (Figure 3.1a and 3.1b). Eleven CC dinucleotides are present within the 1705-1792 CRD region, however, only six were identifiable within the limits of the gel (1738, 1739, 1740, 1741, 1754, 1765). Two of the identifiable CC dinucleotides were weakly cleaved by the endonuclease, including the single-stranded dinucleotides at positions 1740 and 1741. Lastly, there are two identifiable UU dinucleotides within the 1705-1792 CRD RNA (1750 UU and 1756 UU). Only the single-stranded UU dinucleotide at position 1750 was cleaved, very weakly, by the endonuclease.

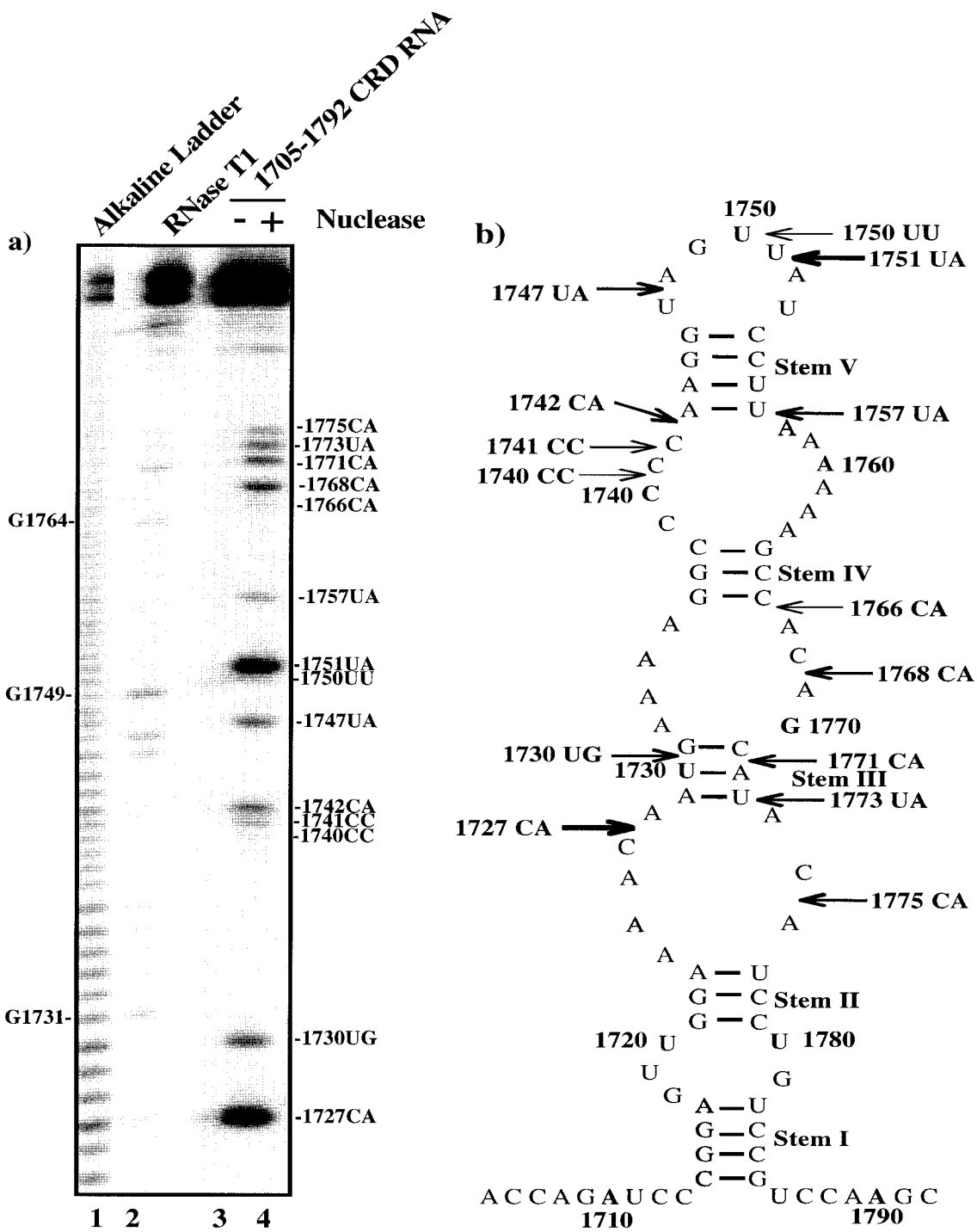

Figure 3.1. Cleavage sites generated by the mammalian endonuclease using the 1705-1792 CRD RNA as a substrate. A, the samples were run on a 12% polyacrylamide/7M urea gel parallel to an alkaline ladder and an RNase T1 digest for band identification. Numbering on the left indicates several guanosine residues cleaved by RNase T1, while bands on the right indicate cleavage sites generated by the endonuclease. B, location of the fourteen cleavage sites generated by the endonuclease. The cleavage intensity is indicated by the thickness of the arrow.

β-globin nts 3018-3159

Upon incubation of the β-globin 3018-3159 RNA with the endonuclease for 5 minutes at 37 ^{0}C, twenty-two cleavage sites were identifiable on the 12% polyacrylamide/7M urea gel (Figures 3.2a and 3.2b). Intense cleavage occurred at the dinucleotides: 2 CA, 39 CA, and 43 CA, whereas weak cleavage occurred at dinucleotides: 4 UU, 5 UU, 6 UG, 8 CU, 9 UU, 10 UC, 11 CU, 23 UG, 27 CA, 47 CA, and 52 UG. Moderate cleavage occurred at dinucleotides: 12 UG, 15 CA, 17 CA, 20 CU, 21 UG, 30 UA, 33 CA, and 50 CA. There is only one UA dinucleotide in the β-globin 3018-3159 RNA. This dinucleotide (30 UA) is present in a single-stranded domain and was cleaved by the mammalian endonuclease (Figures 3.2a and 3.2b) Twelve CA dinucleotides are present within the β-globin 3018-3159 RNA, however, nine of which were identifiable within the limits of the gel (up to dinucleotide 50 CA). The nine identifiable CA dinucleotides were all cleaved by the endonuclease (Figures 3.2a and 3.2b). The endonuclease was able to cleave CA dinucleotides present within single-stranded (2 CA, 15 CA, 33 CA, 39 CA, 43 CA, 47 CA, 50 CA) and double-stranded regions (17 CA, 27 CA). Nineteen UG dinucleotides are present within the β-globin 3018-3159 RNA, however, only five were identifiable using the described gel electrophoresis conditions. All five dinucleotides were cleaved by the endonuclease and all are present within single-stranded domains (6 UG, 12 UG, 21 UG, 23 UG, 52 UG). There are six UU dinucleotides within the β-globin 3018-3159 RNA, however, only four were detectable using the described conditions of the gel. Three of the four detected UU dinucleotides, which are localized in single-stranded domains, were cleaved by the endonuclease (4 UU, 5 UU, 9 UU). The double-stranded 25 UU, however, was not cleaved by the endonuclease. Lastly, there are five detectable CU dinucleotides within the 3018-3159

β-globin RNA. The single-stranded dinucleotides: 8 CU, 11 CU, and 20 CU were all cleaved by the endonuclease, while none of the double-stranded CU dinucleotides (29 CU and 37 CU) were cleaved by the endonuclease.

3.1.2 Sequences of the pUC19 plasmids containing the mutant 1705-1792 cDNAs

The pUC19 plasmids containing the mutant 1705-1792 cDNAs were sequenced by the DNA Sequencing Laboratory at the University of British Columbia (Vancouver, BC). The 1705-1792 c-*myc* plasmid sequences containing the CRD mutants are found in the Appendix of this thesis. All of the sequences were as expected, except those corresponding to CP-10G, CP-13 and CP-22. The sequenced CP-10G CRD mutant (5'-ACCAGAUCCCGGAGUUGGAAAACAAUGAAAAGGCCCCCAAGGUAGUUGUCCU UAAAAAAGCCACAGAUACAUCCUGUCCGUCCAAGC-3') contained the target mutation, however, it lacked the cytidine residue at position 1771. The sequenced CP-13 CRD mutant (5'-ACCAGAUCCCGGAGUUGGAAAACAAGUAAAGGCCCCCAAGGUA GUUAUCCUUAAAAAAGCCACAGCAUACAUCCUGUCCGUCCAAGC-3') consisted of the target mutations: U1730G and G1731U, however, it lacked one of the four adenosine residues located between 1732-1734. The sequenced CP-22 (5'-ACCAGAUCCAGAGUUGGAAAACAAUGAAAAGGCCCCCUAGGUAGUUAUCCUA AAAAAAGCCACAGCAUACAUCCUGUCCGUCCAAGC-3') mutant consisted of the target mutations: A1743U and U1757A, however, other mutations were present. The mutations included the deletion of 1714C and 1715G and the addition of an adenosine residue at position 1714. Although the above three CRD mutants contained unwanted mutations, they were also analyzed for understanding the sequence and structure cleavage specificity of the mammalian endonuclease.

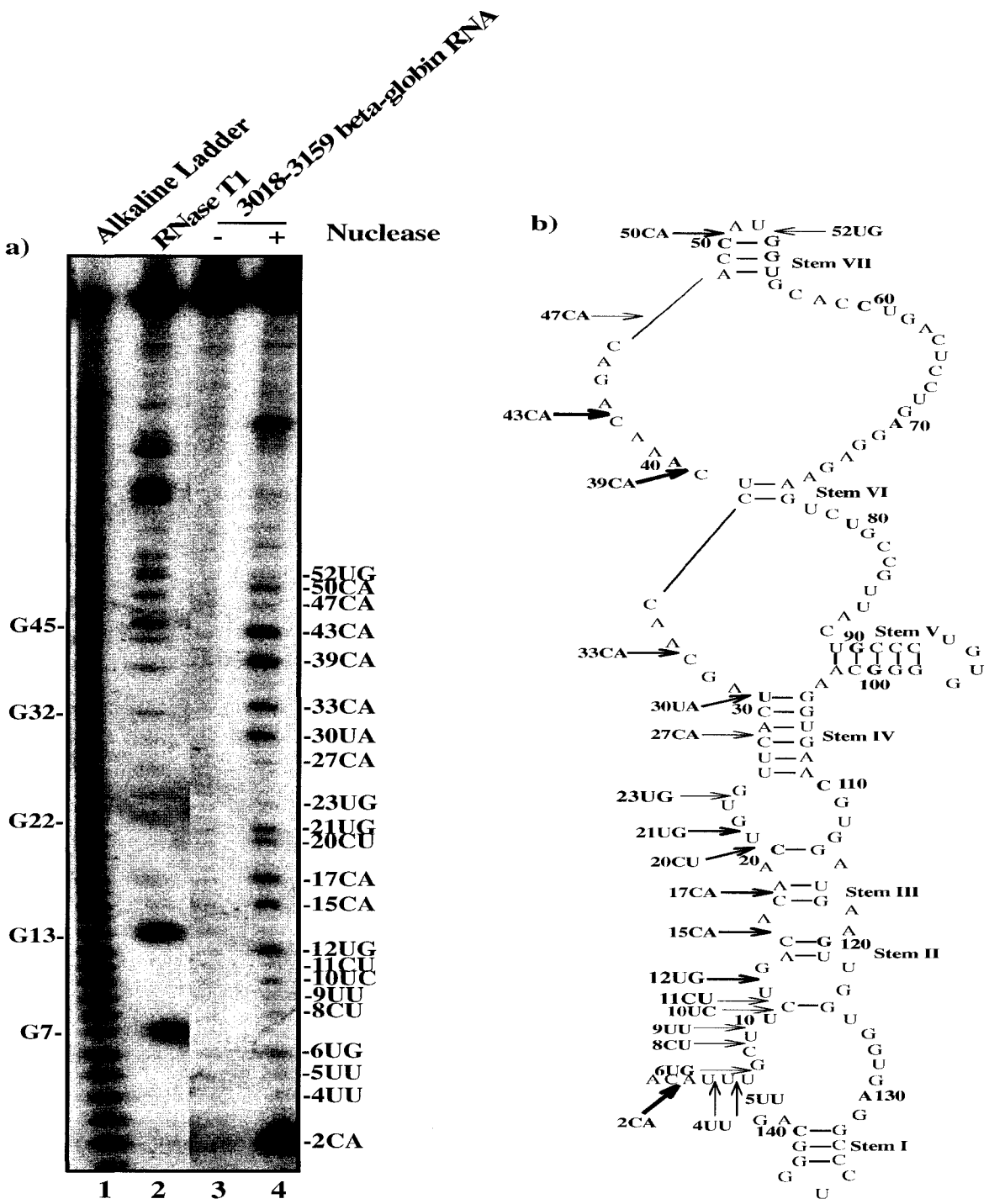

Figure 3.2. Cleavage sites generated by the mammalian endonuclease using the β-globin 3018-3159 RNA as a substrate. A, the samples were run on a 12% polyacrylamide/7M urea gel parallel to an alkaline ladder and a partial RNase T1 digest for band identification. Numbering on the left indicate several guanosine residues cleaved by RNase T1, while numbering on the right indicate cleavage sites generated by the endonuclease. B, location of the twenty-two cleavage sites generated by the endonuclease. The cleavage intensity is indicated by the thickness of the arrow.

3.1.3 The sequence/structure cleavage specificity of the endoribonuclease to the different 1705-1792 CRD RNA mutants.

Specificity to UA dinucleotides

The CP-2 and CP-3 CRD mutants were designed to examine the specificity of the endonuclease to UA dinucleotides. Upon incubation of the CP-2 RNA mutant (1751 UA to AU) with the mammalian endonuclease, cleavage at position 1751 was abolished (lane 6, Figure 3.3a). In addition, the endonuclease was able to cleave the newly-generated single-stranded UA dinucleotide at position 1750 (lane 6, Figure 3.3a; Figure 3.3b). This cleavage was approximately similar in intensity to the cleavage of the 1751 UA dinucleotide in the wild-type (WT) 1705-1792 CRD RNA by the endonuclease (compare lane 4 with 6, Figure 3.3a). Upon incubation of the CP-3 CRD mutant (1757 UA to AU) with the mammalian endonuclease, cleavage at position 1757 was abolished (lane 8, Figure 3.3a; Figure 3.3c). Furthermore, the endonuclease was able to cleave the new single-stranded UA dinucleotide at position 1758, in addition to the cleavage of the new 1756 UA dinucleotide present at a stem-loop junction. Interestingly, while the intensity of the bands related to the other cleavage sites remained unchanged, there was an enhanced band at position 1742 CA, which indicates that this dinucleotide became more accessible for enzymatic cleavage. This is because it changed from being in a stem-loop junction to a single-stranded domain.

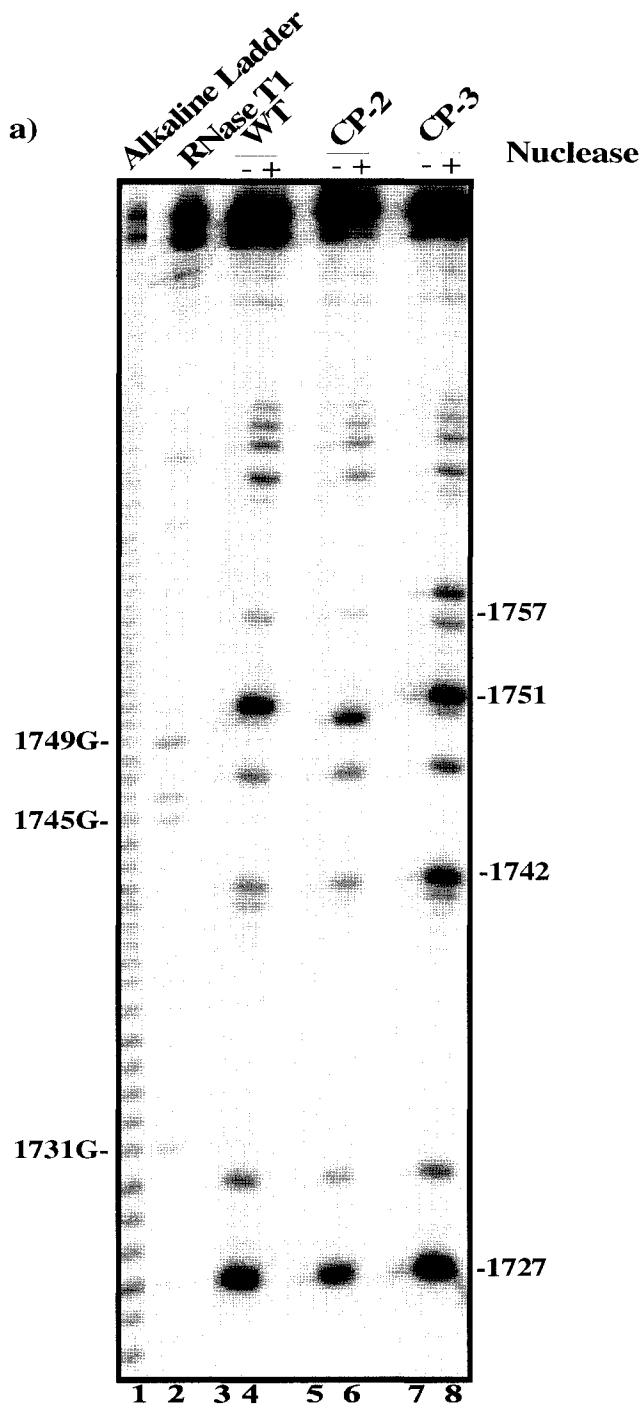

Figure 3.3. The cleavage of the CP-2 and CP-3 CRD mutants by the endonuclease. A), the digested CP-2 and CP-3 CRD mutants were run a 12% polyacrylamide/7M urea gel parallel to an alkaline ladder and an RNase T1 digest. Numbering on the left indicate several of the guanosine residues cleaved by RNase T1, while numbering on the right indicate cleavage sites generated by the endonuclease using the WT RNA as a substrate. B) and C) indicate cleavage sites generated upon incubation of the CP-2 and CP-3 CRD mutants with the endonuclease, respectively. Thick arrows indicate enhanced cleavage, underlined nucleotides indicate mutated residues, and the t-shaped symbol indicates blockage of cleavage.

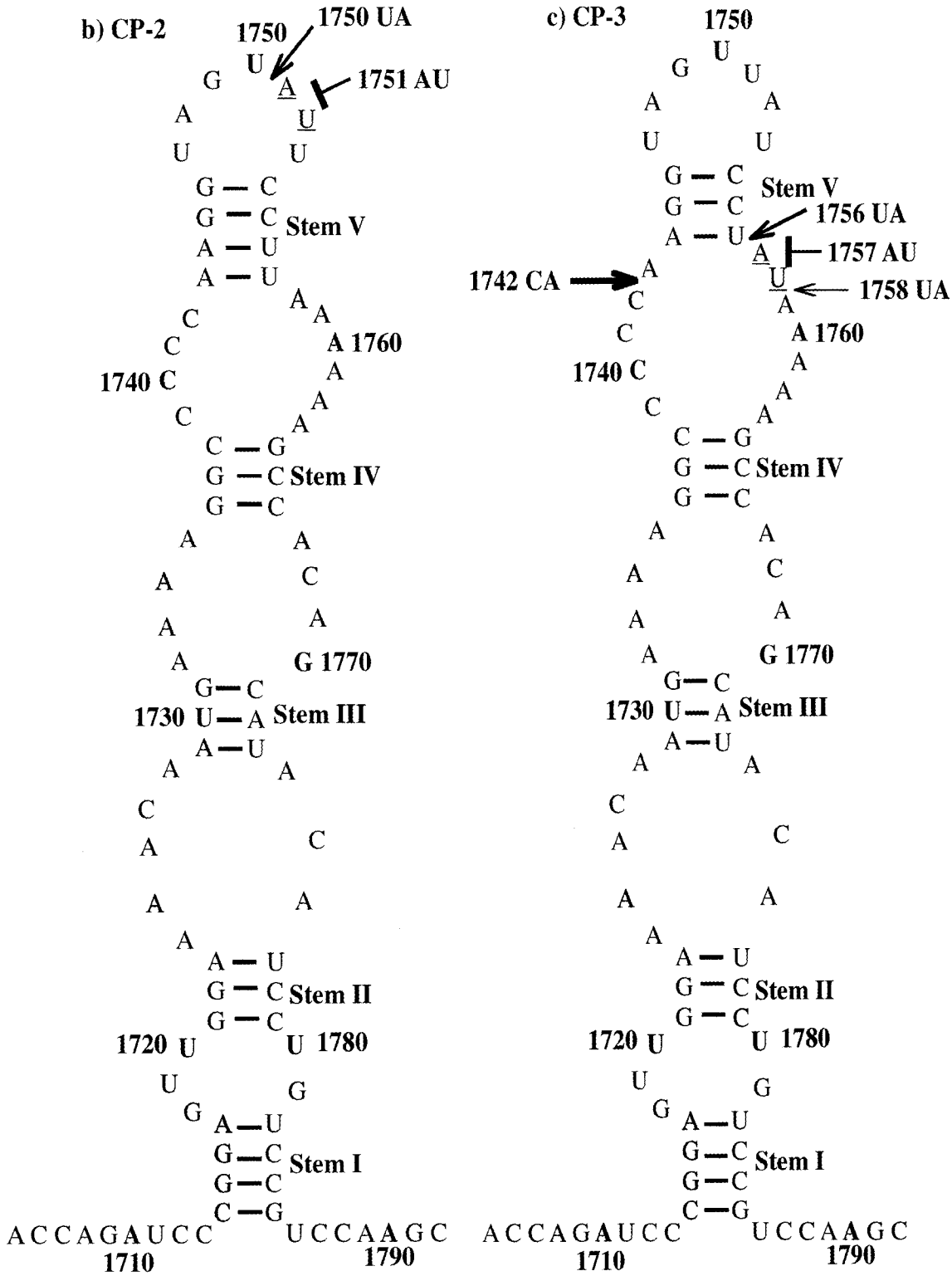
b) CP-2
1750
1750 UA
1751 AU
Stem V
A 1760
1740 C
Stem IV
G 1770
1730 U—A
Stem III
Stem II
1720 U
U 1780
Stem I
ACCAGAUCC
UCCAAGC
1710
1790
c) CP-3
1750
Stem V
1756 UA
1757 AU
1758 UA
1742 CA
A 1760
1740 C
Stem IV
G 1770
1730 U—A
Stem III
Stem II
1720 U
U 1780
Stem I
ACCAGAUCC
UCCAAGC
1710
1790

Upon incubation of the CP-10C RNA mutant (1751 UA to UC) with the mammalian endonuclease, there was a decrease in cleavage at the 1751 dinucleotide (UC dinucleotide) (lane 6, Figure 3.4a; Figure 3.4b) in comparison with the respective WT RNA cleavage (lane 4, Figure 3.4a). Furthermore, the cleavage intensity at the single-stranded 1751 UC was a weak cleavage in comparison with the bands in the same lane. Digestion of the CP-10G RNA mutant (1751 UA to UG) with the mammalian endonuclease, led to a decrease in cleavage at the 1751 UG dinucleotide (lane 8, Figure 3.4a; Figure 3.4c). The absence of cleavage at the 1771 CA dinucleotide was due to an unintentional deletion of the 1771 cytidine residue. This led to the faster migration of the high molecular cleavage sites: 1772 UA and 1774 CA, which correspond to WT dinucleotides: 1773 UA and 1775 CA, respectively. Lastly, upon incubation of the CP-10U RNA mutant (1751 UA to UU) with the mammalian endonuclease, cleavage at position 1751 was abolished (lane 6, Figure 3.5a; Figure 3.5b). There was also a marked decrease in cleavage at the 1747 UA dinucleotide, which is present in the same hairpin loop as the 1751 UU dinucleotide. It is important to note that the discrepancy observed between the migration of the WT and CP-10U RNA bands is due to the unbalanced electric current that was run through the gel, rather than the presence of a nucleotide deletion. The unbalanced current led to the uneven migration of the CP-10U RNA samples, hence, the observed migration difference between the WT and the CP-10U cleavage fragments.

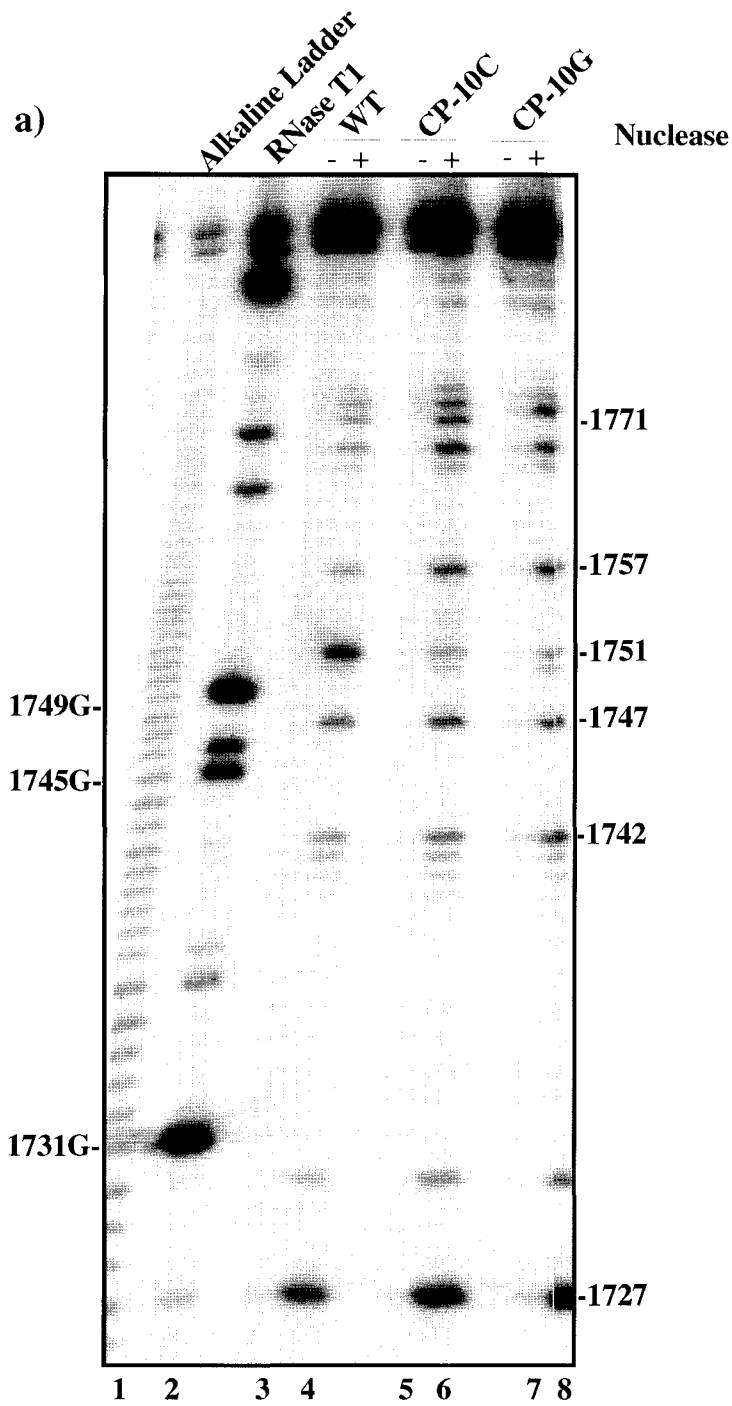

Figure 3.4. The cleavage of the CP-10C and CP-10G CRD mutants by the endonuclease. A), the digested CP-10C and CP-10G were run on a 12% polyacrylamide/7M urea gel parallel to an alkaline ladder and an RNase T1 digest. Numbering on the left indicate several of the guanosine residues cleaved by RNase T1, while numbering on the right indicate cleavage sites generated by the endonuclease using the WT RNA as a substrate. B) and C) indicate cleavage sites generated upon incubation of the CP-10C and CP-10G with the endonuclease, respectively. Dotted arrows indicate decreased cleavage and underlined nucleotides indicate mutated residues.

b) CP-10C

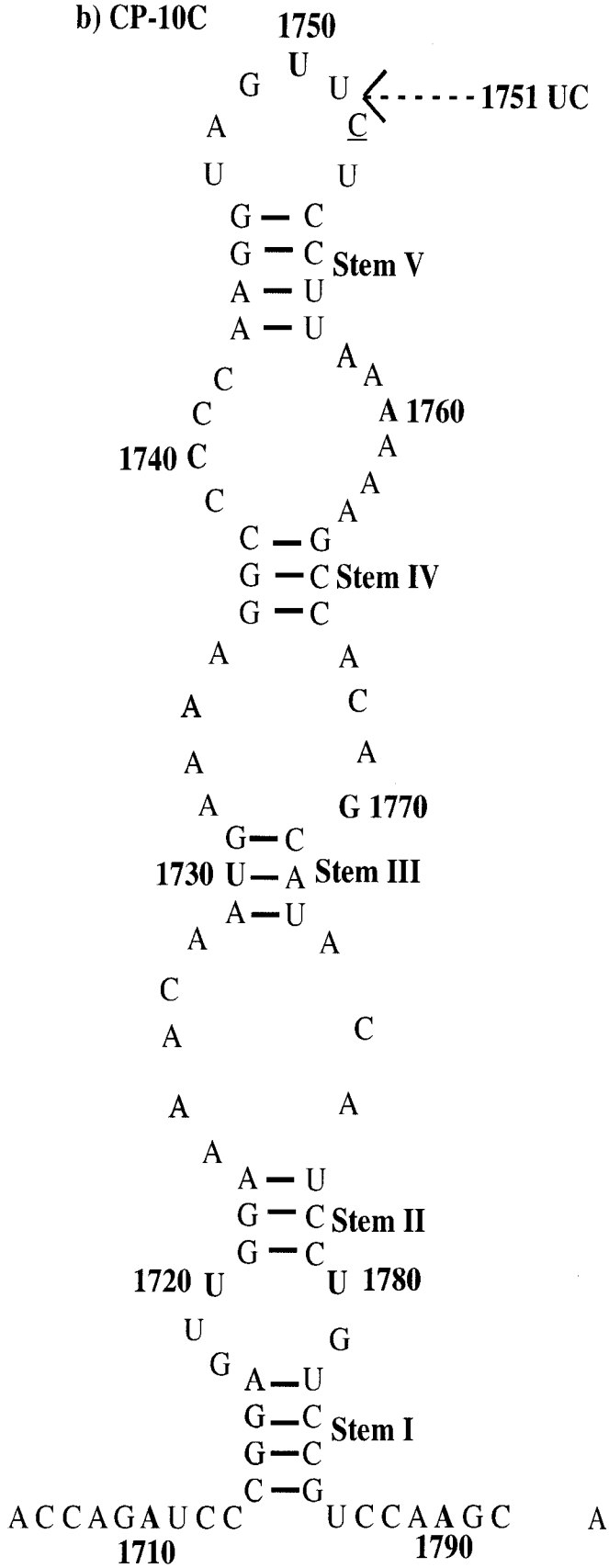

c) CP-10G

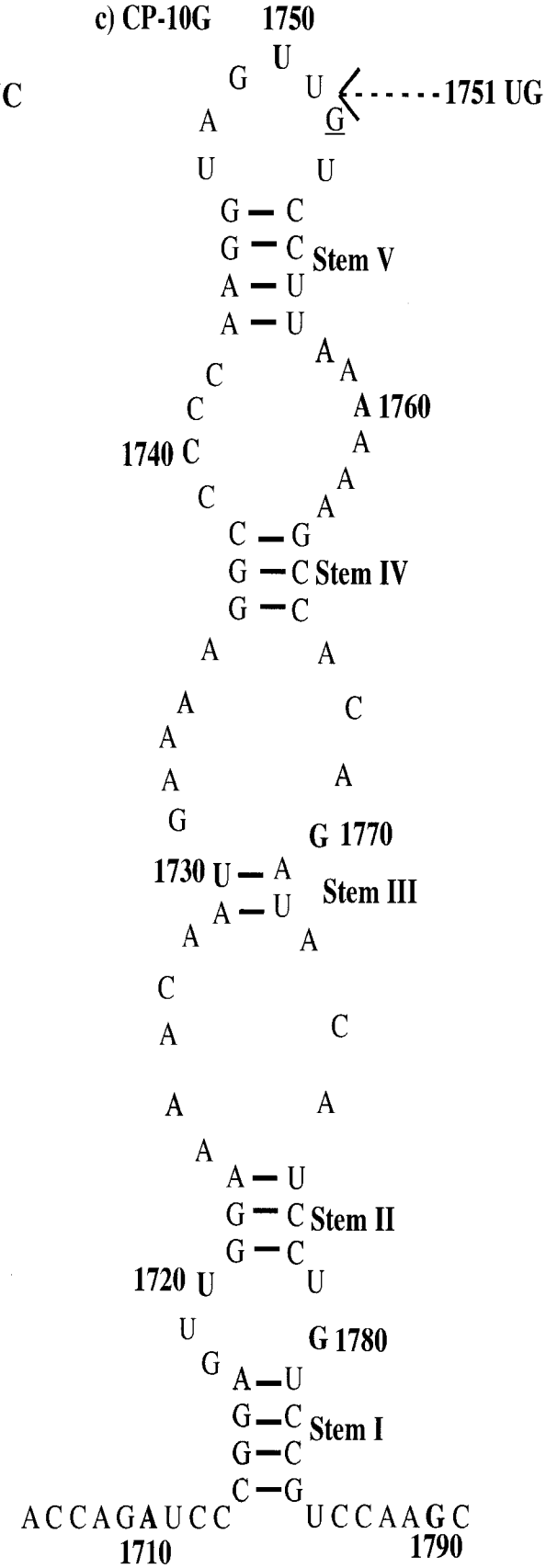

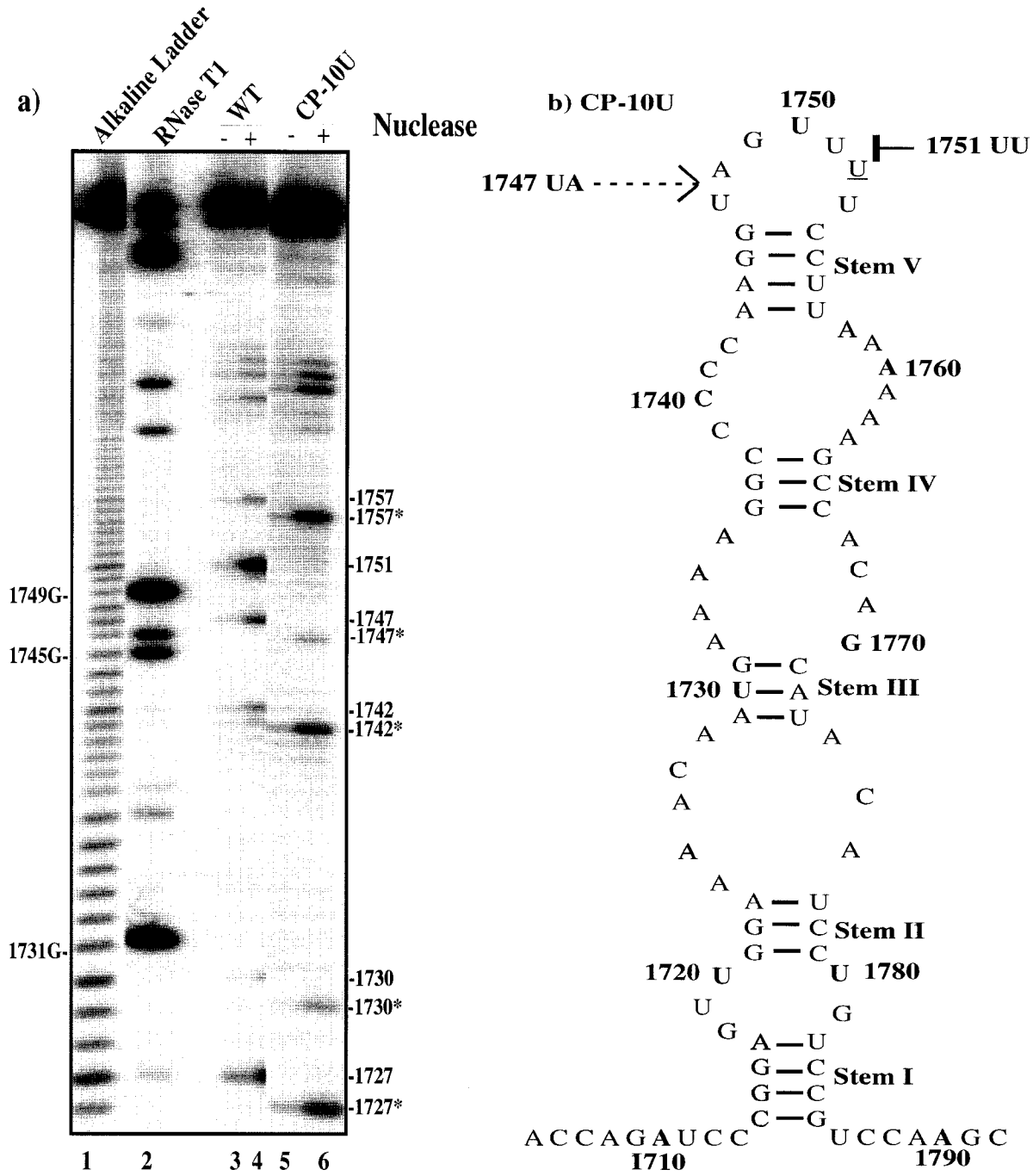

Figure 3.5. The cleavage of the CP-10U CRD mutant by the endonuclease. A), the digested CP-10U CRD mutant was run on a 12% polyacrylamide/7M urea gel parallel to an alkaline ladder and an RNase T1 digest. Numbering on the left indicate several of the guanosine residues cleaved by RNase T1, while numbering on the right indicate cleavage sites generated by the endonuclease using the WT RNA or CP-10U (asterisk) as substrates. B) indicates cleavage sites generated upon incubation of the CP-10U CRD mutant with the endonuclease. Dotted arrows indicate decreased cleavage, underlined nucleotides indicate mutated residues, and the t-shaped symbol indicates blockage of cleavage.

Specificity to CA dinucleotides

Upon incubation of the CP-15 CRD mutant (1727 CA to AC) with the mammalian endonuclease, the cleavage at position 1727 was abolished (lane 6, Figure 3.6a; Figure 3.6b). However, there was cleavage at the newly generated 1728 CA dinucleotide, which is located at a stem-loop junction. Digestion of the CP-19A RNA mutant (1727 CA to AA) with the mammalian endonuclease led to the disappearance of cleavage at position 1727 (lane 6, Figure 3.7a; Figure 3.7b). In addition, there was an enhanced cleavage at the double-stranded 1730 UG dinucleotide and a weak cleavage at the 1726 AA dinucleotide. Upon cleavage of the CP-19G RNA mutant (1727 CA to GA) with the mammalian endonuclease, cleavage at position 1727 was inhibited (lane 8, Figure 3.7a; Figure 3.7c). Lastly, upon mutating dinucleotide 1727 CA to UA (CP-19U), an intense cleavage band was still observed at position 1727 (lane 10, Figure 3.7a; Figure 3.7d). This cleavage corresponds to the new single-stranded 1727 UA dinucleotide.

Specificity to UG dinucleotides

As indicated in section 3.1.2, the CP-13 CRD mutant lacks one of the four adenosines located at position 1732-1734 of the WT 1705-1792 CRD RNA. This is apparent in Figure 3.8a, where the cleavage fragments (cleavage sites at positions 1741 and above) generated by the endonuclease migrated at a faster rate than the corresponding WT fragments and have shifted one nucleotide position below the corresponding WT band. Upon incubation of the CP-13 CRD mutant (1730 UG to GU) with the endonuclease, cleavage at position 1730 was abolished (lane 5, Figure 3.8a; Figure 3.8b). In addition, an intense cleavage is observed at the newly generated single-stranded 1731 UA dinucleotide.

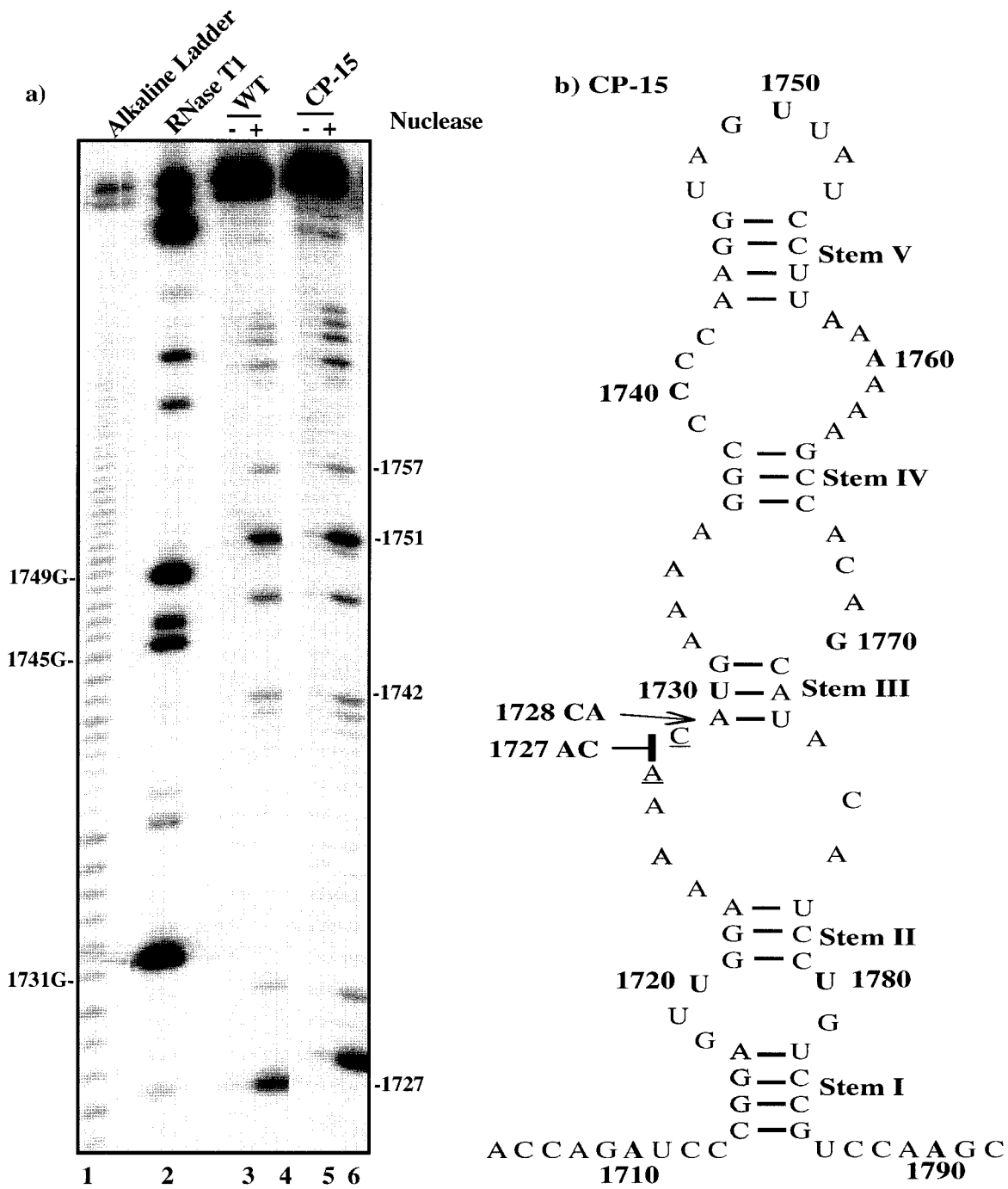

Figure 3.6. The cleavage of the CP-15 CRD mutant by the endonuclease. A), the digested CP-15 was run a 12% polyacrylamide/7M urea gel parallel to an alkaline ladder and an RNase T1 digest. Numbering on the left indicate several of the guanosine residues cleaved by RNase T1, while numbering on the right indicate cleavage sites generated by the endonuclease using the WT RNA as a substrate. B) indicates cleavage sites generated upon incubation of the CP-15 CRD mutant with endonuclease. The arrow indicates new cleavage sites, underlined nucleotides indicate mutated residues, and the t-shaped symbol indicates blockage of cleavage.

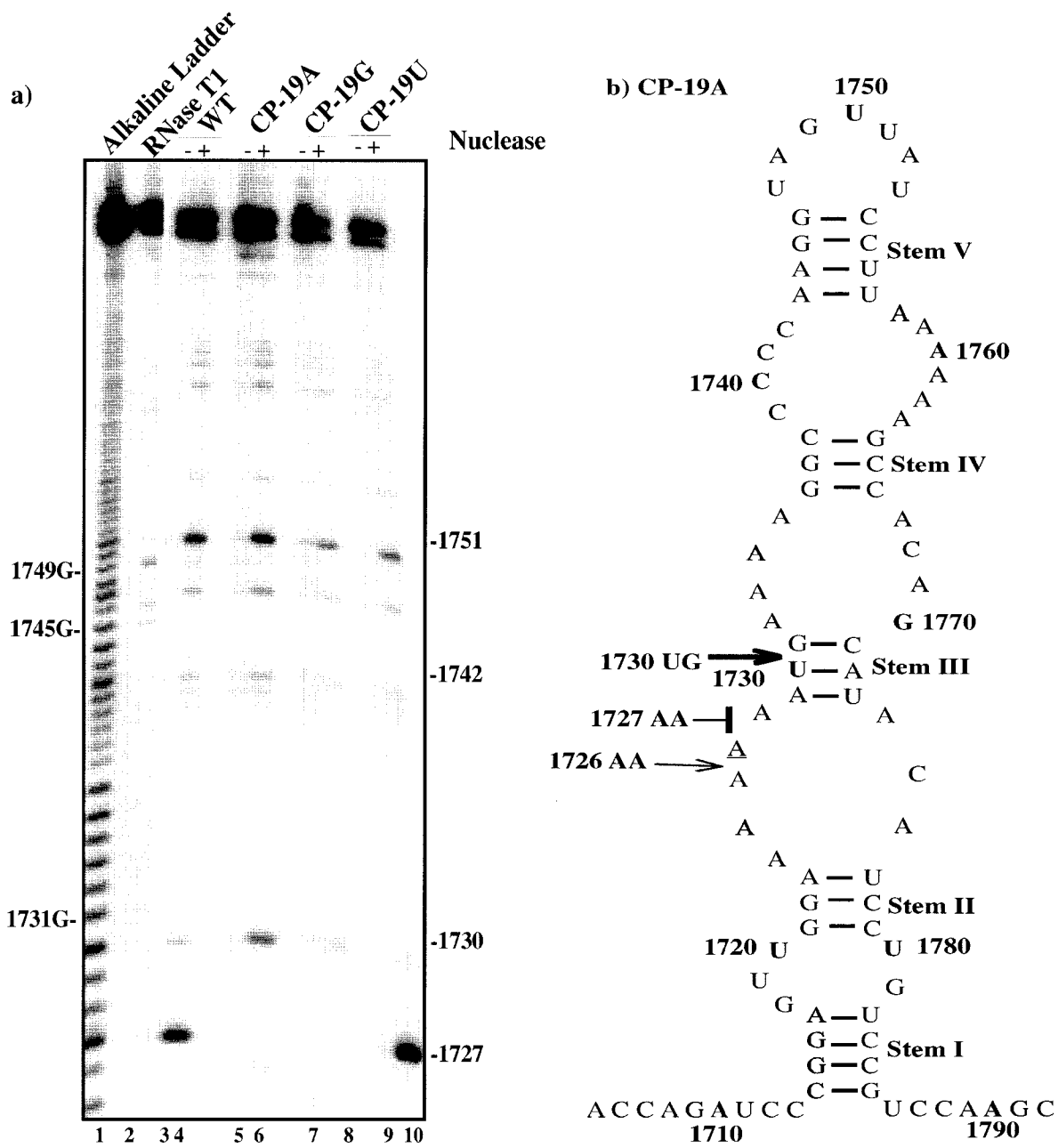

Figure 3.7. The cleavage of the three CP-19 CRD mutants by the endonuclease. A), the digested CP-19A, CP-19G, and CP-19U RNA mutants were run a 12% polyacrylamide/7M urea gel parallel to an alkaline ladder and an RNase T1 digest. Numbering on the left indicate several of the guanosine residues cleaved by RNase T1, while numbering on the right indicate cleavage sites generated by the endonuclease using the WT RNA as a substrate. B), C), and D) indicate cleavage sites generated upon incubation of the CP-19A, CP-19G, and CP-19U, respectively, with the endonuclease. Thick arrows indicate enhanced cleavage, underlined nucleotides indicate mutated residues, and the t-shaped symbol indicates blockage of cleavage.

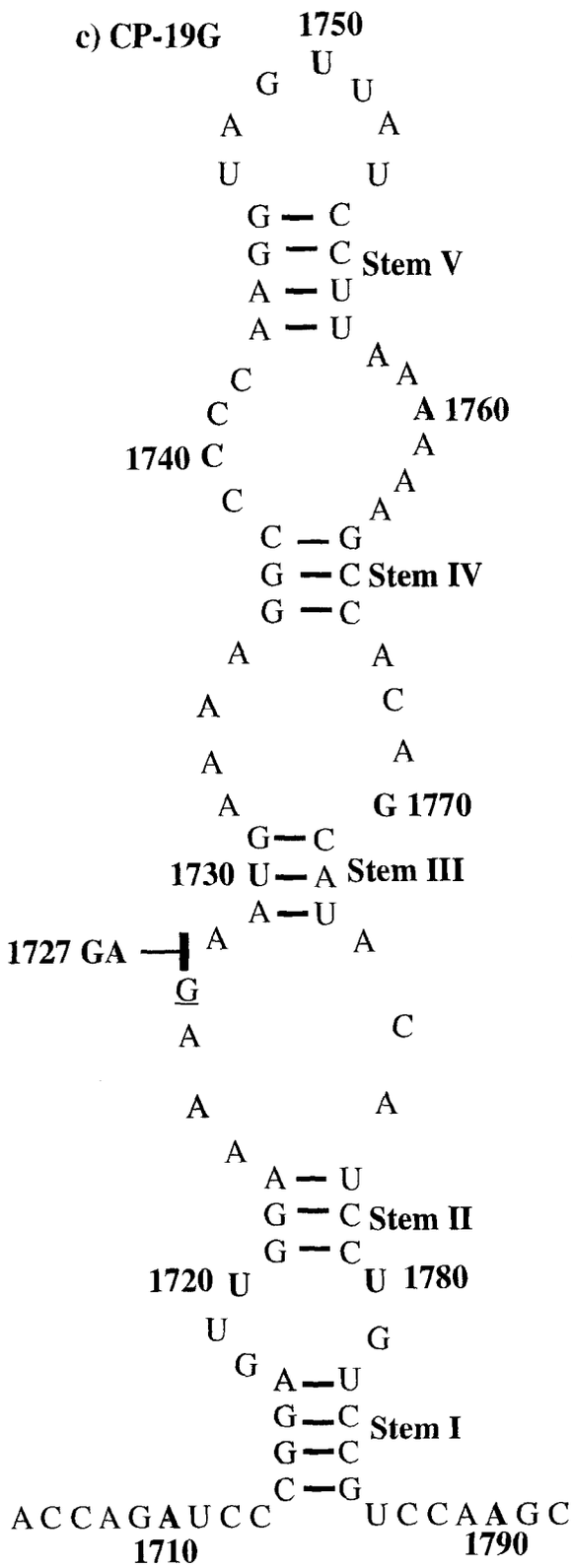
c) CP-19G
1750
Stem V
A 1760
1740 C
Stem IV
G 1770
1730 U—A Stem III
1727 GA
Stem II
1720 U
U 1780
Stem I
ACCAGAUCC
UCCAAGC
1710
1790

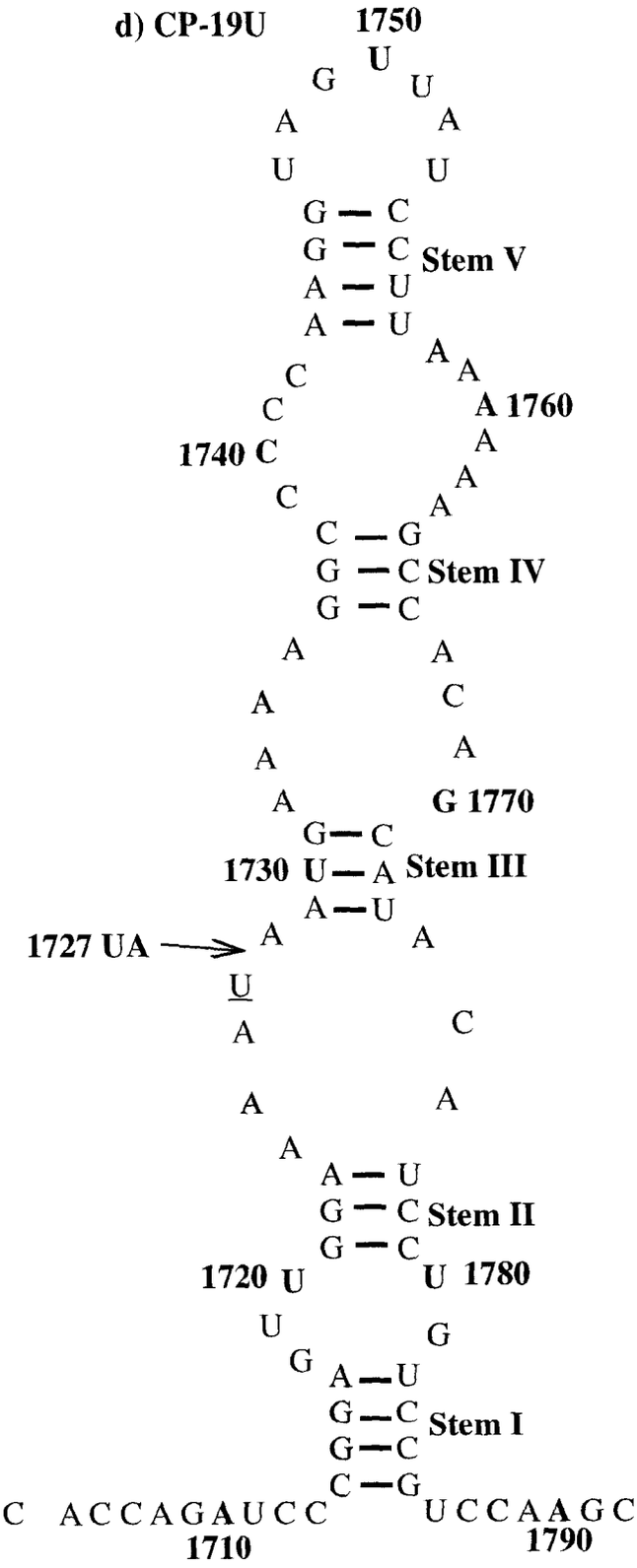
d) CP-19U
1750
Stem V
A 1760
1740 C
Stem IV
G 1770
1730 U—A Stem III
1727 UA
Stem II
1720 U
U 1780
Stem I
ACCAGAUCC
UCCAAGC
1710
1790

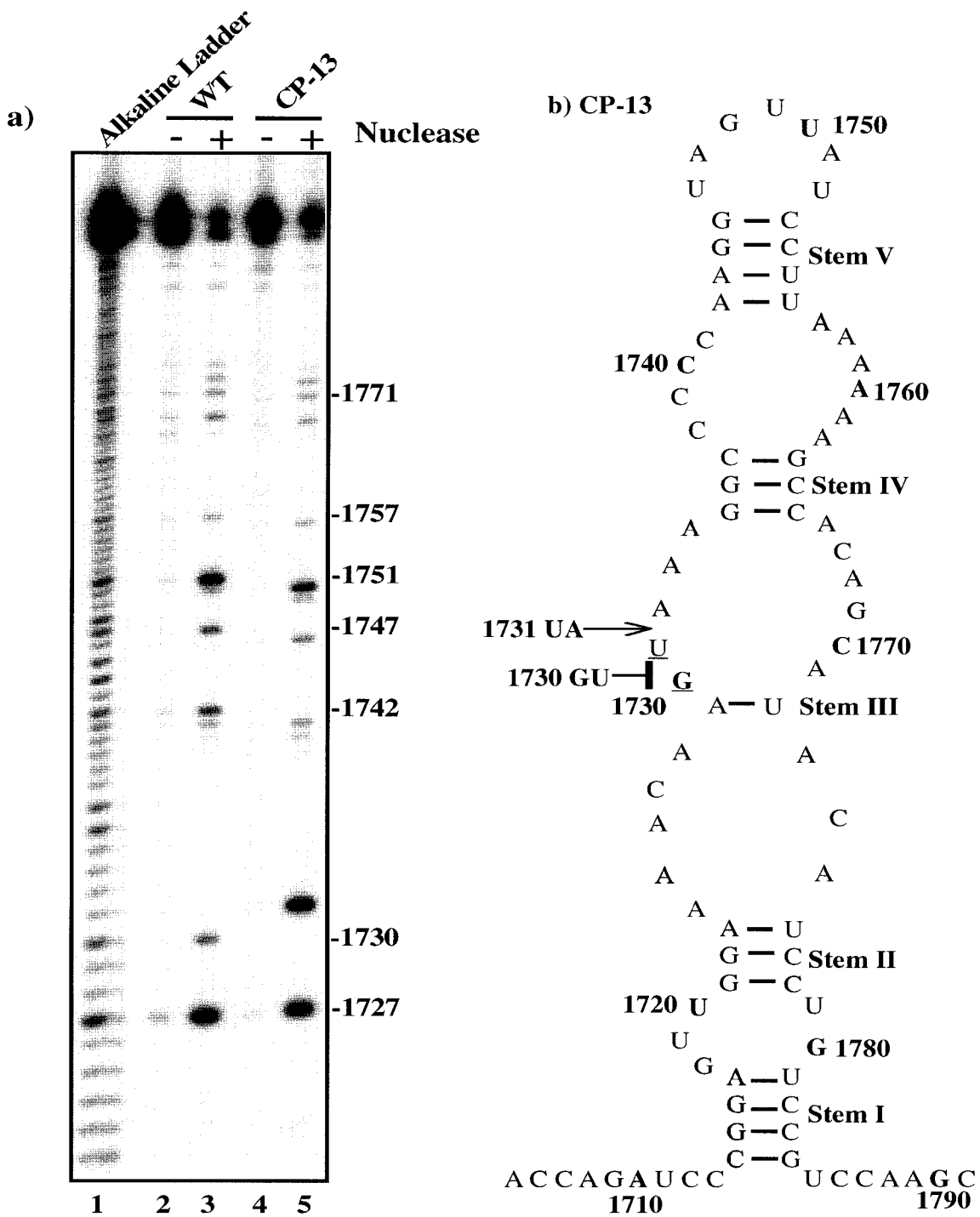

Figure 3.8. The cleavage of the CP-13 CRD mutant by the endonuclease. A), the digested CP-13 was run a 12% polyacrylamide/7M urea gel parallel to an alkaline ladder and an RNase T1 digest. Numbering on the right indicate cleavage sites generated by the endonuclease using the WT RNA as a substrate B) indicates cleavage sites generated upon incubation of the CP-13 with the endonuclease. Arrow indicates cleavage sites, underlined nucleotides indicate mutated residues, and the t-shaped symbol indicates blockage of cleavage.

Structure specificity

As indicated in section 3.1.2, the CP-22 CRD mutant has a deletion of two wild-type nucleotides and an addition of a new residue. Overall, this leads to the faster migration of the CP-22 cleavage fragments (one nucleotide faster) in comparison with the respective wild-type cleavage fragments. The point mutations under investigation are therefore located at positions 1742 (1742 A to U) and 1756 (U to A) in the CP-22 CRD mutant. The deletions of the 1714 cytosine and 1715 guanosine residues and the addition of an adenosine residue at position 1714, may cause the CP-22 CRD mutant to form a different secondary structure than that of the wild-type. The likely secondary structure of the CP-22 CRD mutant was determined using the Mfold program (Zuker, 2003) in conjunction with the RNase A probing data. Digestion of the CP-22 CRD mutant by RNase A generated several identical fragments to those generated upon cleavage of the WT 1705-1792 CRD RNA with RNase A (Lanes 3 and 5, Figure 3.9a). RNase A, however, was also able to cleave at the double-stranded dinucleotide, 1742 U. In addition, there was an enhanced cleavage at position 1739 C (corresponds to WT 1740 C) and an inhibition of cleavage at position 1756. Overall, the probing data is in agreement with the structure determined by the Mfold program (Figure 3.9b).

Upon incubation of the CP-22 CRD mutant with the endonuclease, there was an intense cleavage at the double-stranded 1742 UA dinucleotide and a weak cleavage at the double-stranded 1755 UA dinucleotide (Lane 5, Figure 3.9c; Figure 3.9d). In addition, there was an inhibition of cleavage at position 1756 (corresponds to an AA dinucleotide). Furthermore, there was cleavage at the single-stranded 1741 CU and 1722 AA dinucleotides and enhanced cleavage at the 1739 CC and 1740 CC dinucleotides.

The CP-24 CRD mutant (1752 AU to UA) was designed to generate two double-stranded UA dinucleotides (1747 UA and 1752 UA) within stem V. To confirm the presence of the target secondary structure, the structure of the CP-24 CRD mutant was determined using the Mfold program in conjunction with the RNase A probing data (Figure 3.10a). The cleavage sites generated by RNase A upon incubation with the CP-24 CRD mutant were similar to those generated upon incubation of the WT 1705-1792 CRD RNA with RNase A (lanes 3 and 5, Figure 3.10a). However, RNase A was also able to weakly cleave the double-stranded dinucleotide, 1747 UA. Overall, the RNase A probing data was in agreement with the structure generated by Mfold, which indicated the presence of the intended secondary structure (Figure 3.10b).

Upon incubation of the CP-24 CRD RNA mutant with the mammalian endonuclease, the cleavage at the double-stranded 1747 UA dinucleotide was decreased and there was no cleavage at position 1751 (UU) (lane 5, Figure 3.10c; Figure 3.10d). In addition, there was cleavage at the new UA 1752 UA dinucleotide, which is located in a double-stranded domain. The intensity of cleavage at the 1752 UA dinucleotide was much greater than the effect of RNase A, indicating that the endonuclease has a higher affinity for cleaving this site than RNase A.

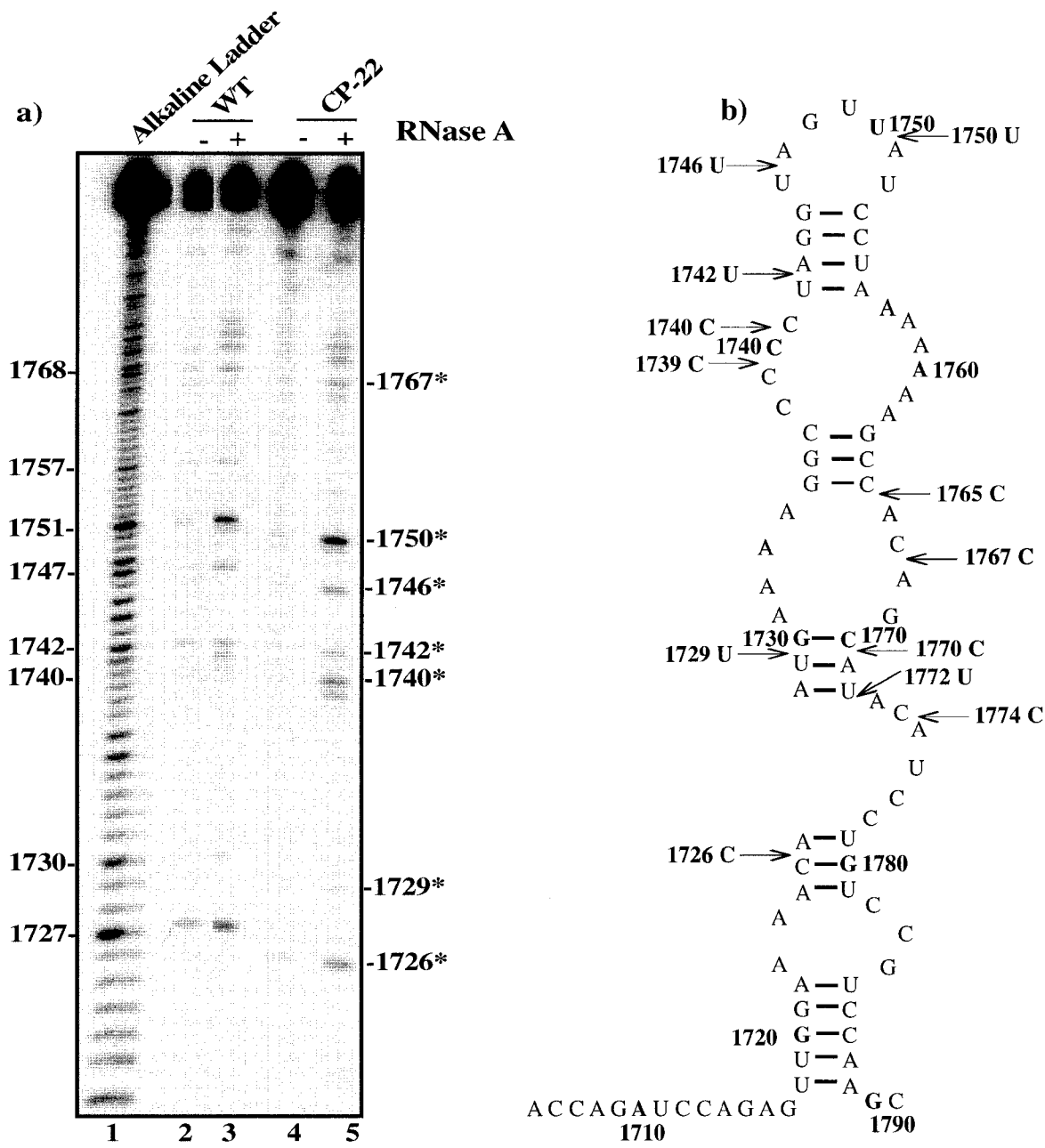

Figure 3.9. Structure probing of the CP-22 CRD mutant using RNase A and cleavage of the CP-22 CRD mutant by the endonuclease. A), CP-22 was digested with RNase A and ran on a 12% polyacrylamide/7M urea gel parallel to an alkaline ladder and an RNase T1 digest. B) corresponds to the CP-22 secondary structure including all the RNase A cleavage sites. C) indicates the 12% polyacrylamide/7M urea gel containing the endonucleolytically digested CP-22 CRD mutant. D) indicates all the cleavage sites generated upon incubation of the CP-22 with the endonuclease. Numbering on the left indicates several cleavage sites generated by incubating the WT RNA with RNase A or the endonuclease, while numbering on the right (*) indicates several cleavage sites generated by incubating the CP-22 CRD mutant with RNase A or the endonuclease.

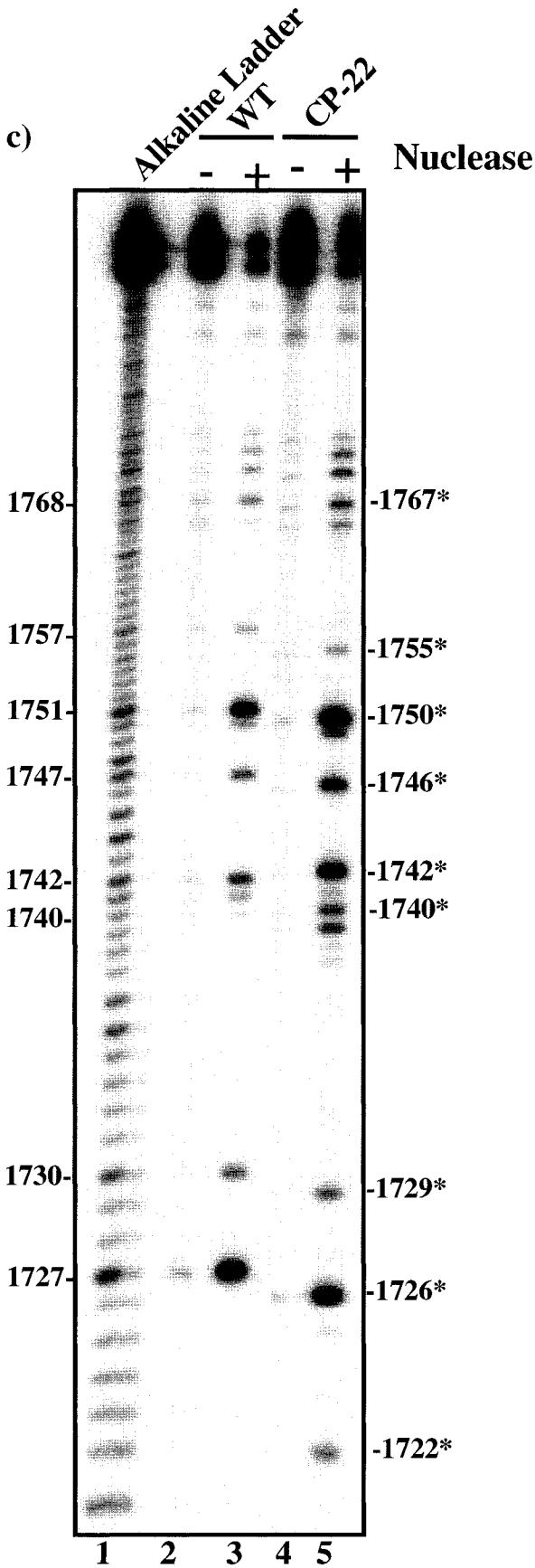
c)
Alkaline Ladder
WT
CP-22
- + - +
Nuclease
1768-
1757-
1751-
1747-
1742-
1740-
1730-
1727-
-1767*
-1755*
-1750*
-1746*
-1742*
-1740*
-1729*
-1726*
-1722*
1 2 3 4 5

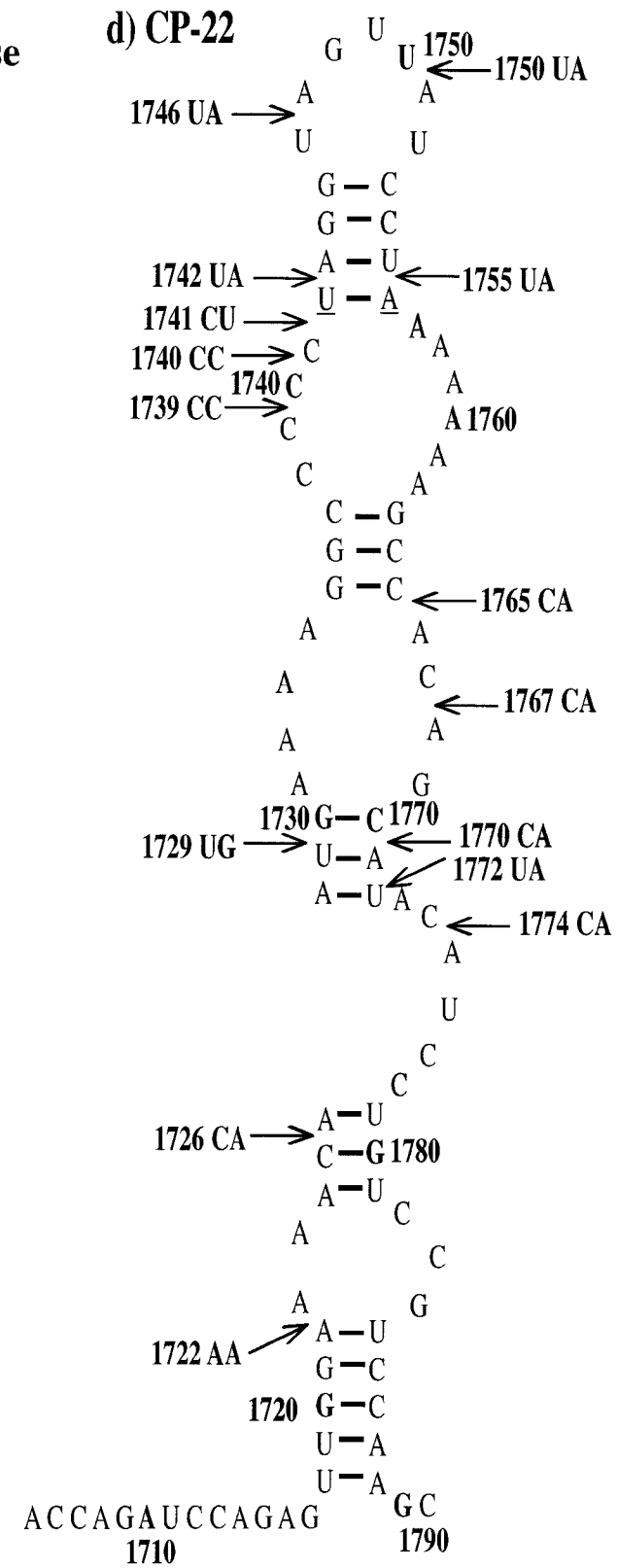
d) CP-22
1750 UA
1746 UA
1742 UA
1755 UA
1741 CU
1740 CC
1740 C
1739 CC
A 1760
1765 CA
1767 CA
1729 UG
1730 G—C 1770
1770 CA
1772 UA
1774 CA
1726 CA
C—G 1780
1722 AA
1720
ACCAGAUCCAGAG
1710
1790

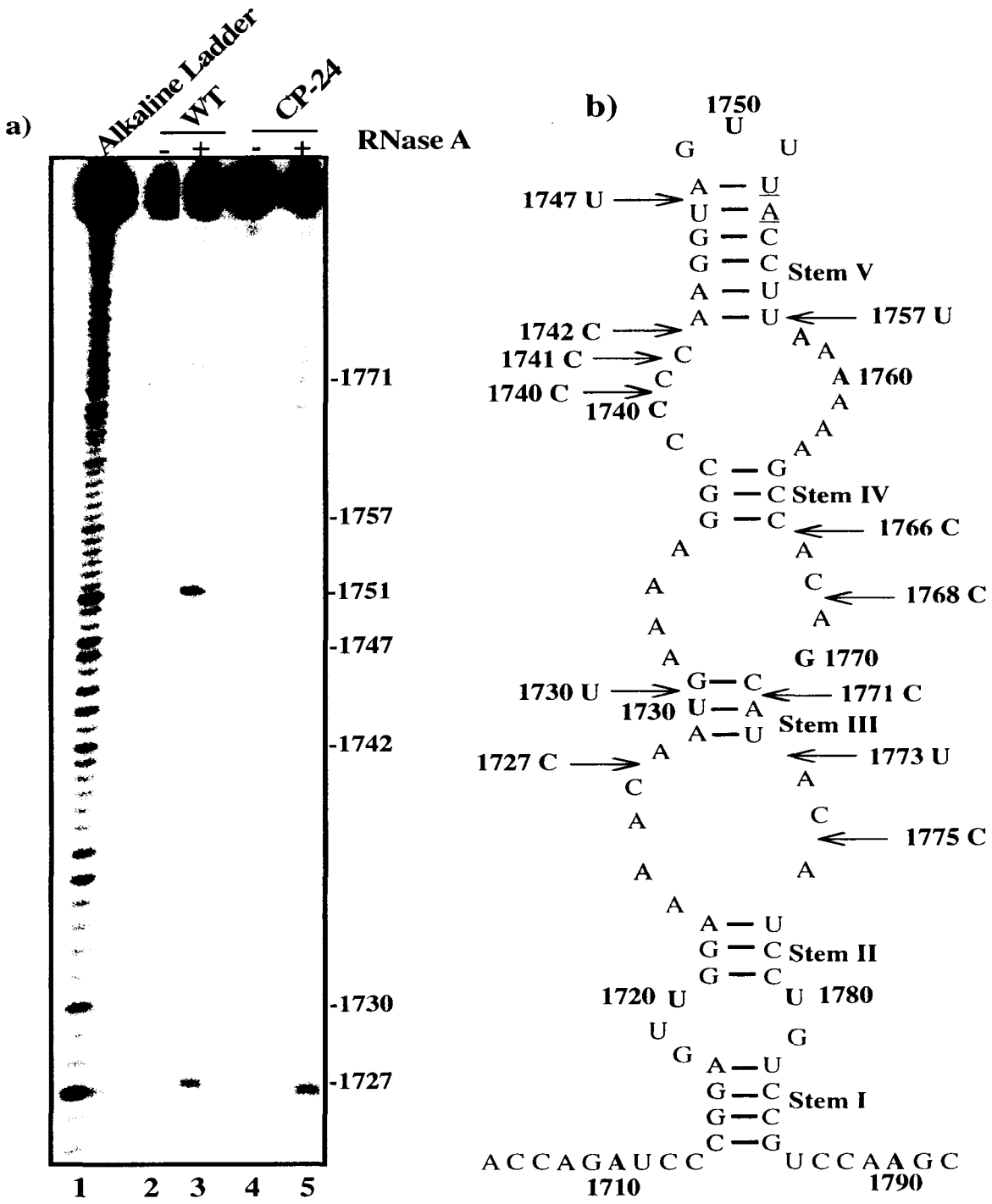

Figure 3.10. Structure probing of the CP-24 CRD mutant using RNase A and cleavage of the CP-24 CRD mutant by the endonuclease. A), CP-24 was digested with RNase A and ran on a 12% polyacrylamide/7M urea gel parallel to an alkaline ladder and an RNase T1 digest. B) corresponds to the CP-24 secondary structure including all the RNase A cleavage sites C) indicates 12% polyacrylamide/7M urea gel containing the endonucleolytically digested CP-24 CRD mutant. D) indicates all cleavage sites generated upon incubation of the CP-24 with the endonuclease. Numbering on the right indicates several cleavage sites generated by RNase A or the endonuclease upon incubation with the WT RNA substrate.

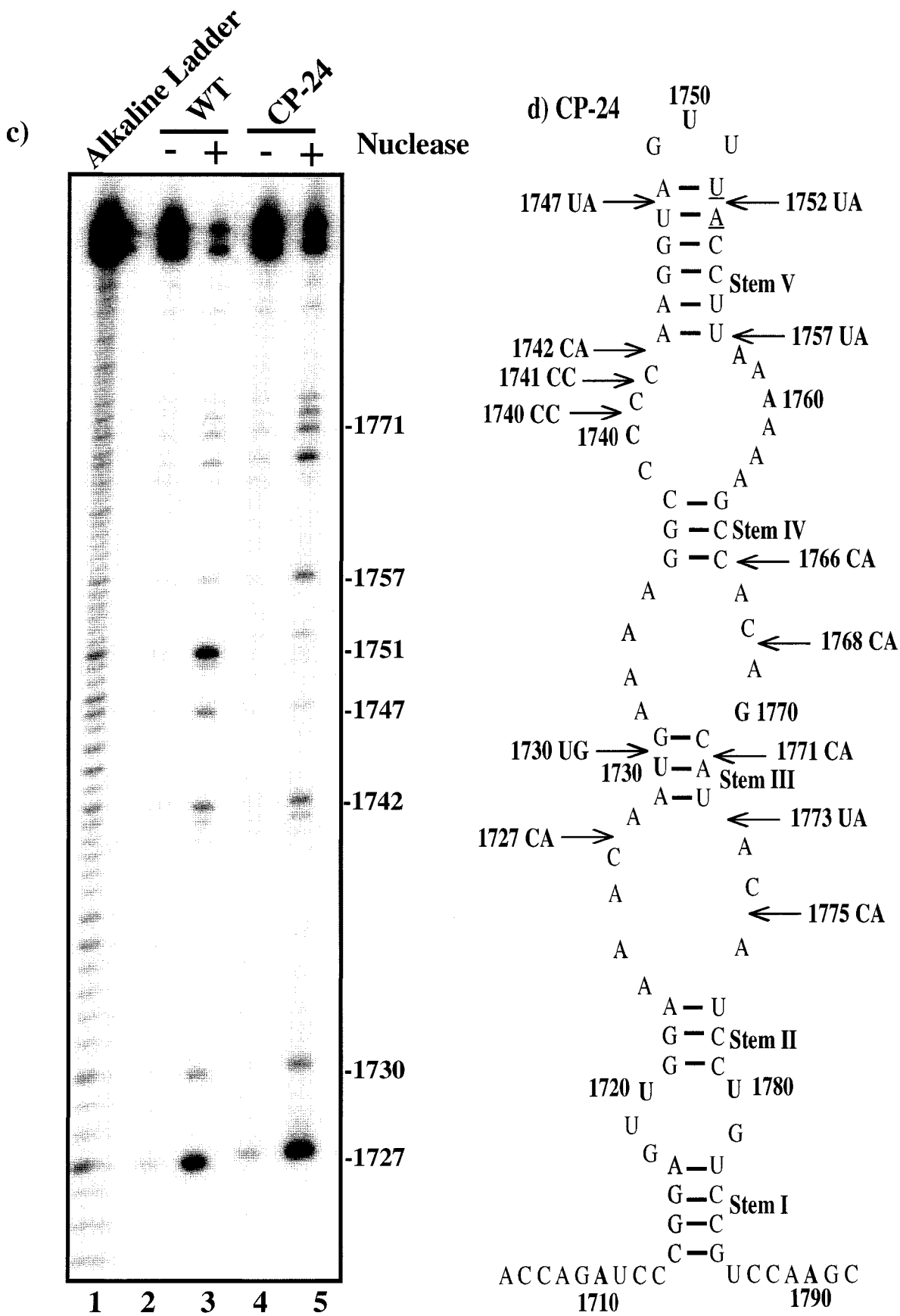
c)
Alkaline Ladder
WT
CP-24
- + - +
Nuclease
-1771
-1757
-1751
-1747
-1742
-1730
-1727
1 2 3 4 5
d) CP-24
1750
U
G U
1747 UA
1752 UA
Stem V
1742 CA
1757 UA
1741 CC
1740 CC
1740 C
A 1760
Stem IV
1766 CA
1768 CA
G 1770
1730 UG
1771 CA
1730
Stem III
1773 UA
1727 CA
1775 CA
Stem II
1720 U
U 1780
Stem I
ACCAGAUCC
UCCAAGC
1710
1790

3.2 Discussion

Overall, the results clearly indicate that one of the sites preferred for cleavage by the endonuclease is 3' to uridines within UA dinucleotides, whether present in single-stranded domains or stem-loop junctions. Evidence of this includes the cleavage of all four UA dinucleotides present in the 1705-1792 CRD region and the UA dinucleotide within the 3018-3159 β-globin RNA. Additional evidence stems from several of the 1705-1792 CRD mutants including CP-2, CP-3, CP-10C, CP-10G, CP-10U, CP-13, CP-19U, and CP-22. Upon mutating the 1751 UA (CP-2) and 1757 UA (CP-3) dinucleotides to AU, cleavage at these positions was inhibited. Mutation of the 1752 adenosine residue to C, G, and U (CP-10C, CP-10G, CP-10U, respectively) led to a large decrease or inhibition of cleavage at the 1751 dinucleotide, therefore indicating the importance of the 3' adenosine residue in promoting strong cleavage by the endonuclease at UA dinucleotides. The decrease in cleavage at the 1747 UA dinucleotide upon digestion of the CP-10U CRD mutant by the endonuclease maybe due to the presence of a pseudo-knot. This pseudo-knot can potentially be generated by base-pairing between the 1750-1753 uridine residues and four of the adenosine residues present between stems IV and V (1758-1763). The formation of the pseudo-knot displaces stems IV and V and may place them in close proximity to each other and to the new UA-rich stem. As a result, the 1747 UA dinucleotide maybe rendered less accessible for cleavage by the endonuclease due to the steric hindrance resulting from the clustering of the three stems.

Additional evidence for preference of the endonuclease towards cleavage of UA dinucleotides includes cleavage of the 1727 UA within the CP-19U CRD mutant. Strong cleavage at position 1727 was only prominent upon mutating the 1727 cytidine to uridine,

therefore, indicating the importance of the uridine residue in promoting cleavage within the UA dinucleotide. Lastly, the strong cleavage at the newly generated single-stranded 1731 UA dinucleotide in the CP-13 CRD mutant and the inhibition of cleavage at the 1756 dinucleotide upon mutating 1756 UA to AA (CP-22), provide further evidence for the affinity of the endonuclease towards UA dinucleotides.

The endonuclease was also found to be capable of cleaving double-stranded UA dinucleotides as evidenced by the CP-22 and CP-24 CRD mutants. The new UA dinucleotides at positions 1742 and 1755 within the CP-22 CRD mutant were cleaved by the endonuclease and are most likely present in double-stranded conformations. As indicated in section 2.2, stem V is highly dynamic due to the breathing of AU base-pairs, which renders them accessible for cleavage by single-strand specific RNase probes. Hence, the breathing of the AU base-pairs may allow the single-strand specific RNase A to cleave at 1742 U. The extremely weak cleavage at the double-stranded 1747 U nucleotide within the CP-24 CRD mutant by RNase A may also be explained by the breathing of AU base-pairs within stem V. Upon folding the CP-22 structure using the Mfold program, several potential structures were obtained, all of which however, show that the 1742 U and 1755 U nucleotides are double-stranded and are localized in stem V. This is not surprising as this mutation is a conservative one that is not expected to alter the RNA secondary structure. The 1747 UA double-stranded dinucleotide in the CP-24 CRD mutant was more strongly cleaved by the novel endonuclease than by RNase A. The decrease in cleavage at position 1747 UA upon localization within a double-stranded domain indicates that the endonuclease preferentially cleaves single-stranded UA dinucleotides. However, additional mutational experiments need to be

completed, in which the strandedness of the remaining three UA dinucleotides are rendered double-stranded, to confirm such a preference.

In addition to UA dinucleotides, the endonuclease appears to have a preference for cleaving 3' to cytidine residues within CA dinucleotides, regardless of the strandedness of the dinucleotide. Evidence includes cleavage of the WT 1705-1792 CRD, 3018-3159 β-globin, CP-15, CP-19A, CP-19G, CP19U, and CP-22 RNAs by the endonuclease. All of the CA dinucleotides present in the 1705-1792 CRD and 3018-3159 β-globin RNAs were cleaved by the endonuclease, regardless of their localization. The specificity to CA dinucleotides is further confirmed by the absence of cleavage at position 1727 within the CP-15 CRD mutant. Upon reversing the orientation of the 1727 CA dinucleotide into AC, the intense cleavage at this position was completely abolished, indicating that cleavage is only induced when the adenosine residue is located 3' to cytidines. The intense cleavage at the 1728 CA dinucleotide within the CP-15 CRD mutant, further confirms the affinity towards CA dinucleotides. The specificity towards CA dinucleotides by the endonuclease was also examined by incubating the endonuclease with the three CP-19 CRD mutants. The intense cleavage at the 1727 position was abolished upon mutating the CA dinucleotide into AA or GA, therefore, indicating that purines cannot be substituted for cytidines in order for cleavage to occur 5' to adenosines. The enhanced cleavage at 1730 UG within the CP-19A CRD mutant can potentially be attributed to an alteration of the tertiary structure of the CRD mutant. The alteration in the RNA tertiary structure may position 1730 UG dinucleotide in a more accessible conformation for cleavage by the endonuclease. The endonuclease was also capable of cleaving double-stranded CA dinucleotides. Evidence of such specificity includes

the cleavage of 1771 CA within the 1705-1792 CRD RNA and the 17 CA and 27 CA dinucleotides within the 3018-3159 β-globin RNA.

The results indicate that the endonuclease is also capable of cleaving UG dinucleotides (3' to the uridine residue), regardless of their strandedness. The five detected single-stranded UG dinucleotides within the 3018-3159 β-globin RNA were all cleaved by the endonuclease. These UG residues are either localized in single-stranded regions or stem-loop junctions. In addition, upon mutating 1751 UA dinucleotide into UG (CP-10G), the endonuclease was capable of cleaving the single-stranded UG dinucleotide, although with less intensity in comparison with the cleavage of the 1751 UA dinucleotide within the WT RNA. Further evidence of specificity towards UG dinucleotides includes the complete disappearance of cleavage at the 1730 position upon mutating the 1730 UG into GU (CP-13). The endonuclease is also capable of cleaving double-stranded UG dinucleotides. Evidence includes the cleavage of the double-stranded 1730 UG dinucleotide within the WT 1705-1792 CRD region within stem III.

The endonuclease was also capable of cleaving CU dinucleotides (3' to the cytidine dinucleotide) only when present in a single-stranded conformation. There are five CU dinucleotides in the 3018-3159 β-globin RNA that are detectable within the limits of the polyacrylamide gel, however, only three of these sites were cleaved by the endonuclease. The three cleaved CU dinucleotides are present in single-stranded domains or stem-loop junctions, whereas the two uncleaved CU dinucleotides are localized within double-stranded domains. Furthermore, the detectable CU dinucleotide (1755 CU) within the 1705-1792 CRD RNA is double-stranded and is not cleaved by the endonuclease. However, upon generation

of a single-stranded CU dinucleotide within the 1705-1792 CRD RNA, there was slight cleavage at this site (1741 CU within the CP-22 CRD mutant).

The endonuclease was also found to be capable of cleaving single-stranded UU, CC, AA, and UC dinucleotides, although the endonuclease does not seem to be specific towards these dinucleotides. There are two UU dinucleotides within the WT 1705-1792 CRD RNA: a single-stranded 1750 UU dinucleotide and a double-stranded 1756 UU. The endonuclease, however, was only capable of cleaving the single-stranded 1750 UU. Additional evidence for the ability of the endonuclease to cleave single-stranded UU dinucleotides included the cleavage of the three single-stranded dinucleotides: 4UU, 5UU, and 9UU and the absence of cleavage at dinucleotide 25 UU in the double-stranded region within the 3018-3159 β-globin RNA. The endonuclease, however, appears to be non-specific to UU dinucleotides as indicated by the following evidence. The new UU dinucleotides within the CP-10U (1751 UU and 1752 UU) and CP-24 (1751 UU) present within single-stranded or stem-loop junctions were not cleaved by the mammalian endonuclease. Therefore, the cleavage of the 1750 UU within the 1705-1792 CRD RNA maybe attributed to the proximity of the 1750 UU dinucleotide to the strongly cleaved 1751 UA site and to the 1747 UA cleavage site.

The non-specificity of the endonuclease towards CC dinucleotides is confirmed by the following evidence. The endonuclease was capable of cleaving two of the six detectable CC dinucleotides within the 1705-1792 CRD RNA. In addition, there was no cleavage at any of the CC dinucleotides present within the 3018-3159 β-globin RNA. The cleavage of the two CC dinucleotides within the 1705-1792 CRD RNA maybe attributed to the proximity of the CC residues to the 1742 CA cleavage site and to the orientation of the CC dinucleotides within the tertiary structure. Such potential orientation may allow the CC dinucleotides to

become more accessible for endonucleolytic cleavage. This finding is in agreement with the cleavage of the same CC residues within the CP-22 CRD mutant. The intense cleavage at the neighboring 1742 UA dinucleotide might have led to the increase in cleavage intensity at both CC dinucleotides: 1739 CC and 1740 CC.

The weak cleavage of the 1726 AA dinucleotide within the CP-19A CRD mutant and the somewhat stronger cleavage at the 1722 AA dinucleotide within the CP-22 CRD mutant is most likely a non-specific cleavage as indicated by the following evidence. There are thirteen AA dinucleotides within the 1705-1792 CRD region and none were cleaved by the endonuclease. In addition, there are four detectable AA dinucleotides in the 3018-3159 β-globin RNA and none were cleaved by the endonuclease. Further confirmation of the non-specificity of the endonuclease towards AA dinucleotides includes the absence of cleavage at the new AA sites at positions 1727 within the CP-19A and 1756 AA within the CP-22 CRD mutants.

The UC dinucleotide is not a preferred site for cleavage by the endonuclease. The cleavage of the single-stranded 10 UC dinucleotide within the 3018-3159 β-globin RNA is a non-specific cleavage and is most likely due to its proximity to the 1-12 nts region of the β-globin RNA, which contains several endonucleolytic cleavage sites. Evidence for the non-specificity of the endonuclease towards UC dinucleotides includes the absence of cleavage at the remaining UC dinucleotides detectable within the limits of the gel (double-stranded 26 UC and single-stranded 38 UC) and the lack of cleavage at the 1753 UC dinucleotide within the 1705-1792 CRD region.

In summary, the results indicate that the endonuclease is sequence-specific towards single-stranded and double-stranded UA, CA, UG dinucleotides and only single-stranded CU

dinucleotides. The enzyme appears to be more specific towards UA dinucleotides compared to CA and UG dinucleotides as indicated by the following evidence. The new UA dinucleotide at position 1727 within the CP-19U CRD mutant was cleaved with more intensity than the wild-type 1727 CA. Furthermore, there was a decrease in cleavage at the 1751 position upon mutating the UA dinucleotide into a UG dinucleotide (CP-10G). The preference of the endonuclease towards UA dinucleotides can further be confirmed by running a time-point experiment where the substrate cleavage sites are analyzed at various time intervals. The cleavage sites generated at the earlier time-points indicate that the endonuclease has more affinity towards cleaving these dinucleotides than those observed at the later time-points. This experiment may also give insights on the preference of the endonuclease towards cleaving single-stranded or double-stranded dinucleotides. Further evidence of the sequence and structure specificity of this endonuclease to RNAs maybe obtained by running the polyacrylamide gel containing the CRD and β-globin transcripts at different time points. This would allow the resolution and identification of all cleavage sites within the RNA, therefore, providing stronger evidence for the endonuclease cleavage specificity. Lastly, incubating the endonuclease with different RNA substrates can potentially provide conclusive information regarding the sequence and structure specificity of the endonuclease to RNAs. The RNA substrates chosen, however, must be non-dynamic in order to confirm the specificity of the endonuclease towards double-stranded dinucleotides.

The results also indicate that the preferred dinucleotides for cleavage are not part of a consensus sequence as the endonuclease seems to cleave at each UA, CA, UG and single-stranded CU dinucleotides. This cleavage property is different from that of PMR-1, which preferentially cleaves single-stranded UG dinucleotides only when present within the

ApyrUGA consensus element (Hanson and Schoenberg, 2001). In addition, the finding that the endonuclease is also capable of cleaving other dinucleotides in a non-sequence specific manner, indicates that the endonuclease is not a restriction enzyme. Such a property is similar to that of PMR-1, which is not thought of as a restriction enzyme in that other nucleotides than the consensus element can also be cleaved (Chernokalskaya et al., 1997).

It is important to point out that the cleavage specificity of the novel endonuclease under study, which was isolated from rat, was determined using human c-*myc* CRD RNA as a substrate. If this endonuclease is challenged with rat c-*myc* nts 1705-1792 CRD RNA, the cleavage specificity of the endonuclease would likely remain the same. Based on the determined cleavage specificity of the endonuclease, it would likely cleave at the following dinucleotides: 1707 CA, 1715 UG, 1720 UG, 1727 CA, 1742 CA, 1747 UA, 1751 UA, 1755 CU, 1757 CA, 1766 CA, 1773 UA, 1775 CA, 1779 CU, 1780 UG, and 1788 CA (Figure 3.11).

The cleavage at the fourteen sites of the 1705-1792 c-*myc* CRD and at the twenty-two sites of 3018-3159 β-globin RNA by the enzyme, *in vitro,* may not necessarily occur *in vivo.* Inside the cell, auxiliary factors such as the CRD-BP is present and binds to the 1705-1792 CRD region, which potentially can cause an alteration in the secondary structure of the CRD RNA. The binding of the CRD-BP may also lead to an inhibition of endonucleolytic cleavage at certain sites within the 1705-1792 CRD. In particular, this effect maybe prominent near the 1763-1777 CRD region, which is thought to be important for CRD-BP binding (Coulis et al., 2000). It is currently unknown whether all five polypeptides comprising the mammalian endonuclease are important for endonucleolytic cleavage of c-*myc in vivo.* The absence of one or more polypeptides *in vivo* may generate different cleavage sites than the ones

observed *in vitro*. In addition, the divalent cations in the cell may cause the c-*myc* and β-globin mRNAs to form tertiary structures, thereby, altering the accessibility of the dinucleotides for endonucleolytic cleavage. In addition, the sequence and structure cleavage specificity of the endonuclease to the 1705-1792 CRD and 3018-3159 β-globin RNAs maybe different *in vivo* due to the presence of auxiliary factors. This is thought to occur with the RNase III and Dicer enzymes, which show little sequence-specificity *in vitro*, but are thought to be sequence-specific *in vivo* (Condon and Putzer, 2002; Doi et al., 2003; Fortin et al., 2002).

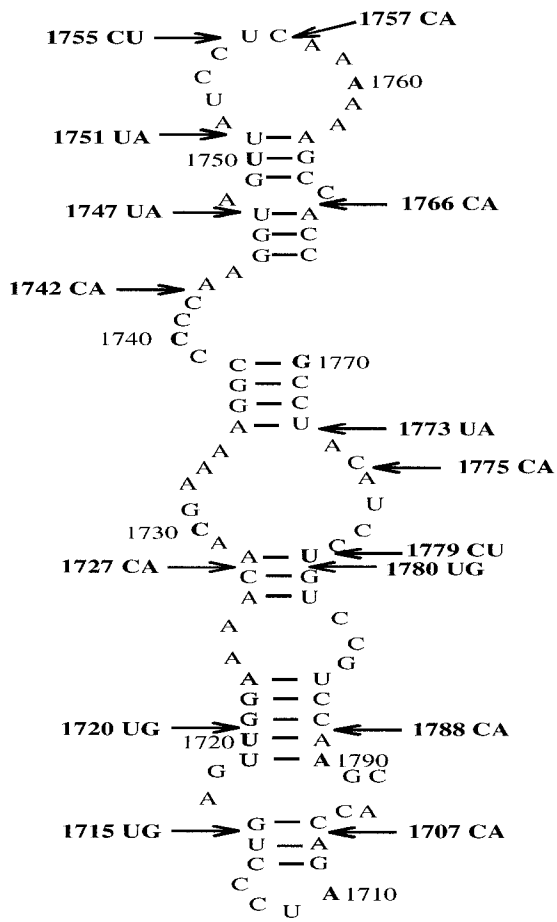

Figure 3.11. The potential cleavages sites that are likely to be generated by the novel mammalian endonuclease upon incubation with rat c-*myc* nts 1705-1792 CRD RNA.

Chapter 4
General Discussion

Post-transcriptional regulation has recently emerged as a major control point of gene expression in many organisms (Brewer, 2002; Dodson and Shapiro, 2002). One mode of mRNA decay is via the deadenylation-independent pathway, which is thought to involve the degradation of mRNAs by endoribonucleases, followed by exonucleolytic degradation (Schoenberg and Cunningham, 1999). In mammals, however, only few endonucleases that degrade mRNAs are known. Several mRNA decay intermediates have been described, however, the responsible endonucleases remain unknown (Dodson and Shapiro, 2002). The importance of controlling gene expression at the post-transcriptional level, underscores the need to understand and characterize the implicated endonucleases.

A comparison between the novel mammalian endonuclease with known vertebrate endoribonucleases

The RNA cleavage specificity of the novel endoribonuclease is different from that of the three other endonucleases responsible for c-*myc* mRNA cleavage *in vitro*: the RasGap-associated G3BP, the ~65 kDa RNase E-like endonuclease, and the ~39 kDa endonuclease. The RasGap-G3BP endonuclease (52 kDa) prefers to cleave only single-stranded CA dinucleotides within the 3'UTR of c-*myc* mRNA (Barnes et al., 2002; Tourriere et al., 2001). This is in contrast to the mammalian endonuclease under study, which preferentially cleaves, among other dinucleotides, both single-stranded and double-stranded CA dinucleotides. It also appears that the cleavage specificity of the mammalian endonuclease is independent of consensus elements in that any region within the c-*myc* mRNA, containing CA dinucleotides, is a potential target for the mammalian endonuclease. Furthermore, the mammalian endonuclease has different cleavage properties in comparison with the ~65 kDa RNase E-like

endonuclease. The dinucleotides cleaved by the mammalian endonuclease do not appear to be part of a consensus sequence, in contrast to the ~65 kDa RNase E-like endonuclease. The RNase E-like endonuclease preferentially cleaves only within the 5'AUUUA 3' motif, present in the 3'UTR of c-*myc* mRNA (Wennborg et al., 1995). The ~39 kDa endonuclease cleaves predominantly in the A-rich 1726-1736 CRD region of c-*myc* mRNA, sparing other A-rich regions (Lee et al., 1998b). This seems to indicate that the ~39 kDa endonuclease is substrate-specific and nucleotide cleavage may depend on the presence of consensus elements. Overall, the distinct cleavage sites generated by the novel mammalian endonuclease, indicates that the enzyme maybe part of a redundant pathway for the control of c-*myc* gene expression in cells. The alternative pathways would ensure steady-state levels of the essential growth-regulator gene, c-*myc*, in the event of inactivation of one pathway.

The novel mammalian endonuclease also exhibits different cleavage properties than those of endonucleases that have been purified from *E.coli* and yeast. Both bacterial RNase E and RNase G cleave only single-stranded regions within RNAs. In addition, these two endonucleases prefer to cleave 5' to AU dinucleotides upstream of stem-loops (Coburn and Mackie, 1999; Wachi et al., 1999). The cleavage properties of the novel mammalian endonuclease are also different from that of bacterial RNase P, MazF, and PemK. All of these endonucleases are thought to cleave their target dinucleotides only when present within a consensus element. Furthermore, the mammalian endonuclease has different cleavage properties than the bacterial RNase III and yeast Rnt1p. Both of these endonucleases cleave only double-stranded RNAs and the Rnt1p endonuclease seems to cleave regions near consensus elements (Lamontagne and Elela, 2004).

In addition, the cleavage specificity of the mammalian endonuclease is distinct in comparison with the specificity of all the vertebrate endonucleases mentioned in Table 1.3. The majority of these endonucleases cleave their target sequence only when present within a consensus element and/or when present in either single-stranded or double-stranded domains, but not both. Furthermore, none of the endonucleases mentioned in Table 1.3 have a preference for cleavage of UA, CA, UG, and CU dinucleotides. PMR-1 relies on consensus elements (ApyrUGA) for RNA cleavage and it degrades its RNA substrates (albumin and vitellogenin) only in the 3' UTR (Cunningham et al., 2001). Furthermore, PMR-1 prefers to cleave UG dinucleotides only when present in single-stranded domains within the consensus element (Bremer et al., 2003; Hanson and Schoenberg, 2004). The polysomal endonuclease that was found to cleave β-globin mRNA is also capable of cleaving UG dinucleotides (Stevens et al., 2002). However, this cleavage occurs only when the dinucleotides are present within single-stranded domains (Stevens et al., 2002). RNase L preferentially cleaves UA and UU dinucleotides, only when present within single-stranded domains (Hua et al., 1993). This is different from the mammalian endonuclease, which is capable of cleaving UA dinucleotides in both single-stranded and double-stranded domains and has no sequence-specificity to UU dinucleotides. Dicer has little sequence specificity *in vitro* and prefers to cleave its target sequences only when present in double-stranded domains (Doi et al., 2003; Fortin et al., 2002). This in contrast to the novel mammalian endonuclease which is also capable of cleaving double-stranded RNA, but with sequence specificity. Lastly, in contrast to the mammalian endonuclease, ErEN appears to be a substrate-specific endonuclease as it preferentially cleaves the α-globin mRNA only at the 63 CU dinucleotide position (strandedness of this CU dinucleotide is unknown) (Rodgers et al., 2002). The remaining

endonucleases mentioned in Table 1.3 are substrate-specific as they cleave their target sequence only when present within or near consensus elements.

Evidence that the novel endonuclease is different from RNase A

Upon incubation of the CP-22 CRD structure mutant with the endonuclease, cleavage was observed at the double-stranded 1755 UA dinucleotide, the single-stranded 1722 AA dinucleotide, and the single-stranded 1741 CU dinucleotide. RNase A was not capable of cleaving at any of these dinucleotides. Upon incubation of the CP-24 CRD structure mutant by the endonuclease, cleavage occurred at the 1752 UA dinucleotide. However, there was no cleavage at this site by RNase A. Furthermore, cleavage at the 1747 UA dinucleotide was more pronounced than the cleavage generated by RNase A at this site. Other evidence indicating that the two enzymes are distinct include the differential cleavage generated upon incubation of a ~ 170 nt region spanning the MDR-1 (multi-drug resistance) RNA with the mammalian endonuclease and RNase A (unpublished observation). The results clearly show that there are several bands that are present in the RNase A lane, but not in the endonuclease lane or vice versa (data not shown). In addition, RNase A is known to generate 5' fragments, each with a 3'phospate terminal (Mishra, 2002), whereas the mammalian endonuclease has been shown to generate a 5' fragment with a 3' hydroxyl terminal (Bergstrom et al., in press). Lastly, RNase A is known to exist as a dimer *in vivo* (Mishra, 2002), whereas the mammalian endonuclease is thought to be composed of five polypeptides in the cell. One of the five polypeptides has a size of ~ 35 kDa and has been tentatively identified to be a SNAP (S-nitroso-N-acetyl-D,L-penicillamine) receptor protein.

The novel mammalian endonuclease maybe part of the RNase A family, due to the slight similarity in the cleavage sites generated between the two enzymes. Two members of

the RNase A family: onconase (11.2 kDa) and bovine-seminal RNase (BS-RNase) (27 kDa) (Bracale et al., 2003; Lee and Raines, 2003) generate similar cleavage sites to RNase A (Kim et al., 1995; Leland and Raines, 2001; Leland et al., 1998). The major difference between onconase and RNase A (~ 30% homology) is attributed to the additional disulfide bond present at the C-terminus of onconase (Lee and Raines, 2003). Furthermore, the three main catalytic sites of RNase A: His^{10}, His^{97}, and Lys^{31} are conserved in onconase (Leland and Raines, 2001; Leland et al., 1998). The other RNase A family member, BS-RNase, contains 80% homology with RNase A and has an identical active site to that corresponding to RNase A (Ercole et al., 2003). In addition to cleaving single-stranded RNA, BS-RNase was also found to cleave double-stranded RNA (sequences cleaved not determined) (Schein et al., 1990), indicating the possibility that the BS-RNase may have a similar mechanism of action as that of the mammalian endonuclease under study. However, to confirm that the mammalian endonuclease is indeed a member of the RNase A family, all five polypeptides must first be identified to determine if there is protein sequence homology with RNase A and the possible existence of an identical active site to that of RNase A.

Despite of the aforementioned differences between the novel mammalian endonuclease and RNase A, the two enzymes possess similar cleavage specificity. However, this cleavage specificity is likely to be different *in vivo*. The potential difference in cleavage specificity between the two enzymes, *in vivo*, may occur to the different compartmentalization of the two enzymes, the different putative protein-protein interactions, and/or whether or not they are phosphorylation-dependent.

Significance of the mammalian endonuclease *in vivo* and future experiments

The mammalian endonuclease maybe the enzyme responsible for the endonucleolytic cleavage of the c-*myc* CRD in the liver (Hanson and Schoenberg, 2001; Pistoi et al., 1996). This endonucleolytic cleavage is potentially the rate-limiting step in the deadenylation-independent pathway of c-*myc* mRNA cleavage *in vivo*. The endonucleolytic fragments generated by the enzyme may then be subjected to exonucleolytic degradation by the 5' to 3' and/or the 3' to 5' exonucleases. Degradation of the 5' fragment by 3' to 5' exonucleases requires the presence of a 3' hydroxyl on the 5' cleavage fragment (Mishra, 2002). The mammalian endonuclease is thought to generate cleavage fragments containing 3' hydroxyl groups (Bergstrom et al., in press), therefore, generating proper substrates for 3' to 5' exonucleases. In addition, the mammalian endonuclease may exist within a multi-protein complex, similar to the bacterial degradosome. The bacterial degradosome consists of the endonuclease, RNase E, a 3' to 5' exonuclease (PNPase), and several other ATP-requiring enzymes (Coburn and Mackie, 1999).

It is also important to note that the experiments in this project were performed *in vitro*. The *in vitro* findings maybe different from those determined *in vivo* due to the presence of auxiliary proteins and divalent cations in the cellular environment. Future experiments must then be undertaken *in vivo* to confirm the secondary structure of the 1705-1792 c-*myc* CRD region and the cleavage specificity of the endoribonuclease to this region. Two potential experiments could be performed to determine the secondary structure of the 1705-1792 c-*myc* CRD *in vivo*. The first experiment would involve isolating total RNA from K562 cell-lines (abundant in c-*myc* mRNA), followed by incubation with the same RNase probes used in this project. Cleavage fragments could then be detected using primer extension

(Ehresmann et al., 1987). Several primers corresponding to the 1705-1792 region can be used to confirm the secondary structure of the 1705-1792 CRD region *in vivo*. The other experiment would involve treating the K562 cell-lines with chemical probes such as dimethylsulfate (DMS) and 1-cyclohexyl-3-(2-morpholinoethyl) carodiimide metho-p-toluene sulfonate (CMCT) which modify single-stranded A,C and U,G residues, respectively (Ehresmann et al., 1987). Total RNA would then isolated from the cell-lines, followed by primer extension.

In order to determine the sequence and structure cleavage specificity of the mammalian endoribonuclease to the 1705-1792 c-*myc* CRD region *in vivo*, the mammalian endonuclease must first be cloned. The cDNA corresponding to the endonuclease could be ligated to an expression vector and transfected into K562 leukemic cell-lines. Any stable degradation products generated by the endonuclease could then be detected using sensitive detection methods such as ligation-mediated PCR (LM-PCR) (Hanson and Schoenberg, 2004; Lee et al., 1998b) and S1 nuclease mapping (Stevens et al., 2002).

Therapeutic implication of the novel mammalian endonuclease

In theory, the novel mammalian endonuclease may have a potential therapeutic application against different types of diseases such as cancer and viral infections. Such application exploits the specificity of the endonuclease to UA, CA, UG, and single-stranded CU residues, which are likely to be abundant in any RNA substrate. The endonuclease maybe used directly to degrade mRNAs present in cancer cells or viral RNAs present in virus-infected cells, thereby inhibiting protein synthesis. The degradation of mRNA by the endonuclease might also lead to apoptosis as has been shown with the two members of the RNase A family, which were used in cancer therapeutics. Both onconase and BS-RNase are

capable of promoting cytotoxic effects in cancer cells (Bracale et al., 2002; Haigis and Raines, 2003). The cytotoxic pathway involves three steps: binding to cell-surface, endocytosis, and cleavage of the RNA target, leading to inhibition of protein synthesis and apoptosis (Bracale et al., 2002; Haigis and Raines, 2003). The primary target for onconase, however, is thought to be tRNA (Irie et al., 1998), whereas the primary target for BS-RNase is thought to be rRNA (Bracale et al., 2002). The limited number of RNA targets cleaved by the two RNase A family members, point to the potential versatility and hence the potency of the mammalian endonuclease in targeting any type of RNA, including mRNA.

The mammalian endonuclease may also be used in conjunction with traditional chemotherapeutic drugs to promote death of chemoresistant cells. This type of therapy has been successfully accomplished utilizing BS-RNase, against human neuroblastoma cancer cell-lines, which contain the multi-drug resistance (MDR) phenotype (Cinatl et al., 1999). This treatment led to the induction of apoptosis in these cell-lines and to the inhibition of cellular growth (Cinatl et al., 1999). The mammalian endonuclease may also be used to target cells infected with viral RNAs. Such application would potentially be similar to that of onconase, that was utilized to target human leukemia cells infected with HIV-1 (Saxena et al., 2002). Such treatment led to the degradation of viral RNAs and eventually led to a decrease in HIV-1 replication (Saxena et al., 2002).

Concluding remarks

This work has revealed important information about the secondary structures of the 1705-1792 c-*myc* CRD RNA and the 3018-3159 β-globin RNA *in vitro*. Both structures are dynamic in that they can alternate between an open and a double-stranded structure. The elucidated structures may provide insight into the secondary structures *in vivo*. Knowledge

of the secondary structures has also allowed for the determination of the structure specificity of the novel mammalian endoribonuclease *in vitro*. Using a series of CRD mutants as substrates, it was determined that the mammalian endonuclease prefers to cleave UA, CA, and UG dinucleotides, regardless of strandedness, while only single-stranded CU dinucleotides are preferentially cleaved. This finding was also confirmed using the 3018-3159 β-globin RNA as a substrate.

The obtained results indicate that the novel mammalian endonuclease is non-substrate specific as other RNAs such as β-globin and MDR-1 were also degraded by the novel mammalian endonuclease, *in-vitro*. In addition, based on the cleavage specificity of the endonuclease, other RNA classes such as rRNA and tRNA are also potential targets by the novel endonuclease. Such cleavage specificity appears to be similar to that of bacterial RNases, which are not dedicated to cleave specific mRNAs or particular RNA classes (Deutscher, 2006). Rather, it was found that the specificity of the endonuclease and the accessibility of the substrate are the sole determinants of whether or not a particular RNA will be targeted (Deutscher, 2006).

Overall, the distinct sequence and structure cleavage specificity of the mammalian endonuclease indicates that it is indeed a novel endonuclease, different from other currently known mammalian endonucleases. The research described here has added significant information to our limited knowledge on RNA cleavage specificity by the recently identified novel mammalian endoribonuclease.

Reference List

Altman S, Kirsebom L, Talbot S. 1993. Recent studies of ribonuclease P. Faseb J 7(1):7-14.

Bachurski CJ, Theodorakis NG, Coulson RM, Cleveland DW. 1994. An amino-terminal tetrapeptide specifies cotranslational degradation of beta-tubulin but not alpha-tubulin mRNAs. Mol Cell Biol 14(6):4076-4086.

Baker KE, Condon C. 2004. Under the Tucson sun: a meeting in the desert on mRNA decay. Rna 10(11):1680-1691.

Baker KE, Mackie GA. 2003. Ectopic RNase E sites promote bypass of 5'-end-dependent mRNA decay in Escherichia coli. Mol Microbiol 47(1):75-88.

Barnes CJ, Li F, Mandal M, Yang Z, Sahin AA, Kumar R. 2002. Heregulin induces expression, ATPase activity, and nuclear localization of G3BP, a Ras signaling component, in human breast tumors. Cancer Res 62(5):1251-1255.

Bashkirov VI, Scherthan H, Solinger JA, Buerstedde JM, Heyer WD. 1997. A mouse cytoplasmic exoribonuclease (mXRN1p) with preference for G4 tetraplex substrates. J Cell Biol 136(4):761-773.

Batey RT, Rambo RP, Doudna JA. 1999. Tertiary Motifs in RNA Structure and Folding. Angew Chem Int Ed Engl 38(16):2326-2343.

Beelman CA, Parker R. 1995. Degradation of mRNA in eukaryotes. Cell 81(2):179-183.

Bergstrom K, Urquhart JC, Tafech A, Doyle E, Lee CH. in press. Purification and characterization of a novel mammalian endoribonuclease. J cell Biochem.

Bernstein PL, Herrick DJ, Prokipcak RD, Ross J. 1992. Control of c-myc mRNA half-life in vitro by a protein capable of binding to a coding region stability determinant. Genes Dev 6(4):642-654.

Binder R, Horowitz JA, Basilion JP, Koeller DM, Klausner RD, Harford JB. 1994. Evidence that the pathway of transferrin receptor mRNA degradation involves an endonucleolytic cleavage within the 3' UTR and does not involve poly(A) tail shortening. Embo J 13(8):1969-1980.

Binder R, Hwang SP, Ratnasabapathy R, Williams DL. 1989. Degradation of apolipoprotein II mRNA occurs via endonucleolytic cleavage at 5'-AAU-3'/5'-UAA-3' elements in single-stranded loop domains of the 3'-noncoding region. J Biol Chem 264(28):16910-16918.

Bonnieu A, Roux P, Marty L, Jeanteur P, Piechaczyk M. 1990. AUUUA motifs are dispensable for rapid degradation of the mouse c-myc RNA. Oncogene 5(10):1585-1588.

Boyer R. 1992. Modern Experimental Biochemistry: Addison Wesley Longman.

Bracale A, Castaldi F, Nitsch L, D'Alessio G. 2003. A role for the intersubunit disulfides of seminal RNase in the mechanism of its antitumor action. Eur J Biochem 270(9):1980-1987.

Bracale A, Spalletti-Cernia D, Mastronicola M, Castaldi F, Mannucci R, Nitsch L, D'Alessio G. 2002. Essential stations in the intracellular pathway of cytotoxic bovine seminal ribonuclease. Biochem J 362(Pt 3):553-560.

Bremer KA, Stevens A, Schoenberg DR. 2003. An endonuclease activity similar to Xenopus PMR1 catalyzes the degradation of normal and nonsense-containing human beta-globin mRNA in erythroid cells. Rna 9(9):1157-1167.

Brennan CM, Steitz JA. 2001. HuR and mRNA stability. Cell Mol Life Sci 58(2):266-277.

Brewer G. 1998. Characterization of c-myc 3' to 5' mRNA decay activities in an in vitro system. J Biol Chem 273(52):34770-34774.
Brewer G. 1999. Evidence for a 3'-5' decay pathway for c-myc mRNA in mammalian cells. J Biol Chem 274(23):16174-16179.
Brewer G. 2002. Messenger RNA decay during aging and development. Ageing Res Rev 1(4):607-625.
Brewer G, Ross J. 1988. Poly(A) shortening and degradation of the 3' A+U-rich sequences of human c-myc mRNA in a cell-free system. Mol Cell Biol 8(4):1697-1708.
Brown BD, Harland RM. 1990. Endonucleolytic cleavage of a maternal homeo box mRNA in Xenopus oocytes. Genes Dev 4(11):1925-1935.
Buratti E, Baralle FE. 2004. Influence of RNA secondary structure on the pre-mRNA splicing process. Mol Cell Biol 24(24):10505-10514.
Butler JS. 2002. The yin and yang of the exosome. Trends Cell Biol 12(2):90-96.
Cai T, Aulds J, Gill T, Cerio M, Schmitt ME. 2002. The Saccharomyces cerevisiae RNase mitochondrial RNA processing is critical for cell cycle progression at the end of mitosis. Genetics 161(3):1029-1042.
Callaghan AJ, Grossmann JG, Redko YU, Ilag LL, Moncrieffe MC, Symmons MF, Robinson CV, McDowall KJ, Luisi BF. 2003. Quaternary structure and catalytic activity of the Escherichia coli ribonuclease E amino-terminal catalytic domain. Biochemistry 42(47):13848-13855.
Campisi J, Gray HE, Pardee AB, Dean M, Sonenshein GE. 1984. Cell-cycle control of c-myc but not c-ras expression is lost following chemical transformation. Cell 36(2):241-247.
Caruccio N, Ross J. 1994. Purification of a human polyribosome-associated 3' to 5' exoribonuclease. J Biol Chem 269(50):31814-31821.
Catapano CV, McGuffie EM, Pacheco D, Carbone GM. 2000. Inhibition of gene expression and cell proliferation by triple helix-forming oligonucleotides directed to the c-myc gene. Biochemistry 39(17):5126-5138.
Charpentier B, Rosbash M. 1996. Intramolecular structure in yeast introns aids the early steps of in vitro spliceosome assembly. Rna 2(6):509-522.
Chen CY, Gherzi R, Ong SE, Chan EL, Raijmakers R, Pruijn GJ, Stoecklin G, Moroni C, Mann M, Karin M. 2001. AU binding proteins recruit the exosome to degrade ARE-containing mRNAs. Cell 107(4):451-464.
Chen CY, Shyu AB. 1995. AU-rich elements: characterization and importance in mRNA degradation. Trends Biochem Sci 20(11):465-470.
Chen CY, Shyu AB. 2003. Rapid deadenylation triggered by a nonsense codon precedes decay of the RNA body in a mammalian cytoplasmic nonsense-mediated decay pathway. Mol Cell Biol 23(14):4805-4813.
Cheng ZF, Deutscher MP. 2005. An important role for RNase R in mRNA decay. Mol Cell 17(2):313-318.
Chernokalskaya E, Dompenciel R, Schoenberg DR. 1997. Cleavage properties of an estrogen-regulated polysomal ribonuclease involved in the destabilization of albumin mRNA. Nucleic Acids Res 25(4):735-742.
Cinatl J, Jr., Cinatl J, Kotchetkov R, Vogel JU, Woodcock BG, Matousek J, Pouckova P, Kornhuber B. 1999. Bovine seminal ribonuclease selectively kills human multidrug-resistant neuroblastoma cells via induction of apoptosis. Int J Oncol 15(5):1001-1009.

Claverie-Martin F, Wang M, Cohen SN. 1997. ARD-1 cDNA from human cells encodes a site-specific single-strand endoribonuclease that functionally resembles Escherichia coli RNase E. J Biol Chem 272(21):13823-13828.
Coburn GA, Mackie GA. 1999. Degradation of mRNA in Escherichia coli: an old problem with some new twists. Prog Nucleic Acid Res Mol Biol 62:55-108.
Coller J, Parker R. 2004. Eukaryotic mRNA decapping. Annu Rev Biochem 73:861-890.
Condon C, Putzer H. 2002. The phylogenetic distribution of bacterial ribonucleases. Nucleic Acids Res 30(24):5339-5346.
Cormack RS, Mackie GA. 1992. Structural requirements for the processing of Escherichia coli 5 S ribosomal RNA by RNase E in vitro. J Mol Biol 228(4):1078-1090.
Cougot N, Babajko S, Seraphin B. 2004. Cytoplasmic foci are sites of mRNA decay in human cells. J Cell Biol 165(1):31-40.
Coulis CM, Lee C, Nardone V, Prokipcak RD. 2000. Inhibition of c-myc expression in cells by targeting an RNA-protein interaction using antisense oligonucleotides. Mol Pharmacol 57(3):485-494.
Culbertson MR, Neeno-Eckwall E. 2005. Transcript selection and the recruitment of mRNA decay factors for NMD in Saccharomyces cerevisiae. Rna 11(9):1333-1339.
Cunningham KS, Dodson RE, Nagel MA, Shapiro DJ, Schoenberg DR. 2000. Vigilin binding selectively inhibits cleavage of the vitellogenin mRNA 3'-untranslated region by the mRNA endonuclease polysomal ribonuclease 1. Proc Natl Acad Sci U S A 97(23):12498-12502.
Cunningham KS, Hanson MN, Schoenberg DR. 2001. Polysomal ribonuclease 1. Methods Enzymol 342:28-44.
Danin-Kreiselman M, Lee CY, Chanfreau G. 2003. RNAse III-mediated degradation of unspliced pre-mRNAs and lariat introns. Mol Cell 11(5):1279-1289.
Decker CJ, Parker R. 1994. Mechanisms of mRNA degradation in eukaryotes. Trends Biochem Sci 19(8):336-340.
Decker CJ, Parker R. 2002. mRNA decay enzymes: decappers conserved between yeast and mammals. Proc Natl Acad Sci U S A 99(20):12512-12514.
Deutscher MP. 2006. Degradation of RNA in bacteria: comparison of mRNA and stable RNA. Nucleic Acids Res 34(2):659-666.
Dodson RE, Shapiro DJ. 2002. Regulation of pathways of mRNA destabilization and stabilization. Prog Nucleic Acid Res Mol Biol 72:129-164.
Doi N, Zenno S, Ueda R, Ohki-Hamazaki H, Ui-Tei K, Saigo K. 2003. Short-interfering-RNA-mediated gene silencing in mammalian cells requires Dicer and eIF2C translation initiation factors. Curr Biol 13(1):41-46.
Doktycz MJ, Larimer FW, Pastrnak M, Stevens A. 1998. Comparative analyses of the secondary structures of synthetic and intracellular yeast MFA2 mRNAs. Proc Natl Acad Sci U S A 95(25):14614-14621.
Doyle GA, Bourdeau-Heller JM, Coulthard S, Meisner LF, Ross J. 2000. Amplification in human breast cancer of a gene encoding a c-myc mRNA-binding protein. Cancer Res 60(11):2756-2759.
Ehresmann C, Baudin F, Mougel M, Romby P, Ebel JP, Ehresmann B. 1987. Probing the structure of RNAs in solution. Nucleic Acids Res 15(22):9109-9128.
Elela SA, Igel H, Ares M, Jr. 1996. RNase III cleaves eukaryotic preribosomal RNA at a U3 snoRNP-dependent site. Cell 85(1):115-124.

Ercole C, Avitabile F, Del Vecchio P, Crescenzi O, Tancredi T, Picone D. 2003. Role of the hinge peptide and the intersubunit interface in the swapping of N-termini in dimeric bovine seminal RNase. Eur J Biochem 270(23):4729-4735.
Facchini LM, Chen S, Marhin WW, Lear JN, Penn LZ. 1997. The Myc negative autoregulation mechanism requires Myc-Max association and involves the c-myc P2 minimal promoter. Mol Cell Biol 17(1):100-114.
Facchini LM, Chen S, Penn LJ. 1994. Dysfunction of the Myc-induced apoptosis mechanism accompanies c-myc activation in the tumorigenic L929 cell line. Cell Growth Differ 5(6):637-646.
Facchini LM, Penn LZ. 1998. The molecular role of Myc in growth and transformation: recent discoveries lead to new insights. Faseb J 12(9):633-651.
Fortin KR, Nicholson RH, Nicholson AW. 2002. Mouse ribonuclease III. cDNA structure, expression analysis, and chromosomal location. BMC Genomics 3(1):26.
Frischmeyer PA, van Hoof A, O'Donnell K, Guerrerio AL, Parker R, Dietz HC. 2002. An mRNA surveillance mechanism that eliminates transcripts lacking termination codons. Science 295(5563):2258-2261.
Gardner L LL, Dang C. 2002. Encyclopedia of cancer: Academic Press.
Gatfield D, Izaurralde E. 2004. Nonsense-mediated messenger RNA decay is initiated by endonucleolytic cleavage in Drosophila. Nature 429(6991):575-578.
Ghora BK, Apirion D. 1978. Structural analysis and in vitro processing to p5 rRNA of a 9S RNA molecule isolated from an rne mutant of E. coli. Cell 15(3):1055-1066.
Gill T, Cai T, Aulds J, Wierzbicki S, Schmitt ME. 2004. RNase MRP cleaves the CLB2 mRNA to promote cell cycle progression: novel method of mRNA degradation. Mol Cell Biol 24(3):945-953.
Grignani F, Lombardi L, Inghirami G, Sternas L, Cechova K, Dalla-Favera R. 1990. Negative autoregulation of c-myc gene expression is inactivated in transformed cells. Embo J 9(12):3913-3922.
Grunberg-Manago M. 1999. Messenger RNA stability and its role in control of gene expression in bacteria and phages. Annu Rev Genet 33:193-227.
Guhaniyogi J, Brewer G. 2001. Regulation of mRNA stability in mammalian cells. Gene 265(1-2):11-23.
Guitard E, Parker F, Millon R, Abecassis J, Tocque B. 2001. G3BP is overexpressed in human tumors and promotes S phase entry. Cancer Lett 162(2):213-221.
Haigis MC, Raines RT. 2003. Secretory ribonucleases are internalized by a dynamin-independent endocytic pathway. J Cell Sci 116(Pt 2):313-324.
Han JQ, Wroblewski G, Xu Z, Silverman RH, Barton DJ. 2004. Sensitivity of hepatitis C virus RNA to the antiviral enzyme ribonuclease L is determined by a subset of efficient cleavage sites. J Interferon Cytokine Res 24(11):664-676.
Hanson MN, Schoenberg DR. 2001. Identification of in vivo mRNA decay intermediates corresponding to sites of in vitro cleavage by polysomal ribonuclease 1. J Biol Chem 276(15):12331-12337.
Hanson MN, Schoenberg DR. 2004. Application of ligation-mediated reverse transcription polymerase chain reaction to the identification of in vivo endonuclease-generated messenger RNA decay intermediates. Methods Mol Biol 257:213-222.

Heise T, Guidotti LG, Cavanaugh VJ, Chisari FV. 1999a. Hepatitis B virus RNA-binding proteins associated with cytokine-induced clearance of viral RNA from the liver of transgenic mice. J Virol 73(1):474-481.
Heise T, Guidotti LG, Chisari FV. 1999b. La autoantigen specifically recognizes a predicted stem-loop in hepatitis B virus RNA. J Virol 73(7):5767-5776.
Heise T, Guidotti LG, Chisari FV. 2001. Characterization of nuclear RNases that cleave hepatitis B virus RNA near the La protein binding site. J Virol 75(15):6874-6883.
Henriksson M, Luscher B. 1996. Proteins of the Myc network: essential regulators of cell growth and differentiation. Adv Cancer Res 68:109-182.
Herrick DJ, Ross J. 1994. The half-life of c-myc mRNA in growing and serum-stimulated cells: influence of the coding and 3' untranslated regions and role of ribosome translocation. Mol Cell Biol 14(3):2119-2128.
Hodgson SV ME. 1993. A practical Guide to Human Cancer Genetics: Cambridge University Press.
Hua J, Garner R, Paetkau V. 1993. An RNasin-resistant ribonuclease selective for interleukin 2 mRNA. Nucleic Acids Res 21(1):155-162.
Huang Z, Zhou TH, Guo BJ. 2004. [Progress on cis-acting regulatory elements in nonsense-mediated mRNA decay]. Yi Chuan Xue Bao 31(11):1321-1326.
Hutvagner G, Zamore PD. 2002. RNAi: nature abhors a double-strand. Curr Opin Genet Dev 12(2):225-232.
Irie M, Nitta K, Nonaka T. 1998. Biochemistry of frog ribonucleases. Cell Mol Life Sci 54(8):775-784.
Irvine K, Stirling R, Hume D, Kennedy D. 2004. Rasputin, more promiscuous than ever: a review of G3BP. Int J Dev Biol 48(10):1065-1077.
Ji X, Kong J, Liebhaber SA. 2003. In vivo association of the stability control protein alphaCP with actively translating mRNAs. Mol Cell Biol 23(3):899-907.
Jiang X, Belasco JG. 2004. Catalytic activation of multimeric RNase E and RNase G by 5'-monophosphorylated RNA. Proc Natl Acad Sci U S A 101(25):9211-9216.
Kelly K, Cochran BH, Stiles CD, Leder P. 1983. Cell-specific regulation of the c-myc gene by lymphocyte mitogens and platelet-derived growth factor. Cell 35(3 Pt 2):603-610.
Kim JS, Soucek J, Matousek J, Raines RT. 1995. Mechanism of ribonuclease cytotoxicity. J Biol Chem 270(52):31097-31102.
Klaff P, Riesner D, Steger G. 1996. RNA structure and the regulation of gene expression. Plant Mol Biol 32(1-2):89-106.
Koeller DM, Casey JL, Hentze MW, Gerhardt EM, Chan LN, Klausner RD, Harford JB. 1989. A cytosolic protein binds to structural elements within the iron regulatory region of the transferrin receptor mRNA. Proc Natl Acad Sci U S A 86(10):3574-3578.
Kong J, Ji X, Liebhaber SA. 2003. The KH-domain protein alpha CP has a direct role in mRNA stabilization independent of its cognate binding site. Mol Cell Biol 23(4):1125-1134.
Korner CG, Wahle E. 1997. Poly(A) tail shortening by a mammalian poly(A)-specific 3'-exoribonuclease. J Biol Chem 272(16):10448-10456.
Kren BT, Trembley JH, Steer CJ. 1996. Alterations in mRNA stability during rat liver regeneration. Am J Physiol 270(5 Pt 1):G763-777.

Kushner SR. 2002. mRNA decay in Escherichia coli comes of age. J Bacteriol 184(17):4658-4665; discussion 4657.
Lachman HM, Cheng GH, Skoultchi AI. 1986. Transfection of mouse erythroleukemia cells with myc sequences changes the rate of induced commitment to differentiate. Proc Natl Acad Sci U S A 83(17):6480-6484.
Lai WS, Kennington EA, Blackshear PJ. 2002. Interactions of CCCH zinc finger proteins with mRNA: non-binding tristetraprolin mutants exert an inhibitory effect on degradation of AU-rich element-containing mRNAs. J Biol Chem 277(11):9606-9613.
Lamontagne B, Elela SA. 2004. Evaluation of the RNA determinants for bacterial and yeast RNase III binding and cleavage. J Biol Chem 279(3):2231-2241.
Lamontagne B, Hannoush RN, Damha MJ, Abou Elela S. 2004. Molecular requirements for duplex recognition and cleavage by eukaryotic RNase III: discovery of an RNA-dependent DNA cleavage activity of yeast Rnt1p. J Mol Biol 338(2):401-418.
Lee CH, Bradley G, Ling V. 1998a. Increased P-glycoprotein messenger RNA stability in rat liver tumors in vivo. J Cell Physiol 177(1):1-12.
Lee CH, Leeds P, Ross J. 1998b. Purification and characterization of a polysome-associated endoribonuclease that degrades c-myc mRNA in vitro. J Biol Chem 273(39):25261-25271.
Lee JE, Raines RT. 2003. Contribution of active-site residues to the function of onconase, a ribonuclease with antitumoral activity. Biochemistry 42(39):11443-11450.
Lejeune F, Li X, Maquat LE. 2003. Nonsense-mediated mRNA decay in mammalian cells involves decapping, deadenylating, and exonucleolytic activities. Mol Cell 12(3):675-687.
Leland PA, Raines RT. 2001. Cancer chemotherapy--ribonucleases to the rescue. Chem Biol 8(5):405-413.
Leland PA, Schultz LW, Kim BM, Raines RT. 1998. Ribonuclease A variants with potent cytotoxic activity. Proc Natl Acad Sci U S A 95(18):10407-10412.
Levens DL. 2003. Reconstructing MYC. Genes Dev 17(9):1071-1077.
Levy NS, Chung S, Furneaux H, Levy AP. 1998. Hypoxic stabilization of vascular endothelial growth factor mRNA by the RNA-binding protein HuR. J Biol Chem 273(11):6417-6423.
Li XL, Blackford JA, Judge CS, Liu M, Xiao W, Kalvakolanu DV, Hassel BA. 2000. RNase-L-dependent destabilization of interferon-induced mRNAs. A role for the 2-5A system in attenuation of the interferon response. J Biol Chem 275(12):8880-8888.
Li Y, Altman S. 2003. A specific endoribonuclease, RNase P, affects gene expression of polycistronic operon mRNAs. Proc Natl Acad Sci U S A 100(23):13213-13218.
Lingel A, Izaurralde E. 2004. RNAi: finding the elusive endonuclease. Rna 10(11):1675-1679.
Liu H, Rodgers ND, Jiao X, Kiledjian M. 2002. The scavenger mRNA decapping enzyme DcpS is a member of the HIT family of pyrophosphatases. Embo J 21(17):4699-4708.
Liu J, Carmell MA, Rivas FV, Marsden CG, Thomson JM, Song JJ, Hammond SM, Joshua-Tor L, Hannon GJ. 2004. Argonaute2 is the catalytic engine of mammalian RNAi. Science 305(5689):1437-1441.

Loflin P, Chen CY, Shyu AB. 1999. Unraveling a cytoplasmic role for hnRNP D in the in vivo mRNA destabilization directed by the AU-rich element. Genes Dev 13(14):1884-1897.

Lowman HB, Draper DE. 1986. On the recognition of helical RNA by cobra venom V1 nuclease. J Biol Chem 261(12):5396-5403.

Lundberg U, Melefors O, Sohlberg B, Georgellis D, von Gabain A. 1995. RNase K: one less letter in the alphabet soup. Mol Microbiol 17(3):595-596.

Lundberg U, von Gabain A, Melefors O. 1990. Cleavages in the 5' region of the ompA and bla mRNA control stability: studies with an E. coli mutant altering mRNA stability and a novel endoribonuclease. Embo J 9(9):2731-2741.

Ma WJ, Cheng S, Campbell C, Wright A, Furneaux H. 1996. Cloning and characterization of HuR, a ubiquitously expressed Elav-like protein. J Biol Chem 271(14):8144-8151.

Ma WJ, Chung S, Furneaux H. 1997. The Elav-like proteins bind to AU-rich elements and to the poly(A) tail of mRNA. Nucleic Acids Res 25(18):3564-3569.

Mackie GA, Genereaux JL. 1993. The role of RNA structure in determining RNase E-dependent cleavage sites in the mRNA for ribosomal protein S20 in vitro. J Mol Biol 234(4):998-1012.

Manohar CF, Short ML, Nguyen A, Nguyen NN, Chagnovich D, Yang Q, Cohn SL. 2002. HuD, a neuronal-specific RNA-binding protein, increases the in vivo stability of MYCN RNA. J Biol Chem 277(3):1967-1973.

Marcu KB, Bossone SA, Patel AJ. 1992. myc function and regulation. Annu Rev Biochem 61:809-860.

McAllister RM HS, Gilder RV. 1993. Cancer.HarperCollins Publishers Inc.

McEwan IJ, Dahlman-Wright K, Ford J, Wright AP. 1996. Functional interaction of the c-Myc transactivation domain with the TATA binding protein: evidence for an induced fit model of transactivation domain folding. Biochemistry 35(29):9584-9593.

Meinsma D, Scheper W, Holthuizen PE, Van den Brande JL, Sussenbach JS. 1992. Site-specific cleavage of IGF-II mRNAs requires sequence elements from two distinct regions of the IGF-II gene. Nucleic Acids Res 20(19):5003-5009.

Mishra N. 2002. Nucleases: Molecular Biology and Applications: Wiley-Interscience Publications.

Mitchell P, Petfalski E, Shevchenko A, Mann M, Tollervey D. 1997. The exosome: a conserved eukaryotic RNA processing complex containing multiple 3'-->5' exoribonucleases. Cell 91(4):457-466.

Mitchell P, Tollervey D. 2000. Musing on the structural organization of the exosome complex. Nat Struct Biol 7(10):843-846.

Moore JP, Hancock DC, Littlewood TD, Evan GI. 1987. A sensitive and quantitative enzyme-linked immunosorbence assay for the c-myc and N-myc oncoproteins. Oncogene Res 2(1):65-80.

Morello D, Lavenu A, Babinet C. 1990. Differential regulation and expression of jun, c-fos and c-myc proto-oncogenes during mouse liver regeneration and after inhibition of protein synthesis. Oncogene 5(10):1511-1519.

Mudd EA, Prentki P, Belin D, Krisch HM. 1988. Processing of unstable bacteriophage T4 gene 32 mRNAs into a stable species requires Escherichia coli ribonuclease E. Embo J 7(11):3601-3607.

Munoz-Gomez AJ, Santos-Sierra S, Berzal-Herranz A, Lemonnier M, Diaz-Orejas R. 2004. Insights into the specificity of RNA cleavage by the Escherichia coli MazF toxin. FEBS Lett 567(2-3):316-320.

Nicholson AW. 1999. Function, mechanism and regulation of bacterial ribonucleases. FEMS Microbiol Rev 23(3):371-390.

Nicholson RH, Nicholson AW. 2002. Molecular characterization of a mouse cDNA encoding Dicer, a ribonuclease III ortholog involved in RNA interference. Mamm Genome 13(2):67-73.

Nielsen FC, Christiansen J. 1992. Endonucleolysis in the turnover of insulin-like growth factor II mRNA. J Biol Chem 267(27):19404-19411.

Pandey M, Rath PC. 2004. Expression of interferon-inducible recombinant human RNase L causes RNA degradation and inhibition of cell growth in Escherichia coli. Biochem Biophys Res Commun 317(2):586-597.

Parker JS, Roe SM, Barford D. 2004. Crystal structure of a PIWI protein suggests mechanisms for siRNA recognition and slicer activity. Embo J 23(24):4727-4737.

Parker R, Song H. 2004. The enzymes and control of eukaryotic mRNA turnover. Nat Struct Mol Biol 11(2):121-127.

Penn LJ, Brooks MW, Laufer EM, Land H. 1990. Negative autoregulation of c-myc transcription. Embo J 9(4):1113-1121.

Piecyk M, Wax S, Beck AR, Kedersha N, Gupta M, Maritim B, Chen S, Gueydan C, Kruys V, Streuli M, Anderson P. 2000. TIA-1 is a translational silencer that selectively regulates the expression of TNF-alpha. Embo J 19(15):4154-4163.

Pistoi S, Roland J, Babinet C, Morello D. 1996. Exon 2-mediated c-myc mRNA decay in vivo is independent of its translation. Mol Cell Biol 16(9):5107-5116.

Posch M, Sutterluety H, Skern T, Seiser C. 1999. Characterization of the translation-dependent step during iron-regulated decay of transferrin receptor mRNA. J Biol Chem 274(23):16611-16618.

Prokipcak RD, Herrick DJ, Ross J. 1994. Purification and properties of a protein that binds to the C-terminal coding region of human c-myc mRNA. J Biol Chem 269(12):9261-9269.

Provost P, Dishart D, Doucet J, Frendewey D, Samuelsson B, Radmark O. 2002. Ribonuclease activity and RNA binding of recombinant human Dicer. Embo J 21(21):5864-5874.

Rand TA, Ginalski K, Grishin NV, Wang X. 2004. Biochemical identification of Argonaute 2 as the sole protein required for RNA-induced silencing complex activity. Proc Natl Acad Sci U S A 101(40):14385-14389.

Rauhut R, Klug G. 1999. mRNA degradation in bacteria. FEMS Microbiol Rev 23(3):353-370.

Redko Y, Tock MR, Adams CJ, Kaberdin VR, Grasby JA, McDowall KJ. 2003. Determination of the catalytic parameters of the N-terminal half of Escherichia coli ribonuclease E and the identification of critical functional groups in RNA substrates. J Biol Chem 278(45):44001-44008.

Richardson N, Navaratnam N, Scott J. 1998. Secondary structure for the apolipoprotein B mRNA editing site. Au-binding proteins interact with a stem loop. J Biol Chem 273(48):31707-31717.

Robertson HD, Webster RE, Zinder ND. 1968. Purification and properties of ribonuclease III from Escherichia coli. J Biol Chem 243(1):82-91.
Rodgers ND, Wang Z, Kiledjian M. 2002. Characterization and purification of a mammalian endoribonuclease specific for the alpha -globin mRNA. J Biol Chem 277(4):2597-2604.
Ross J. 1995. mRNA stability in mammalian cells. Microbiol Rev 59(3):423-450.
Ross J, Peltz SW, Kobs G, Brewer G. 1986. Histone mRNA degradation in vivo: the first detectable step occurs at or near the 3' terminus. Mol Cell Biol 6(12):4362-4371.
Saxena SK, Sirdeshmukh R, Ardelt W, Mikulski SM, Shogen K, Youle RJ. 2002. Entry into cells and selective degradation of tRNAs by a cytotoxic member of the RNase A family. J Biol Chem 277(17):15142-15146.
Schein CH, Haugg M, Benner SA. 1990. Interferon-gamma activates the cleavage of double-stranded RNA by bovine seminal ribonuclease. FEBS Lett 270(1-2):229-232.
Scheper W, Holthuizen PE, Sussenbach JS. 1996. The cis-acting elements involved in endonucleolytic cleavage of the 3' UTR of human IGF-II mRNAs bind a 50 kDa protein. Nucleic Acids Res 24(6):1000-1007.
Schiavi SC, Belasco JG, Greenberg ME. 1992. Regulation of proto-oncogene mRNA stability. Biochim Biophys Acta 1114(2-3):95-106.
Schmitt ME, Clayton DA. 1992. Yeast site-specific ribonucleoprotein endoribonuclease MRP contains an RNA component homologous to mammalian RNase MRP RNA and essential for cell viability. Genes Dev 6(10):1975-1985.
Schoenberg DR, Cunningham KS. 1999. Characterization of mRNA endonucleases. Methods 17(1):60-73.
Schwarz DS, Hutvagner G, Haley B, Zamore PD. 2002. Evidence that siRNAs function as guides, not primers, in the Drosophila and human RNAi pathways. Mol Cell 10(3):537-548.
Shiman R, Draper DE. 2000. Stabilization of RNA tertiary structure by monovalent cations. J Mol Biol 302(1):79-91.
Silverman RH. 2003. Implications for RNase L in prostate cancer biology. Biochemistry 42(7):1805-1812.
Smith RF, Wiese BA, Wojzynski MK, Davison DB, Worley KC. 1996. BCM Search Launcher--an integrated interface to molecular biology data base search and analysis services available on the World Wide Web. Genome Res 6(5):454-462.
Sommer A, Bousset K, Kremmer E, Austen M, Luscher B. 1998. Identification and characterization of specific DNA-binding complexes containing members of the Myc/Max/Mad network of transcriptional regulators. J Biol Chem 273(12):6632-6642.
Spencer CA, Groudine M. 1991. Control of c-myc regulation in normal and neoplastic cells. Adv Cancer Res 56:1-48.
Steege DA. 2000. Emerging features of mRNA decay in bacteria. Rna 6(8):1079-1090.
Stevens A, Wang Y, Bremer K, Zhang J, Hoepfner R, Antoniou M, Schoenberg DR, Maquat LE. 2002. Beta -Globin mRNA decay in erythroid cells: UG site-preferred endonucleolytic cleavage that is augmented by a premature termination codon. Proc Natl Acad Sci U S A 99(20):12741-12746.

Supino R, Perego P, Gatti L, Caserini C, Leonetti C, Colantuono M, Zuco V, Carenini N, Zupi G, Zunino F. 2001. A role for c-myc in DNA damage-induced apoptosis in a human TP53-mutant small-cell lung cancer cell line. Eur J Cancer 37(17):2247-2256.
Tannock IF HR. 1998. The Basic Science of Oncology: McGraw -Hill.
Thisted T, Sorensen NS, Gerdes K. 1995. Mechanism of post-segregational killing: secondary structure analysis of the entire Hok mRNA from plasmid R1 suggests a fold-back structure that prevents translation and antisense RNA binding. J Mol Biol 247(5):859-873.
Tock MR, Walsh AP, Carroll G, McDowall KJ. 2000. The CafA protein required for the 5'-maturation of 16 S rRNA is a 5'-end-dependent ribonuclease that has context-dependent broad sequence specificity. J Biol Chem 275(12):8726-8732.
Tourriere H, Gallouzi IE, Chebli K, Capony JP, Mouaikel J, van der Geer P, Tazi J. 2001. RasGAP-associated endoribonuclease G3Bp: selective RNA degradation and phosphorylation-dependent localization. Mol Cell Biol 21(22):7747-7760.
Uchida N, Hoshino S, Katada T. 2004. Identification of a human cytoplasmic poly(A) nuclease complex stimulated by poly(A)-binding protein. J Biol Chem 279(2):1383-1391.
van Dijk EL, Sussenbach JS, Holthuizen PE. 1998. Identification of RNA sequences and structures involved in site-specific cleavage of IGF-II mRNAs. Rna 4(12):1623-1635.
van Dijk EL, Sussenbach JS, Holthuizen PE. 2001. Kinetics and regulation of site-specific endonucleolytic cleavage of human IGF-II mRNAs. Nucleic Acids Res 29(17):3477-3486.
van Hoof A, Frischmeyer PA, Dietz HC, Parker R. 2002. Exosome-mediated recognition and degradation of mRNAs lacking a termination codon. Science 295(5563):2262-2264.
Vermeulen A, Behlen L, Reynolds A, Wolfson A, Marshall WS, Karpilow J, Khvorova A. 2005. The contributions of dsRNA structure to Dicer specificity and efficiency. Rna 11(5):674-682.
Wachi M, Umitsuki G, Shimizu M, Takada A, Nagai K. 1999. Escherichia coli cafA gene encodes a novel RNase, designated as RNase G, involved in processing of the 5' end of 16S rRNA. Biochem Biophys Res Commun 259(2):483-488.
Walker SC, Avis JM. 2005. Secondary structure probing of the human RNase MRP RNA reveals the potential for MRP RNA subsets. Biochem Biophys Res Commun 335(2):314-321.
Wang Z, Kiledjian M. 2000. Identification of an erythroid-enriched endoribonuclease activity involved in specific mRNA cleavage. Embo J 19(2):295-305.
Wennborg A, Sohlberg B, Angerer D, Klein G, von Gabain A. 1995. A human RNase E-like activity that cleaves RNA sequences involved in mRNA stability control. Proc Natl Acad Sci U S A 92(16):7322-7326.
Wilusz CJ, Wormington M, Peltz SW. 2001. The cap-to-tail guide to mRNA turnover. Nat Rev Mol Cell Biol 2(4):237-246.
Wisdom R, Lee W. 1990. Translation of c-myc mRNA is required for its post-transcriptional regulation during myogenesis. J Biol Chem 265(31):19015-19021.
Wisdom R, Lee W. 1991. The protein-coding region of c-myc mRNA contains a sequence that specifies rapid mRNA turnover and induction by protein synthesis inhibitors. Genes Dev 5(2):232-243.

Xu N, Chen CY, Shyu AB. 2001. Versatile role for hnRNP D isoforms in the differential regulation of cytoplasmic mRNA turnover. Mol Cell Biol 21(20):6960-6971.

Yang F, Schoenberg DR. 2004. Endonuclease-mediated mRNA decay involves the selective targeting of PMR1 to polyribosome-bound substrate mRNA. Mol Cell 14(4):435-445.

Yang J, Stern DB. 1997. The spinach chloroplast endoribonuclease CSP41 cleaves the 3'-untranslated region of petD mRNA primarily within its terminal stem-loop structure. J Biol Chem 272(19):12874-12880.

Yeilding NM, Procopio WN, Rehman MT, Lee WM. 1998. c-myc mRNA is down-regulated during myogenic differentiation by accelerated decay that depends on translation of regulatory coding elements. J Biol Chem 273(25):15749-15757.

Zekri L, Chebli K, Tourriere H, Nielsen FC, Hansen TV, Rami A, Tazi J. 2005. Control of fetal growth and neonatal survival by the RasGAP-associated endoribonuclease G3BP. Mol Cell Biol 25(19):8703-8716.

Zhang J, Zhang Y, Zhu L, Suzuki M, Inouye M. 2004. Interference of mRNA function by sequence-specific endoribonuclease PemK. J Biol Chem 279(20):20678-20684.

Zhang Y, Zhang J, Hara H, Kato I, Inouye M. 2005. Insights into the mRNA cleavage mechanism by MazF, an mRNA interferase. J Biol Chem 280(5):3143-3150.

Zhang Y, Zhang J, Hoeflich KP, Ikura M, Qing G, Inouye M. 2003. MazF cleaves cellular mRNAs specifically at ACA to block protein synthesis in Escherichia coli. Mol Cell 12(4):913-923.

Zhao Z, Chang FC, Furneaux HM. 2000. The identification of an endonuclease that cleaves within an HuR binding site in mRNA. Nucleic Acids Res 28(14):2695-2701.

Zuker M. 2003. Mfold web server for nucleic acid folding and hybridization prediction. Nucleic Acids Res 31(13):3406-3415.

APPENDIX

The Obtained Sequences of the CRD Mutants

```
                                        1710      1720      1730    1740        1750      1760     1770

         A             B                                                          C
CP-2    GGATCCATTTAGGTG ACACTATAGACCAGA TCCCGGAGTTGGAAA ACAATGAAAAGGCCC CCAAGGTAGTATTCC TTAAAAAAGCCACAG
CP-10G  GGATCCATTTAGGTG ACACTATAGACCAGA TCCCGGAGTTGGAAA ACAATGAAAAGGCCC CCAAGGTAGTTGTCC TTAAAAAAGCCACAG
CP-10C  GGATCCATTTAGGTG ACACTATAGACCAGA TCCCGGAGTTGGAAA ACAATGAAAAGGCCC CCAAGGTAGTTCTCC TTAAAAAAGCCACAG
CP-3    GGATCCATTTAGGTG ACACTATAGACCAGA TCCCGGAGTTGGAAA ACAATGAAAAGGCCC CCAAGGTAGTTATCC TATAAAAAGCCACAG
CP-24   GGATCCATTTAGGTG ACACTATAGACCAGA TCCCGGAGTTGGAAA ACAATGAAAAGGCCC CCAAGGTAGTTTACC TTAAAAAAGCCACAG
CP-10U  GGATCCATTTAGGTG ACACTATAGACCAGA TCCCGGAGTTGGAAA ACAATGAAAAGGCCC CCAAGGTAGTTTTCC TTAAAAAAGCCACAG
CP-15   GGATCCATTTAGGTG ACACTATAGACCAGA TCCCGGAGTTGGAAA AACATGAAAAGGCCC CCAAGGTAGTTATCC TTAAAAAAGCCACAG
CP-19A  GGATCCATTTAGGTG ACACTATAGACCAGA TCCCGGAGTTGGAAA AAAATGAAAAGGCCC CCAAGGTAGTTATCC TTAAAAAAGCCACAG
CP-19G  GGATCCATTTAGGTG ACACTATAGACCAGA TCCCGGAGTTGGAAA AGAATGAAAAGGCCC CCAAGGTAGTTATCC TTAAAAAAGCCACAG
CP-19U  GGATCCATTTAGGTG ACACTATAGACCAGA TCCCGGAGTTGGAAA ATAATGAAAAGGCCC CCAAGGTAGTTATCC TTAAAAAAGCCACAG
CP-13   GGATCCATTTAGGTG ACACTATAGACCAGA TCCCGGAGTTGGAAA ACAA-GTAAAGGCCC CCAAGGTAGTTATCC TTAAAAAAGCCACAG
CP-22   GGATCCATTTAGGTG ACACTATAGACCAGA TCCAG-AGTTGGAAA ACAATGAAAAGGCCC CCTAGGTAGTTATCC TAAAAAAAGCCACAG


                    1780      1790

                      C            D
CP-2    CATACATCCTGTCCG TCCAAGCGAATTC
CP-10G  -ATACATCCTGTCCG TCCAAGCGAATTC
CP-10C  CATACATCCTGTCCG TCCAAGCGAATTC
CP-3    CATACATCCTGTCCG TCCAAGCGAATTC
CP-24   CATACATCCTGTCCG TCCAAGCGAATTC
CP-10U  CATACATCCTGTCCG TCCAAGCGAATTC
CP-15   CATACATCCTGTCCG TCCAAGCGAATTC
CP-19A  CATACATCCTGTCCG TCCAAGCGAATTC
CP-19G  CATACATCCTGTCCG TCCAAGCGAATTC
CP-19U  CATACATCCTGTCCG TCCAAGCGAATTC
CP-13   CATACATCCTGTCCG TCCAAGCGAATTC
CP-22   CATACATCCTGTCCG TCCAAGCGAATTC
```

Figure A.1. Alignment of the 12 sequenced CRD mutants using the BCM Search Launcher (Smith et al., 1996). Region A (bold) represent the *Bam*HI Restriction site, region B represents the SP-6 RNA polymerase promoter (underlined), region C represents the 1705-1792 CRD sequence, while Region D (bold) represents the *Eco*RI restriction site. Numbering indicates the CRD regions.